THE UNIVERSITY OF CHICAGO

THE ROLE OF THE LATERODORSAL TEGMENTAL NUCLEUS IN NICOTINE WITHDRAWAL

A DISSERTATION SUBMITTED TO
THE FACULTY OF THE DIVISION OF THE BIOLOGICAL SCIENCES
AND THE PRITZKER SCHOOL OF MEDICINE
IN CANDIDACY FOR THE DEGREE OF
DOCTOR OF PHILOSOPHY

INTERDISCIPLINARY SCIENTIST TRAINING PROGRAM:
NEUROBIOLOGY

BY

ALEXIS MONICAL

CHICAGO, ILLINOIS

AUGUST 2023

To all my family and friends that made this journey vibrant and joyful through the fun times and the hard ones. You made me feel like I was never alone.

TABLE OF CONTENTS

LIST OF FIGURES……..vi

LIST OF TABLES……..viii

ACKNOWLEDGMENTS……ix

ABSTRACT……xi

INTRODUCTION……1

Overview of nicotine addiction and withdrawal…….1

Vulnerable populations to nicotine addiction…….4

Addiction cycle in an average smoker…….7

Dopamine dynamics in nicotine withdrawal……11

Laterodorsal tegmental nucleus in reward and addiction……11

The interpeduncular nucleus is a main driver of nicotine withdrawal aversion……..13

Outlook on current treatments of nicotine addiction.....……15

Aims of this thesis: Critical gaps in knowledge that will be addressed……18

MATERIALS AND METHODS……19

Animals…….....19

Nicotine administration……..19

Drugs and reagents……..21

ELISA cotinine assay……..21

Surgical procedures…….....22

Slice preparation……..23

Slice recording……..……..23

Histology……24

Behavior…….……26

Fiber photometry……..……..29

Randomization and blinding…….……..30

Data analysis..……31

RESULTS - GABAERGIC NEURONS FROM THE INTERPEDUNCULAR NUCLEUS TO THE LATERODORSAL TEGMENTAL NUCLEUS DRIVE AFFECTIVE AND SOMATIC NICOTINE WITHDRAWAL SYMPTOMS…..…….....32

LDTg activity attenuates during nicotine withdrawal……..…....32

IPN GABAergic neurons synapse to the LDTg cell types differentially…….32

Blocking inhibitory inputs from IPN to LDTg is preferred in nicotine withdrawal……..40

Inhibition of IPN-LDTg GABAergic terminals alleviates nicotine withdrawal somatic signs……45

LDTg mediates nicotine withdrawal behavioral response to novelty……...……..45

LDTg mediates nicotine withdrawal behavioral response to hedonic stimuli……..……..50

Dopamine in the NAc lateral shell aligns with LDTg activity……..…..…..52

DISCUSSION……...74

Translatability of nicotine dependence and withdrawal in mice……..……....74

LDTg activity is suppressed during nicotine withdrawal……..……..79

The IPN sends GABAergic synaptic connections differentially to cell types in LDTg…...81

Whole brain mapping reveals differential inputs to LDTg cholinergic and GABAergic cells……86

The habenulo-peduncular system regulates nicotine withdrawal through LDTg…..……88

Inhibition of IPN-LDTg GABAergic terminals relieves somatic nicotine withdrawal….91

Inhibition of IPN-LDTg GABAergic terminals relieves affective nicotine withdrawal….94

Nicotine withdrawal alters normal LDTg response and dopamine release to novel object…….……96

Coordination of LDTg activity and dopamine release in NAc lateral shell…..…….100

Conclusions……...…….……103

Future Directions.……104

REFERENCES……106

LIST OF FIGURES

Figure 1: Nicotine addiction is a chronically relapsing disorder…...……...…….10

Figure 2: Proposed neural circuitry involved in nicotine withdrawal…….……..…….……14

Figure 3: Nicotine drinking for 4-weeks..…….……20

Figure 4: LDTg is spontaneously active and attenuates activity after nicotine withdrawal…...…….33

Figure 5: Mecamylamine decreases LDTg activity after chronic nicotine treatment …….34

Figure 6: Nicotine withdrawal increases activity in IPN GABAeric neurons.…….35

Figure 7: Starter cells in LDTg label monosynaptic inputs in a cell type specific manner…..…….37

Figure 8: IPN subregions connect to different LDTg cell types …….……...…38

Figure 9: Whole brain inputs to LDTg GABAergic and cholinergic cells……..…..…..39

Figure 10: Optogenetic inhibition of IPN GABAergic terminals in LDTg……..41

Figure 11: cfos expression in LDTg after photoinhibition of IPN GABAergic terminals …….42

Figure 12: Inhibition of IPN-LDTg GABAergic terminals during nicotine withdrawal results in place preference ..……43

Figure 13: Context dependent conditioning for photoinhibition in nicotine withdrawal…..……44

Figure 14: Silencing GABAergic IPN projections to LDTg decreases somatic sign duration…….46

Figure 15: Silencing GABAergic IPN-LDTg projections increases open-field exploration..……..47

Figure 16: LDTg activity during novel object interaction……..…...48

Figure 17: Nicotine withdrawal decreases LDTg responsiveness to novel object interaction……....49

Figure 18: IPN-LDTg inhibition prevents nicotine withdrawal anhedonia to social odor..……..51

Figure 19: Spontaneous DA release in the NAc lateral shell to SAL and MEC injections..……..54

Figure 20: DA release in the NAc lateral shell is depressed after nicotine withdrawal..……..55

Figure 21: DA dynamics to novel object interaction in NAc lateral shell……..……..56

Figure 22: Nicotine withdrawal alters DA dynamics to novel object response……57

LIST OF TABLES

Table 1: Public health facts for U.S. tobacco and nicotine use…..…….……...2

Table 2: FDA-approved therapeutic options for tobacco use disorder….……...17

Table 3: Statistical significance…….....…….……...58

Table 4: Statistical tests and outputs…….....…….……..59

Table 5: Statistical abbreviations…….....…….……..73

ACKNOWLEDGEMENTS

I would like to thank my mentor, Daniel McGehee, for embracing me into the lab and teaching me how to be a scientist. Dan fostered an environment that allowed for scientific curiosity. I felt like I was given the mentorship to succeed and the freedom to ask questions that were meaningful and interesting to me. Without Dan this project would not have been possible, and I am thankful for the opportunity to learn the intricacies of neuroscience and the complexity of designing thoughtful experiments in this lab. Dan cares about his lab on a personal level. He took us out for our birthdays, and during COVID Dan even let me borrow his car to get to work. I could not have asked for a more caring and attentive mentor.

I would also like to thank my committee, Ruth Anne Eatock, Xiaoxi, Zhuang, Andrea King, and Mitchell Roitman. Ruth Anne was an ever-positive presence throughout my PhD, contributing invaluable scientific knowledge and thoughtful insights. As the chair of my committee, she always made sure I had space to be heard. Xiaoxi Zhuang was a calm and levelheaded member of the committee that always brought a new and fresh perspective to my research. I am thankful for his attention to the important details and alternative interpretations of my research. Andrea King was a vigilant committee member that always pushed me to think about the research from the clinical perspective. I am grateful for Andrea's perspective on nicotine addiction in humans and helping me work through the translatability of mouse research. Mitchell Roitman joined my committee late but was an amazing addition to my committee. Not only did he bring a wealth of knowledge that my project needed, but he brought additional collaboration efforts to the lab. Mitch is a good hearted and warm person that always made committee meetings a joy. I thank all my committee and their commitment to my project.

This dissertation would not be possible without the support of my friends and family. I would love to thank my best friend Nonna how has been my friend since high school, my roommate through college and the entirety of my PhD. She has seen me through my highest highs and my lowest lows. She has been nothing but kind and supportive and always knows exactly what I need. I would also like to thank my large family who has supported me through thick and thin. They have given me access to good education, given me unconditional love and support. I would like to thank my mom who has always taken a deep interest in my education and will support me in all my milestones. I would like to thank my grandma who was a huge presence throughout my childhood. She has a lot of love in her heart and is always curious about my life and my adventures. I also need to thank my aunt and uncle who raised me since I was six. None of this would be possible without their unwavering love and support. Thank you to all of my friends, mentors and colleagues I've met along the way.

ABSTRACT

Nicotine is the main addictive component in cigarettes. After chronic exposure to nicotine, neural adaptations in key brain areas lead to an aversive state upon withdrawal from nicotine consumption. This withdrawal state is accompanied by unpleasant behavioral manifestations that increases susceptibility to nicotine relapse. These withdrawal symptoms encompass somatic and affective components. These negative symptoms are associated with activity in the interpeduncular nucleus (IPN), a midbrain structure that increases activity with presentation of aversive stimuli, including aversion to high doses of nicotine and withdrawal from chronic nicotine. While it has been shown that the IPN mediates negative effects of nicotine withdrawal, how the IPN mediates this aversive state through the efferent connections to downstream targets has not been clearly elucidated. Based on previous studies in the lab, activation of inhibitory GABAergic connections from the IPN to the laterodorsal tegmentum (LDTg) is aversive and silencing these projections prevents aversive response to an acute high dose of nicotine in mice. We hypothesize that the GABAergic projections from IPN to LDTg are recruited during withdrawal from chronic nicotine promoting an aversive state and withdrawal symptoms. This thesis explores the use optogenetics for control over circuit activation and inhibition to study its contribution to nicotine withdrawal behavior and physiology. By studying the IPN to LDTg circuit in the context of nicotine withdrawal we may elucidate areas with novel drug targets, which have therapeutic potential to relieve nicotine withdrawal symptoms and improve cessation outcomes.

INTRODUCTION

Overview of nicotine addiction and withdrawal

Tobacco use disorder affects over 1 billion people worldwide and the associated adverse health consequences establishes it as one of the most severe threats to public health[1-3], as seen in Table 1. Despite the health campaigns and policy changes to combat the health risks of smoking, it remains the leading cause of preventable premature death in the United States[4]. Nicotine is the main psychoactive addictive compound in tobacco and electronic cigarette products[5-7], and the transition from occasional use to dependence is much more likely for nicotine than other addictive drugs[8]. While nicotine alone is not carcinogenic, it does have separate adverse health implications[5,9], summarized in Table 1.

One of the most challenging aspects of nicotine addiction is the remarkably high percentage of relapse for individuals who attempt to quit[10,11]. An important driver of relapse is avoidance of the aversive effects associated with nicotine withdrawal[10-12], which is characterized by a range of physical and psychological symptoms, including anxiety, depression, irritability, and restlessness [13,14]. The severity of withdrawal symptoms can vary depending on factors such as the duration of nicotine use and the method of cessation[8,15-17]. Preventing relapse is crucial in improving health outcomes. Smoking cessation can result in immediate health benefits, including partial or full reversal of the reduced life expectancy, depending on age that the smoker successfully quits[4,18]. Understanding the neural mechanisms underlying nicotine withdrawal is essential for developing improved treatments for addiction.

a. TOBACCO HEALTH STATISTICS AND FACTS			
	Description		**Ref**
Consumption	>Smoke (Cigarettes, Cigars, Cigarillos, Hookah, Pipe, etc.) >Smokeless (Snuff, Chew, Dip, Snus, etc.) >Dissolvable (gel or ground) >Heat-not-burn		3,19,20
Components	>Nicotine (addictive) >Acetaldehyde (reinforcing) >Carbon monoxide (combustion byproduct) >Flavor and absorption enhancers >Over 7,000 chemicals >Approximately 69 carcinogens		4,21
# Deaths	> Over 480,000/year		4
Mortality Risk	>2x in smokers over 60 years of age vs. non-smokers >About 6-year decrease in life expectancy		4
Use	>About 28.3 million US adults smoke cigarettes (11.5% as of 2021) >About 61.6 million US adults use tobacco or nicotine (22% as of 2021)		4
b. SMOKING ASSOCIATED DISEASE			
	Description		**Ref**
Cancer	>Lung, mouth, pharynx, larynx, esophagus, stomach, pancreas, cervix, kidney, bladder, myeloid >Responsible for at least 30% of all cancer deaths >80-90% of all lung cancers, increasing risk 5-10-fold vs. non-smokers >Smokeless tobacco also causes cancer		4
Lung Disease	>Bronchitis, emphysema, asthma, chronic obstructive pulmonary disease		4
Heart Disease	>Stroke, heart attack, vascular disease, aneurysm		4
Other	>Rheumatoid arthritis, inflammation, immune deficiency, type II diabetes, Alzheimer's Disease		4,22
c. E-CIGARETTE HEALTH STATISTICS AND FACTS			
	Description		**Ref**
Components	>Nicotine (addictive) >Over 7,000 flavors >Over 100 Chemicals >Carcinogens, toxicants, metal particles		4,23
Use	>Over 2.5 million US middle (3.3% as of 2022) and high school students (14.1% as of 2022) >Over 11.6 million US adults (4.5% as of 2021)		24,25
d. NICOTINE ASSOCIATED HEALTH CONSEQUENCES			
	Effect	**Description**	**Ref**
Sympathetic drug	Catecholamine release	>Elevates heart rate and blood pressure >Increases cardiac contractility and constricts vessels	26
Implicated adverse effects	Endothelial dysfunction	>Arteriosclerotic cardiovascular disease >Oxidative inflammation, thrombosis, atherogenesis, angiogenesis, vasoconstriction, insulin resistance >No risk observed with NRT	9,27

Table 1. Public health facts for U.S. tobacco and nicotine use

Table 1, continued

Tobacco has been consumed by humans for millennia and commercialized in the U.S. since the 17th century. To date, cigarette companies are still a part of a multibillion-dollar industry with millions of consumers. **a.** Tobacco is consumed in a variety of forms and the associated components cause increased risk of mortality. Tobacco is still used by millions of people in the U.S. alone **b.** The diseases associated with smoking tobacco products can negatively impact every organ system in the body. Smoking cessation decreases risk of disease development and improves health outcomes. **c.** E-cigarettes do not contain the combustible tar of tobacco that contains the bulk of toxins and carcinogens. E-cigarettes contain nicotine and they are addictive. Research is ongoing surrounding the health risk of vaping these products. **d.** Nicotine alone is not carcinogenic. Nicotine increases risk of endothelial disease and contributes to cardiovascular pathologies.

Vulnerable populations to nicotine addiction

Adolescents

While cigarette use is reportedly lower in the adolescent population (0.8%, 1.7%, and 4% in 8th, 10th and 12th graders respectively), the numbers of adolescents using nicotine vapor products is high (8.7%, 15.1% and 24.8% of 8th, 10th, and 12th graders respectively)[4]. Since e-cigarettes hit the market in 2007, they have rapidly gained popularity[4]. With the sleek, inconspicuous design and the barrage of different flavors, they have successfully marketed to a younger population[28]. E-cigarette use is prevalent in both adolescent smokers and non-smokers[4]. Early, adolescent exposure to nicotine is predictive of future drug use, including transition to cigarette use[29,30]. Within the adult population there is a belief that e-cigarettes are a form of smoking cessation, however, that belief is not maintained in the adolescent population[4]. Adolescents also report low belief that nicotine vape products are harmful and addictive[4]. Social factors are one of the primary motivators for nicotine use at young ages including peer use, parental use, psychological stress, and low socioeconomic status[4,31]. E-cigarettes do not contain the harmful constituents of combustible tar, however, the research surrounding safety of these products is ongoing[32]. The FDA gained regulation of e-cigarettes in 2016[4]. Since then, they raised the legal age from 18 to 21 in 2019 and issued regulations on flavoring in 2020[4]. However, use is still prevalent in the adolescent population.

Comparison of Sex

Male and female smokers have differences in tobacco use. Men tend to use tobacco products at higher rates than women (13.1% vs 10.1%)[4]. One theory is that men smoke for the rewarding effects and have higher levels of nicotine positive reinforcement, while women smoke

for mood regulatory effects[4]. Women have stronger withdrawal symptoms and craving, especially from stress[4]. One study showed that women obtain equal relief from withdrawal symptoms by smoking nicotine cigarettes or de-nicotinate cigarettes, while men only found relief from the cigarettes with nicotine included[33]. This suggests that women find nicotine less rewarding than men and women have stronger cue association responses. There is no difference in the number of men and women who report wanting to quit, however men are 30% more likely to be successful[4]. In addition to stronger withdrawal symptoms, cessation aids are more effective in men[34]. This may be due to differences in metabolism and hormonal cycles but is also a product of preclinical and clinical research excluding female participants[35].

Mental disorders

As of 2018, those diagnosed with a mental health disorder were almost 2x more likely to smoke[4]. Schizophrenia and bipolar disorder have particularly high rates of smoking, with an estimated 70-85% of patients diagnosed with schizophrenia reporting smoking and about 50-70% of patients with bipolar disorder[4]. The link between these mental states and smoking is still under investigation[36], although some researchers have identified a link between the decreased functional connectivity of the anterior cingulate cortex and limbic system as being a risk for schizophrenia and nicotine addiction[37]. Other mental disorders with higher levels of smoking include anxiety, depression, and addiction to other substances[4]. There is evidence that smoking regulates some of the psychological symptoms of these disorders, including concentration, mood, and stress[4], but the degree to which individual self-medicate nicotine to relieve mental health symptoms is still actively debated[38]. Nicotine enhances serotonin, norepinephrine, and reduces MAO (enzyme that breaks down dopamine and norepinephrine in the synapse), which is a common goal of many anti-

depressants[39]. Those with a mental health disorder have a harder time quitting than the general public[4], although they show no difference in desire to quit[40]. Of note, smoking cessation improves mental health in the long term with these conditions, stressing the importance of continued research and outreach to help this population of smokers successfully quit[41]. Current research is trying to identify the genetic markers for susceptibility to nicotine addiction and mental disorders, which may lead to more effective individualized treatment options.

Pregnant smokers

The number of pregnant smokers has been steadily declining since 2016[42]. As of 2021, about 4.6% of mothers smoked during pregnancy (~168,000 women)[42]. The adverse health outcomes for newborns with mothers that smoke during pregnancy include low birth weight, premature delivery, restricted head growth, placental dysfunction, higher still births and miscarriages, poor lung function, chronic wheezing, asthma, and visual deformations[4].

Secondhand and thirdhand smoke

Secondhand smoke (environmental exposure of cigarette smoke to non-smokers) and thirdhand smoke (exposure to tobacco chemical residue from surfaces exposed to cigarette smoke) are known to pose risk of disease to non-smokers[4]. An estimated >53,000 deaths/year are attributed to secondhand smoke[4]. Adolescents exposed to secondhand smoke increases risk for lung cancer, asthma, and nicotine addiction[4]. There is still active research into the negative consequences of injected chemicals from thirdhand smoke.

Addiction cycle in an average smoker

The road to nicotine addiction is not the same across all smokers, but there are commonalities in the cycle, as illustrated in Fig. 1. The cycle begins with acute exposure to nicotine. When cigarette smoke is initially inhaled, there are immediate actions of nicotine in the peripheral and central nervous systems. The next part of the cycle comes from chronic nicotine use. The reinforcing effects of acute nicotine, along with conditioned pairing of those reinforcing effects with certain cues, may lead casual smokers to transition to more chronic, continual use. About 2/3 of casual smokers will transition to continual, chronic use.

1. THE "HIGH"
    - Inhaled nicotine has a stimulant effect by acting on the nicotinic acetylcholine receptors (nAChRs) on chromaffin cells in the adrenal glands causing epinephrine release[5].
    - Epinephrine leads to vasoconstriction, increased blood pressure, heightened respiration, elevated heart rate, and increased blood sugar[5].
2. POSITIVE REINFORCEMENT
    - Inhaled cigarette smoke is efficient at delivering nicotine to the brain, skipping intestinal and hepatic metabolism. With rapid absorption into the bloodstream, nicotine reaches peak concentration in the brain within 10 seconds, being as effective as direct intravenous infusion[4,43].
    - Within the brain, nicotine facilitates release of dopamine, serotonin, norepinephrine, acetylcholine, vasopressin, beta-endorphins and adrenocorticotropic hormone primarily through nAChRs activation, leading to euphoric and addictive effects[44].
    - Nicotine temporarily boosts cognition, including attention and memory[45].

3. DEPENDENCE

- Nicotine is rapidly metabolized, and the acute effects quickly dissipate, along with the feelings of reward. Nicotine's half-life in systemic circulation is about 1-3 hours and its main byproduct, cotinine (metabolized by cytochrome P450 26A) is 15-20 hours[5]. Smokers with a faster nicotine metabolism tend to be heavier smokers and are less likely to quit[5].
- A regular smoker receives ~1-2mg of nicotine per cigarette. A typical smoker takes 10 puffs on a cigarette over 5-minutes. For a pack of 20 cigarettes this leads to about 200 "hits" [4].
- Smoking allows for precise nicotine titration, making it almost impossible to overdose[4,5]. High doses of nicotine produce aversive effects[7,46]. Those with a negative experience associated with nicotine consumption are less likely to develop dependence[47].
- Smokers develop conditioned associations (moods, situations, and environmental factors) with the rewarding effects of smoking[5]. These become cues that trigger craving[48]. This can include feel, smell, and sight of cigarettes or the ritual of obtaining, handling, lighting and smoking the cigarette[48]. Environmental cues can also include situations – such as smoking after a meal, with coffee or alcohol or with a specific person[48].
- Repeated exposure changes sensitivity and tolerance to nicotine, through desensitization and upregulation of nAChRs, adjusting the body to nicotine consumption[5].

4. NEGATIVE REINFORCEMENT

- Smokers continually dose nicotine to maintain pleasurable effects and avoid withdrawal symptoms[5].
- During periods of abstinence, such as sleep, smokers no longer have saturation of their nAChRs[5]. The first cigarette after abstinence is often described by smokers as the most pleasurable[49]. The lack of nicotinic stimulation and the learned cues associated with smoking contribute to increased craving and smoking compulsivity[5].
- Without nicotine consumption, symptoms of irritability, craving, depression, anxiety, impaired attention, sleep disturbances, and increased appetite occur[5].
- Typically, peak withdrawal symptoms occur within the first few days and subside within a few weeks[4]. However, symptoms may persist for many months, and severity is based on variety of factors such as genetics and cessation-aids[4].

5. RELAPSE

- After a period of cessation, escalation of nicotine intake to mitigate withdrawal symptoms, acquire euphoric effects, or in response to conditioned cues may occur[5].
- While many smokers wish to quit, those who successfully abstain are low, about 7% of smokers abstain for one year[50].
- Most smokers will require multiple relapse cycles before permanently quitting[10].

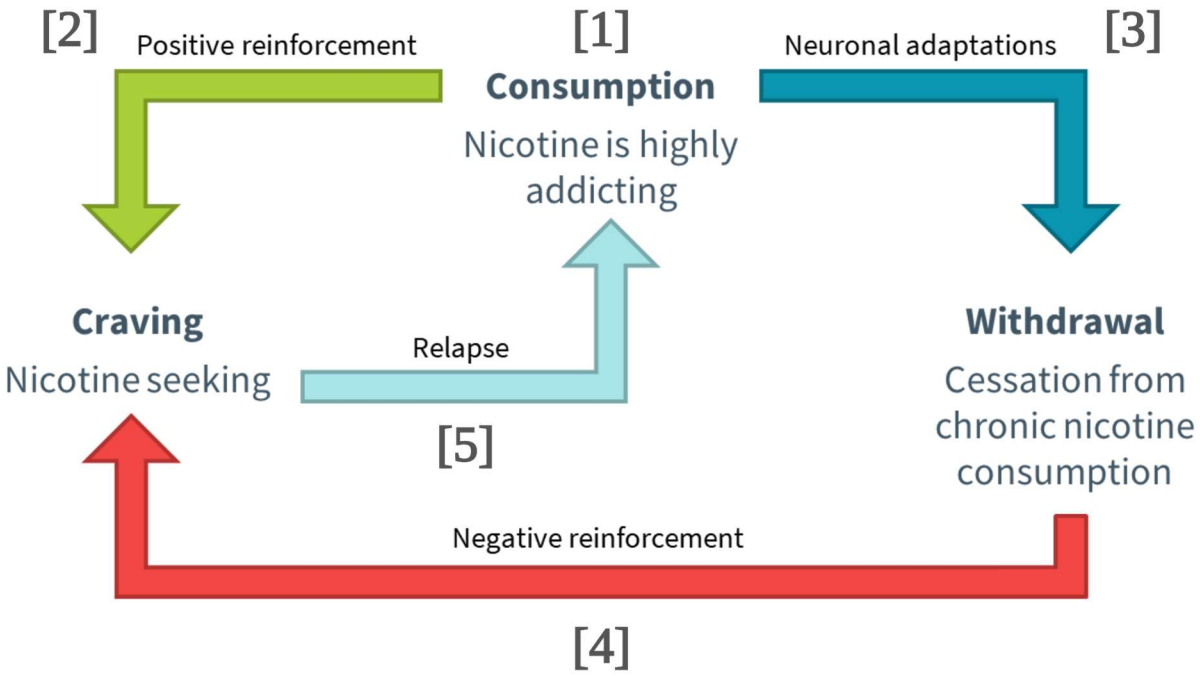

Figure 1. Nicotine addiction is a chronically relapsing disorder

If initial experimentation or infrequent use of nicotine has positive reinforcing effects within an individual, this leads to continued, chronic use. Nicotine mediated changes in neural circuitry leads to aversive effects upon cessation of use. The negative reinforcement from withdrawal combined with the positive reinforcement from nicotine consumption leads to relapse. SOURCE: Author

Dopamine dynamics in nicotine withdrawal

Nicotine addiction is described as chronically, relapsing disorder of compulsive drug-seeking behavior despite negative consequences[48,51], as seen in Fig. 1. A primary mechanism underlying addiction to nicotine and other drugs is the activation of the mesolimbic pathway and release of the neuromodulator, dopamine (DA)[48,52-55]. While the precise role of DA has been debated over the years, we know it plays a key role in addiction, including aspects such as motivation, reward, aversion, and reinforcement[51,56-59]. Nicotine consumption activates the mesolimbic DA circuitry, leading to a surge of DA release from the ventral tegmental area (VTA) projections to the nucleus accumbens (NAc)[60-62]. This connection is required for nicotine self-administration and enhanced locomotor behaviors[63-66]. Chronic nicotine exposure leads to upregulation of nAChRs, notably the high affinity α4β2 receptors[67-70]. Additionally, tonic levels of DA release within the NAc, as measured by microdialysis, produce a hypodopaminergic state during withdrawal that can vary in severity, depending on length of dependence and days of withdrawal[71-75]. Consequently, this DA dysregulation raises reward thresholds contributing to depression-like symptoms, heightened sensitivity to unpleasant stimuli and increased irritability[76-78]. Relief from these symptoms is a driver of nicotine relapse, as the individual attempts to normalize DA levels and correct their affect and behavior[17,45,48,79,80]. Although the precise neural mechanisms underlying nicotine withdrawal are not fully understood, research has identified several brain regions that may play a key role driving DA dysregulation.

Laterodorsal tegmental nucleus in reward and addiction

One such region is the laterodorsal tegmental nucleus (LDTg), a brainstem structure that modulates reward processing and motivation via GABA, glutamate, and acetylcholine projections

to the mesolimbic DA system[81-90]. Cell phenotypic studies reveal the LDTg to be very heterogeneous with approximately 40-46% GABAergic, 22% cholinergic, and 31-38% glutamatergic[81,89]. In recent years, the LDTg has been a subject of addiction related research. Studies have shown the LDTg is activated under rewarding concentrations of nicotine in slice electrophysiology and LDTg lesion dampens nicotine locomotor effects[91,92]. Selective ablation or pharmacological blockade of cholinergic neurons decreases cocaine self-administration, CPP and reinstatement[93-95]. These addiction related behaviors are partially mediated through the LDTg functional synaptic connections onto VTA DA neurons that project to the NAc[96-101]. LDTg neurons regulate the VTA through many differential circuits. Electrical stimulation of LDTg evokes both excitatory and inhibitory responses within VTA[102], and DA release in the NAc through glutamatergic and cholinergic receptors[103,104]. Cholinergic and glutamatergic drive from the LDTg to the VTA has been shown to be critical regulating tonic DA neuron population activity and in gating the transition of DA neurons to burst activity, a firing pattern necessary for several measures of behavioral reinforcement[83,105-108]. These LDTg excitatory projections elicit place preference, self-stimulation, and reinforces operant behaviors[87,88,102,103,109]. There is a connectivity bias for LDTg glutamatergic neurons to synapse on DA over non-DA neurons[110]. There are also some direct connections from LDTg to NAc that promote DA release, place preference and motivation to work for reward[86,111].

Additionally, LDTg inhibitory GABAergic neurons project to the VTA and NAc[84,86]. LDTg GABAergic neurons are activated along with glutamatergic neurons in response to nicotine[91]. The precise role of the LDTg GABAergic neurons and their projections to VTA remains unclear. LDTg GABAergic neurons have been shown to influence both VTA GABAergic and VTA DAergic neurons [84,112]. As with most non-local GABAergic neurons, LDTg GABA neurons

show a connectivity bias for VTA GABAergic neurons over VTA-DA neurons[110]. Many non-local GABAergic inputs disinhibit DA neurons by suppressing activity of local GABAergic interneurons[66,113,114]. However, recent research reveals more complex connections between the LDTg and the VTA, observing LDTg GABAergic neurons directly inhibiting VTA DA neurons to attenuate reward or promote aversion[84,115]. It is likely there are region-specific circuits, with projections to lateral and medial VTA having separate and distinct pathways[84,116]. While the LDTg is an important regulator of VTA DA neurons, the role of the LDTg in nicotine withdrawal and the associated aversive state is unknown.

The interpeduncular nucleus is a main driver of nicotine withdrawal aversion

We hypothesize that during nicotine withdrawal, there is enhanced inhibitory drive to the LDTg to suppress DA output from the VTA to the NAc, as seen in Figure 2. Our focus is on the interpeduncular nucleus (IPN), a midbrain GABAergic nucleus, that mediates the cognitive and behavioral processes of aversion and addiction[117-120]. Withdrawal from chronic nicotine activates the IPN through recruitment of excitatory inputs from the medial habenula (MHb), and this activation is associated with both somatic and affective withdrawal symptoms[14,118-124]. There is upregulation of low affinity nAChRs in this area after chronic nicotine exposure, specifically those located on chromosome 15 containing the α5, α3, and β4 subunits[121,125-128]. This is of particular interest because these receptors are part of a genetic cluster identified to be a risk factor for heavy smoking and relapse[128,129]. Of note, these receptors are not targeted in current therapeutics, such as the standard of care drug, varenicline, a partial agonist of the α4β2 receptors[130].

Despite the evidence implicating the IPN in nicotine withdrawal, the impact of IPN activation on LDTg during the withdrawal state is currently unknown. Recent studies have

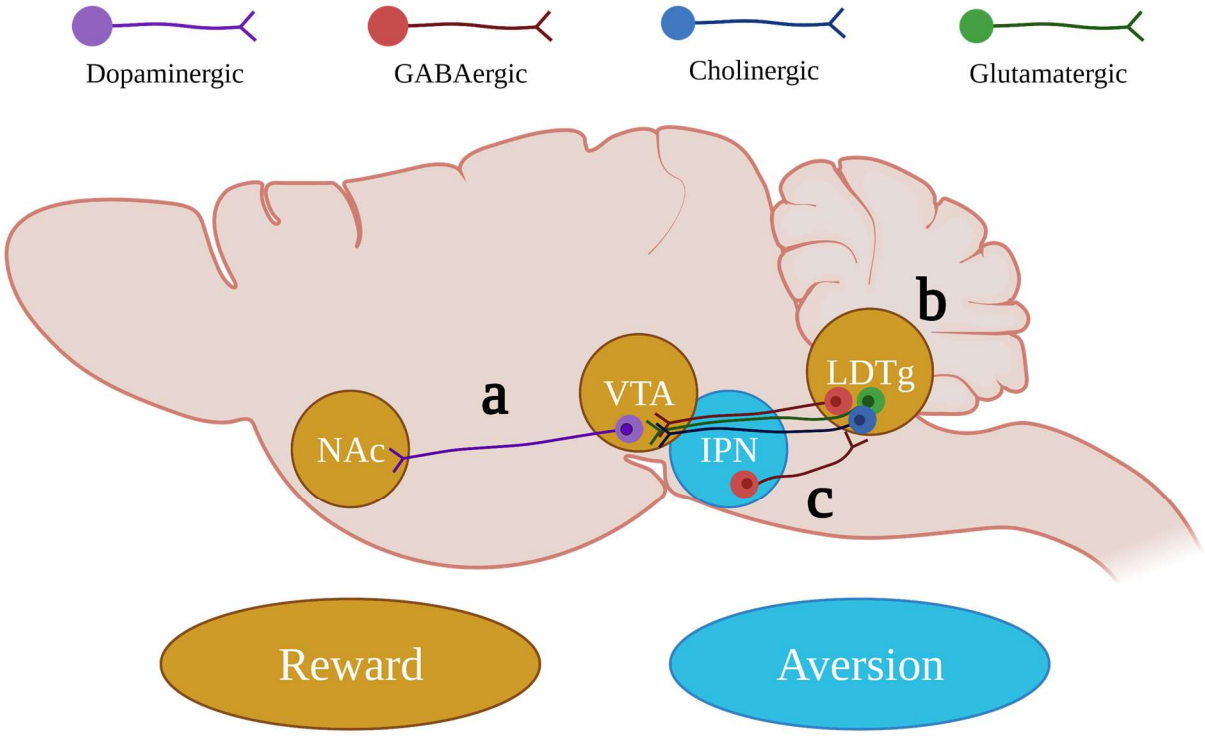

Figure 2. Proposed neural circuitry involved in nicotine withdrawal

During nicotine withdrawal, there are many areas that are responsible for the aversive somatic and affective symptoms. **a.** Mesolimbic dopamine system contains DA neurons that project from the VTA to the NAc. Chronic nicotine hijacks the dopamine reward system, increasing dopamine release on nicotine intake and depleting dopamine during cessation of use. **b.** LDTg projects GABAergic, cholinergic, and glutamatergic neurons to the VTA to modulate dopamine neuron firing and release. The precise role of the LDTg in nicotine addiction is still unclear. **c.** The IPN is a GABAergic nucleus that becomes highly activate during nicotine withdrawal and mediates the somatic and affective aversive symptoms including, anxiety and anhedonia. SOURCE: Author, image made with BioRender

implicated IPN projections to the LDTg in the aversive effects of high nicotine doses[46,117,131-134]. While low doses of nicotine are highly reinforcing, higher concentrations of nicotine lead to highly aversive effects[46,135]. Although high doses of nicotine and nicotine withdrawal are two very different aversive physiological and behavioral states, both are known to activate the MHb-IPN pathway [119,121,136]. We previously reported GABAergic projections from the IPN to the LDTg contributed to the aversive state underlying acute high dose nicotine aversion, and that blocking these projections blocks nicotine conditioned place aversion[46]. We reason that IPN inhibition of excitatory LDTg neurons during nicotine withdrawal may contribute to the hypodopaminergic conditions in the NAc. The LDTg may be the link between IPN activation under nicotine withdrawal and suppression of VTA DA output.

Outlook on current treatments of nicotine addiction

Developing effective treatment strategies for tobacco cessation is extremely important for public health. While around 70% of smokers wish to quit, about 80% will relapse within the first month[130]. Studies suggest less than 10% remain abstinent for 6 months and only about 3% obtain long term abstinence for over one year[130]. FDA approved treatments for tobacco use disorder include a variety of pharmaco- and behavioral therapies, and in more recent years transcranial magnetic stimulation (TMS)[137]. During WWII, the cytisus plant was smoked by soldiers as a tobacco substitute and later cytisine was extracted and developed as smoking cessation aid[130]. Cytisine is a partial agonist of the α4β2 nAChR and while it proved moderately effective as a cessation aid, it has poor absorption, permeability to blood-brain barrier, and severe side effects including cold/flu symptoms, heavy nausea and vomiting, and sleep disorders[130]. However, the discovery of its role in smoking cessation led to the development of varenicline, a partial agonist

of the α4β2 nAChR, with a similar chemical structure to cytisine. In addition to being safe to use, varenicline boosts smoking cessation outcomes including decreased ventral striatal and orbitofrontal cortex activation by smoking cues, attenuated withdrawal, and reduced cravings[130].

While varenicline has been shown to be the most effective pharmacotherapeutic intervention for tobacco cessation, both bupropion and nicotine replacement therapies (NRT) improve cessation outcomes compared to no treatment[137]. Bupropion works as a norepinephrine-DA reuptake inhibitor (NDRI) and as a non-specific nAChR antagonist[137]. While there are reports of bupropion decreasing craving, there is some contradictory evidence if bupropion has any effect on withdrawal symptoms[138]. Bupropion has increased effectiveness in populations of depressed smokers due to its anti-depressive effects[139]. NRT releases nicotine into the body without the additives of combustible nicotine products. Outcomes may improve by combining multiple NRT types, combining NRT with other pharmacotherapies, or by combining pharmacotherapies with behavioral therapies[137,140]. Advances in precision medicine may help determine the best treatment for an individual, considering their motivation to quit, environmental and genetic factors[141,142].

While there are several therapeutic measures to combat tobacco use disorder, the first line treatments still show abstinence rates < 30% at 6 months and these rates are even worse after one year. Part of this relapse cycle is the aversive effects associated with nicotine withdrawal, which are not effectively diminished with current treatments[143,144]. As with other medication for tobacco dependence, nAChRs remain targets of interest to combat this disorder. Exploring areas with high densities of nAChRs containing the α5, α3, and β4 subunits, such as the IPN, could inform further drug development that better combat nicotine withdrawal symptoms.

a. MEDICATION				
	Drug target	**Quit Rate (6 mo.)**	**Notes**	**Ref**
Varenicline	α4β2 nAChR partial agonist	~18-26%	> dampens rewarding effects of inhaled nicotine (partial agonist) > reduces withdrawal symptoms	130,140
Bupropion	NDRI & nAChR antagonist	~10-19%	> dampens rewarding effects of inhaled nicotine (antagonism) > combats dopamine depletion	138,139
NRT	nAChRs agonist	~6-17%	> Types: patch, spray, gum, lozenges, inhaler > Difference in onset and peak level	137,145
b. BEHAVIORAL				
		Quit Rate (6 mo.)	**Description**	**Ref**
Cognitive Behavioral Therapy		~8-10%	> relapse-prevention skills > coping strategies to triggers	142,146
Motivational Interviewing		~14-20%	> counseling to enhance motivation > patient focused, non-confrontational, self-efficacy and optimism	142,146
Telephone/ Web-based support		~7-14%	> help lines with counselor providing information and support > online, accessible, emotional support, community	142,146
c. OTHER				
	Regions	**Quit Rate (6 mo.)**	**Notes**	**Ref**
TMS	Deep insula/ prefrontal cortex	Ongoing studies	> low access due to limited number of sites, equipment, personnel, and cost > need for further studies to determine efficacy on cessation outcomes	137,142

Table 2. FDA-approved therapeutic options for tobacco use disorder

a. The FDA has approved the use of pharmacotherapies including varenicline, bupropion and NRT. All of these treatments have quit rates under 30% after 6 months and there is a drop off of efficacy as cessation time increases. **b.** Behavioral therapies are effective treatment strategies, and their efficacy increases when combined with medication. **c.** TMS within the insula/prefrontal cortex has been approved to treat several diseases including smoking cessation.

Aims of this thesis: Critical gaps in knowledge that will be addressed

Previous studies have analyzed the relationship between nicotine withdrawal and VTA DA dysregulation, while others have investigated IPN activity. The LDTg is uniquely positioned between the IPN and the VTA, however, no studies have explored the role of the LDTg in nicotine withdrawal. The aim of this thesis is to assess how the LDTg is related to the activity in the IPN and DA release within the NAc during nicotine withdrawal.

Aim 1: Investigate the role of IPN-LDTg connections in aversive nicotine withdrawal behavior. Relieving nicotine withdrawal symptoms may help improve cessation rates. We hypothesize that inhibiting the connection from the IPN-LDTg will alleviate nicotine withdrawal symptoms. The purpose of this aim is to test the necessity of IPN-LDTg projections in the maintenance of an aversive nicotine withdrawal state.

Aim 2: Investigate the correspondence between LDTg activity and NAc DA release in response to salient stimuli during nicotine dependence and withdrawal. Nicotine withdrawal alters the processing of salient stimuli, and the effects of these stimuli on LDTg activity under baseline and withdrawal conditions are unknown. The purpose of this aim is to measure LDTg activity in comparison to NAc DA release under a withdrawal context.

Aim 3: Identify postsynaptic LDTg cell types contacted by IPN GABAergic projections. Nicotine withdrawal is complex partly due to the many cell types present in the brain and their region-specific connections. The LDTg has 3 major cell types – GABAergic, cholinergic, and glutamatergic. These cell types play different roles in control of DA release. The purpose of this aim is to identify the major cell types receiving withdrawal signals from IPN.

MATERIALS AND METHODS

Animals

All experiments were done in compliance with the animal care guidelines set forth by the National Institutes of Health and were approved by the University of Chicago's Institutional Animal Care and Use Committee. Adult male and female mice were balanced across experimental conditions and the sexes were combined for analysis (>8weeks old, no significant sex differences observed). Mice were group housed in a colony room on a standard light-dark cycle (6AM – 6PM). The following mouse strains (C57BL/6J background, backcrossed for at least 10 generations) were used: C57BL/6J (JAX stock number: 000664), Gad2-IRES-Cre (JAX stock number: 028867), Vglut2-IRES-Cre (JAX stock number: 028863), and ChAT-IRES-Cre (JAX stock number: 006410). Water and standard chow were available ad libitum, and cages were changed twice/week. Experiments were conducted during the day, during the animal's light period.

Nicotine administration

Chronic tartrate or nicotine-tartrate (200μg/ml, free base) solution was administered orally (pH 6.5-7.0) for >4-weeks via drinking water with 2% saccharin sweetener added for palatability [147]. Body weight was measured twice a week for the duration of the experiment to monitor change in weight. A threshold of >20% weight loss was set as an exclusion criterion, and no mice were excluded due to excessive weight loss (Fig. 3B). Forced nicotine drinking at this concentration for 4 weeks generates serum cotinine levels of 150-300 ng ml−1 (Fig. 3A), which is similar to those observed in heavy smokers [148,149]. This treatment paradigm results in nicotine withdrawal behaviors following cessation of nicotine drinking or mecamylamine administration (2 mg/kg)[150].

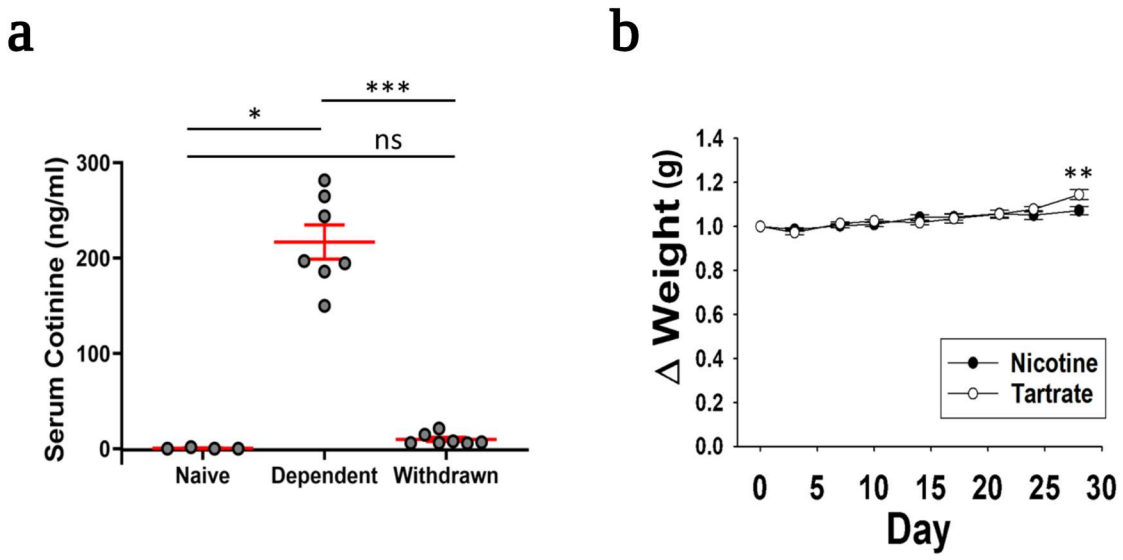

Figure 3. Nicotine drinking for 4-weeks

Mice underwent 4-weeks of forced nicotine (200µg/ml) drinking. **a.** Serum cotinine levels were measured by ELISA in mice that drank tartrate water (nicotine naïve), mice that drank nicotine water for 4-weeks (nicotine dependent), and mice that had nicotine water removed for 24 hours at the end of the 4 weeks. **b.** Change in weight from baseline on day 1 was tracked across the drinking experiments. SOURCE: Author

Drugs and reagents

For nicotine drinking, (-)-nicotine hydrogen tartrate salt (Glentham Life Sciences) or L-(+)-tartaric acid (Sigma-Aldrich) was used in combination with saccharin sodium salt hydrate (Acros Organics, 99+% purity). For precipitated withdrawal, mecamylamine hydrochloride (Abcam) was used. Additional reagents used were S-(-)-eticopride hydrochloride (Sigma-Aldrich), MK0677 (Tocris), sucrose (Sigma-Aldrich), quinine hydrochloride dihydrate (Sigma-Aldrich).

ELISA cotinine assay

In a subset of animals, serum cotinine levels were measured using an ELISA kit from Calbiotech (Lot #: CO096D-100). After experimentation (5 weeks of drinking water), mice were taken under three different contexts, 1) nicotine naïve remained on tartrate water, 2) nicotine dependent remained on nicotine water, and 3) nicotine withdrawn replaced nicotine with tartrate water for 24 hours. Using a 23ga needle, 150-300µl of cardiac blood was collected from the left atrium. Syringe with cardiac blood was removed and replaced with perfusion tubing for perfusion as described below. Cardiac blood was transferred to a polypropylene tube and rested at room temperature for 20-minutes. Blood was centrifuged for 10-minutes at 3000rpm in 4°C. Clear serum was extracted and aliquoted into vials stored at -80°C.

Samples were diluted to 1:3 concentration in PBS and were run in duplicate according to the kit instructions. Absorbances were read on a microplate reader (BioTek Epoch) at 450nm within 15-minutes of the Stop Solution. Six standards (0, 5, 10, 25, 50, 100 ng/ml cotinine) were included in duplicate to generate a standard curve (absorbance vs. concentration) and unknown cotinine concentrations were calculated from standard curve equation.

Surgical procedures

One week after initiation of nicotine drinking, mice undergo surgery, and then are given 3-week recovery and viral expression time before experimentation. Stereotaxic surgeries were performed under 1% isoflurane anesthesia.

For all nicotine withdrawal somatic and affective withdrawal behavioral experiments viral vectors expressing AAV5.Ef1a.DIO.eNpHR3.0-EYFP or AAV5.Ef1a.DIO-EYFP (500nL, infusion rate 150nL/min) were injected into IPN (AP: -3.5mm, ML: 0.9mm, DV: -4.8mm from Bregma at 10° angle) of Gad2-cre mice with an optical fiber (200μm) placed 0.2mm above the LDTg (AP: -5.0mm, ML: 1.8mm, DV: -3.3mm from Bregma at 20° angle).

For fiber photometry experiments: AAV9.Syn.GCaMP6s.WPRE.SV40 (500nL, infusion rate 100nL/min) was injected into the LDTg (AP: -5.0mm, ML: 1.8mm, DV: -3.5mm from Bregma at 20° angle) or AAV9.hSyn.GRAB_DA1h (500nL, infusion rate 100nL/min) was injected in the NAc lateral shell (AP: 1.0mm, ML: 2.0mm, DV: -4.3mm from Bregma). An optical fiber (400μm) was placed 0.2mm above the targets. Viruses were obtained from Addgene (stock #s: 26966, 27056, 100843, 113050, respectively). To ensure a tight connection, all headcaps contained two skull screws and were secured using dental acrylic (Lang Dental Mfg. Co., Jet Denture Repair Powder and Jet Liquid).

For rabies transsynaptic tracing, AAV8.hSyn.FLEX.TVA.P2A.eFGP.2A.oG (400nL, 100nL/min) was injected into the LDTg (AP: -5.0mm, ML: 1.8mm, DV: -3.5mm from Bregma at 20° angle) of Gad2-Cre, ChAT-Cre and Vglut2-Cre mice. Subsequently, 14 days after helper virus injection, EnVA G-deleted Rabies-mcherry (200nL, 100nL/min) was injected into the LDTg at the same coordinates. Viruses were obtained from Salk Institute for Biological Studies.

Slice preparation

Brain slices were obtained using a neuroprotective recovery method as previously described[46]. Mice were rapidly decapitated following anesthesia with isoflurane. Brains were dissected in a solution of ice-cold protective artificial cerebrospinal fluid (aCSF) including (in mM): 92 N-methyl-D-glucamine, 2.5 KCl, 1.25 NaH2PO4, 30 NaHCO3, 20 HEPES, 25 glucose, 12 N-acetyl cysteine, 2 thiourea, 5 Na-ascorbate, 3 Na-pyruvate, 0.5 CaCl2·4H2O, and 10 MgSO4·7H2O, pH adjusted to 7.3–7.4 with HCl and then bubbled continuously with 95% O2–5% CO2. 250-μm-thick IPN coronal slices were cut with a vibratome (VT100S, Leica) and incubated in a holding chamber at 32–34 °C for ≤15–20 min in the same protective aCSF. Slices were then transferred to a holding chamber containing room temperature aCSF including (in mM): 119 NaCl, 2.5 KCl, 1.25 NaH2PO4, 26 NaHCO3, 20 HEPES, 12.5 glucose, 5 N-acetyl cysteine, 2 thiourea, 5 Na-ascorbate, 3 Na-pyruvate, 2 CaCl2·4H2O and 2 MgSO4·7H2O, bubbled continuously with 95% O2–5% CO2 and perfused at a rate of 20 ml min−1 for at least 30 min before recording.

Slice recording

Recording chambers were superfused (~2 ml min^{-1}) with room temperature aCSF (in mM, 125 NaCl, 25 NaHCO3, 20 glucose, 2.5 KCl, 2.5 CaCl2, 1 MgCl2, 1 NaH2PO4, at pH 7.4, saturated with 95% O2 and 5% CO2). Neurons were visualized under infrared illumination using a fixed-stage upright microscope (Axioskop, Zeiss). Data were acquired with a Multiclamp 700A/Axo-patch 200B amplifier and pCLAMP 9 software (Molecular Devices). Whole-cell patch-clamp recordings were achieved with microelectrodes (3–6 MΩ) pulled on a Flaming/Brown micropipette puller (model P-97, Sutter Instrument, Novato, CA). All electrophysiology experiments were performed on neurons in the IPN that expressed NpHR (verified by EYFP

fluorescence). Recording electrodes were filled with potassium gluconate internal solution (in mM): 154 K-Gluconate, 1 KCl, 1 EGTA, 10 HEPES, 10 Glucose, 5 ATP, 0.1 GTP, pH 7.4 with KOH). To activate light-sensitive NpHR, light was delivered through the objective at maximal power (>40 mW; 532 nm). Light evoked inhibitory currents were recorded in voltage clamp mode with 3ms stimulation. Light evoked membrane hyperpolarization was recorded in current clamp mode with prolonged 10s stimulation.

Histology

Animals were anesthetized with isoflurane and transcardially perfused with 4% paraformaldehyde. Brains were kept in paraformaldehyde for >24 h and then transferred to 30% sucrose in phosphate-buffered saline (PBS) for >24 h. Brains were frozen in embedding medium (OCT Compound, Fisher). Injection sites and optical fiber placements were confirmed in all animals by taking coronal slices (60µm) of perfused tissue using a cryostat (Leica CS3050 S). Animals with incorrect placement of either fiber optics (>200µm from target) or viral injections were excluded from analysis. Viral injection criteria for exclusion were: >10% expression outside of nucleus for optogenetic experiments and >0% starter cells within 1mm of tissue outside of LDTg at injection site for rabies transsynaptic tracing.

For optogenetic experiments, in a subset of slices (20µm), immunohistochemistry (IHC) was used to confirm cre-dependent expression of NpHR using rabbit α-GAD65+67 (1:1000, Abcam 11070) with Alexa donkey α-rabbit 647 (1:1000, Thermofisher A-31573).

For cFos experiments, slices were taken at 40µm and IHC using rabbit α-c-Fos primary antibody (1:1000, Lot # 092315) with Alexa goat α-rabbit 594 secondary antibody (1:1000, Thermofisher A-11012).

For rabies transsynaptic tracing, slices were taken at 40μm and down sampled to every other slice throughout the entire brain. IHC was performed to boost helper virus expression (GFP), rabies virus expression (mCherry), and stain for GAD67 using the following primary antibodies: rabbit α-GFP (1:2000, Abcam ab290), chicken α-mCherry (1:1000, Origene TA150127), and goat α-Gad67 (1:1000, R&D AF2086). Respectively, secondary antibodies used were: Alexa donkey α-rabbit 488 (1:2000, Thermofisher A-21206), Alexa donkey α-chicken 594 (1:1000, Thermofisher A-78951), and Alexa donkey α-goat 647 (1:1000, Thermofisher A-21447).

For all IHC, slices were washed in PBS in between the following steps, incubation in blocking solution (1% BSA, 10% NDS, and 0.1% Triton-X in PBS) for 2 hours at room temperature, in primary antibodies for 24 hours in PBS + blocking solution at 4°C, and in secondary antibodies for 2 hours at room temperature in PBS. Slices were mounted on slides (Fisherbrand, Superfrost Plus) with DAPI Fluoromount-G (Southern Biotech) and cover-slipped (Fisher Scientific). Images were taken on a 3i Marianas Spinning Disk Confocal or Olympus VS200 Slideview Research Slide Scanner.

Cell detection and fluorescent cell counts were done on QuPath software. Cell detection was done using DAPI nucleus staining, and cytoplasm estimates were determined given parameters for area (max/min), intensity threshold, and cell expansion. A Gaussian filter was applied for noise reduction. For positive cell detection with fluorescent staining, a single measurement classifier was used to detect positive nuclei or cytoplasm containing intensity levels above target threshold. For co-localization, classifiers were applied sequentially to region of interest.

Behavior

Behavioral experiments occurred after 4 weeks of chronic tartrate (nicotine naïve) or nicotine drinking (nicotine dependent), which overlaps with viral expression and recovery time from surgery.

Real-time place preference

Prior to testing, mice were handled and habituated to injections for ≥ 3 days. A 2-chambered box (each chamber 25cm x 25cm x 25cm) was used to assess place preference in a real-time assay (20-min/day). Each chamber of the boxes has different patterned walls (vertical vs. horizontal black and white stripes) and different textured floors (ribbed lines vs. patchwork). Mice were hooked up to optical fiber cord all experimental days.

Experimental groups included 1) nicotine naïve, 2) nicotine dependent and 3) MEC-precipitated withdrawal states. Within these three groups mice underwent control (EGFP) or halorhodopsin (NpHR) viral surgeries. Mice received an injection immediately preceding real-time test. *Day 1:* All mice received a saline injection (SAL). *Day 2-4:* Nicotine naïve and nicotine withdrawn mice received an injection of 2mg/kg mecamylamine (MEC). Nicotine dependent mice received a SAL injection. *Day 5:* Nicotine naive and withdrawn mice received either SAL or 2mg/kg MEC. Nicotine dependent mice received a SAL injection.

Real-time place preference test timeline: *Day 1:* This was a pretest day to assess baseline preference with the laser off. Any mice with a >70% preference for either chamber was excluded from the experiment. *Days 2-4:* In an unbiased design, mice received constant 532 nm light delivered through a DPSS laser (SLOC) and gated to turn on while in one of the two chambers controlled using Master-9 pulse stimulator. The light-paired chamber was kept consistent within

animals across the 3 days of real-time place preference and counterbalanced across animals. Power output was tested using a digital power meter (Thorlabs) and was checked before and after each experimental animal. Output during light stimulation was estimated to be 4-6 mW/mm2 at the targeted tissue 0.2 mm from the fiber tip. *Day 5:* This was a posttest day to assess conditioning of the light-paired chamber after 3 days of light-paired inhibition with a specific chamber.

Open-field and Novel Object Test

In a separate set of animals, mice were split into nicotine naïve and nicotine dependent groups with either EGFP or NpHR virus expressed. Prior to testing mice were handled and habituated to injections for ≥ 3 days. A large-chambered box (each chamber 20cm x 43cm x 43cm) was used to assess locomotion in a 20-min open field test. Immediately preceding open field test, mice were injected with 2mg/kg MEC and placed immediately in the center of the arena. Constant 532 nm light delivery occurred during the entirety of the test. After 10-minutes, a novel object was presented into the center of the chamber. Object interaction was defined when the mouse touched the object with its nose within 2cm or less.

Somatic signs and Anhedonia

In a separate set of animals, mice were split into nicotine naïve and nicotine dependent groups with either EGFP or NpHR virus expressed. Prior to testing mice were handled and habituated to injections for ≥ 3 days. One hour before experimentation, mice habituated to 2 cotton swabs affixed to the sides of the home cage. After injection of 2mg/kg MEC, mice were placed in their home cage with one swab dipped in water and one swab dipped in the urine of a mouse of the opposite sex. During the 3-min test, mice were allowed to freely explore the home cage and

sniff the two swabs with constant 532 nm light delivery. Immediately after the social odor preference assay, mice were moved to a large plexiglass box with an angled mirror underneath to assess somatic signs for 10-minutes. Time spent sniffing and somatic signs were analyzed through video analysis by a scorer blinded to experimental conditions.

Behavioral analyses

All exposures to the apparatus were recorded with a video camera and analyzed using Ethovision 11 (Noldus). For the real-time place preference test, a preference score (%time spent in light-paired chamber - %time spent in non-light paired chamber) and a change in preference (preference score on experimental day – preference score on pretest day) were calculated. Position traces were automated by Ethovision software using center-point detection of the mouse and dynamic subtraction from the background. For the open-field test, time spent and number of visits to the center zone (21cmx21cm) was automatically counted by the software. For novel object test, time spent and number of object interactions was measured by a third party blind scorer. For somatic signs, a blind scorer counted the following signs and their durations that were visible by camera (Logitech) analysis: grooming, paw licking, straub tail, shaking, rearing, backing, retropulsion, head nodding, abdominal gasps, and jumping. Some reported signs were excluded due to inability to distinguish on camera including yawning, chewing, facial fasciculations, cage scratching, ptosis, and piloerection. Individual signs were analyzed for behaviors that had >3 occurrences, otherwise signs were only included in combined analysis. Blinded scorer was trained on wild type behavioral data, previously verified by 3 separate scorers. For social odor test, a blinded scorer and a live unblinded scorer counted sniffing time. If discrepancy was >0.5s the blind score was used, otherwise, an average was taken.

Cfos

In a separate set of animals, mice were placed in a circular (ht. 23 cm, dia. 20 cm) container for 20-min with 532nm constant laser delivery. Prior to testing, mice were handled and habituated to injections for ≥ 3 days. Immediately prior to experiments, mice were given an injection of SAL or 2mg/kg MEC. Mice were separated into nicotine naïve and nicotine dependent groups with either EGFP or NpHR viral expression. After 90-minutes, mice were sacrificed and perfused in according to the methods described in the histology section.

Fiber photometry

Mice were habituated to handling, vehicle injection, and recording apparatus for ≥ 3 days prior to experimentation. Photometry recordings were performed on a rig with optical components from Doric lenses controlled by a real-time processor from Tucker Davis Technologies (TDT; RZ5P). TDT Synapse software was used for data acquisition. Two excitation wavelengths of 465nm (calcium dependent) and 405nm (isosbestic control) LEDs were modulated at 210 Hz and 330 Hz, respectively. The emitted fluorescence is recorded using a photodetector and sent to a data acquisition device via mini cube port to isolate individual signals. LED currents were adjusted to return a comparable baseline voltage in the calcium dependent and isosbestic channels, and this level was maintained within animals across experiments. Signal was collected with 8 Hz lowpass frequency filter. Behavioral timestamps were fed into the real-time processor as TTL signals for alignment with the neural data or timestamped from a camera log.

In LDTg (GCaMP6) and NAc (GRAB-DA) recordings, mice were habituated to the recording room for 1 hour. Mice were hooked up to the cable and allowed to explore the apparatus for 5-minutes. After recording started baseline signal was recorded for at least 5-minutes in freely

moving mice. Mice were injected with SAL or 2mg/kg MEC and recorded for 10-minutes. Response to novel object (10-minute test) and social odor (3-minute test) occurred on a separate day post injection of SAL or 2mg/kg MEC as described previously. New novel objects were used for SAL and MEC recordings for within-animal comparisons.

To test the specificity of GRAB-DA, a modified D2R, in the NAc some mice were injected with 1 mg/kg eticlopride, a D2R antagonist. Mice were injected after a 10-minute baseline period.

In a subset of LDTg (GCaMP6) and NAc (GRAB-DA) mice, an assortment of rewarding and aversive salient stimuli was tested including: 0.5 M sucrose, 0.003 M quinine, tail pinch, looming and air puff.

For analysis, the signal from the 405nm and 465nm channels were extracted on MATLAB software and the 405nm channel was fitted to the 465nm channel using linear regression. The fitted control was used to calculate the change in fluorescence ($\Delta F/F$) or z-score. Parameters including number of peaks, peak amplitude, peak half-width and AUC were measured from z-score.

Randomization and blinding

Mice were not selected for any experimental condition based on previous observations or tests. Cages were selected arbitrarily to receive viral injections (EGFP vs. NpHR) and drinking water (tartrate vs. nicotine). Mice were randomly assigned to behavioral boxes and light-pairing was randomized across behavioral boxes, taking care to alternate orientation of chamber (vertical vs. horizontal stripes) within the behavior room. Behavioral tests and electrophysiological data acquisition were performed by investigators with knowledge of the experimental groups. Where possible, behavioral experiments were controlled by computer systems, and data was collected and analyzed in an automated and unbiased way. For somatic signs, novel object interaction, and social

odor tests the behavior was scored by an experimenter blinded to drinking water and viral expression groups. The experimenter was trained on wild type data that was previously standardized by 3 other blinded observers. Histological verifications always took place prior to analysis of behavioral data. Experimenters were not blinded to the groups during this verification step but were blinded to the actual observed behavior of individuals and groups.

Data analysis

Data were tested for normal distribution using Shapiro-Wilk or D'Agostino & Pearson (repeated measures) tests. For data that conformed to normal distribution, student's t tests (paired and unpaired), one-way, two-way, or three-way ANOVA (normal or repeated measures) tests, and mixed effects analyses were used to determine statistical differences using GraphPad Prism 9 (GraphPad Software). Tukey's HSD or Holm-Sidak's post hoc analysis was applied when an ANOVA or mixed effects analysis showed a significant main effect or significant interaction for multiple comparisons. For non-normal distribution, Kruskal-Wallis or a Mann Whitney test was used followed by Dunn's multiple comparisons test (as needed) when analysis showed a significant main effect. A Welch's correction was done for data where equal SD could not be assumed. Statistical significance (p-value) is listed in Table 2. All data are presented as means – SEM. All details of the statistical analysis including means, SEMs, and number of animals used are summarized in Table 4 with abbreviations defined in Table 5.

RESULTS— GABAERGIC NEURONS FROM THE INTERPEDUNCULAR NUCLEUS TO THE LATERODORSAL TEGMENTAL NUCLEUS DRIVE AFFECTIVE AND SOMATIC NICOTINE WITHDRAWAL SYMPTOMS

LDTg activity attenuates during nicotine withdrawal

IPN is activated during nicotine withdrawal[121] and is known to send inhibitory projections to the LDTg[46]. However, it is currently unknown how the LDTg responds during nicotine withdrawal. To test this, we grouped housed wild type mice into cages with sipper bottles of either nicotine (200µg/ml free base) or tartrate added to the water for at least 4 weeks (Fig. 4A), sweetened with 2% saccharin for palatability. This duration and dose of nicotine increases serum cotinine levels and mice maintain a healthy weight (Fig. 3A,B) [147,149,151]. We expressed a calcium indicator (GCaMP6s) into the LDTg to record neuronal activity through a fiber optic implanted directly above the nucleus (Fig. 4B-D). We observed the activity of LDTg before and after an injection of saline (SAL) or 2mg/kg mecamylamine (MEC) in nicotine naïve and dependent mice (Fig. 4E,F). This dose of MEC has been shown to precipitate withdrawal in mice chronically exposed to nicotine[150]. In nicotine dependent mice, but not in tartrate controls, MEC injection decreased the amplitude and AUC of identified peaks without changing the peak frequency (Fig. 5A-D), within the 5-minutes post injection compared to the baseline period. This resulted in an overall suppression of activity, as seen by the averaged trace (Fig. 4f).

IPN GABAergic neurons synapse to the LDTg cell types differentially

The decrease in LDTg activity during withdrawal may be due to increased GABAergic drive to these neurons during a withdrawal state. GABAergic neurons in the IPN become active during nicotine withdrawal[121] (Fig. 6A-C) and send dense projections to the LDTg (Fig. 10G). Our

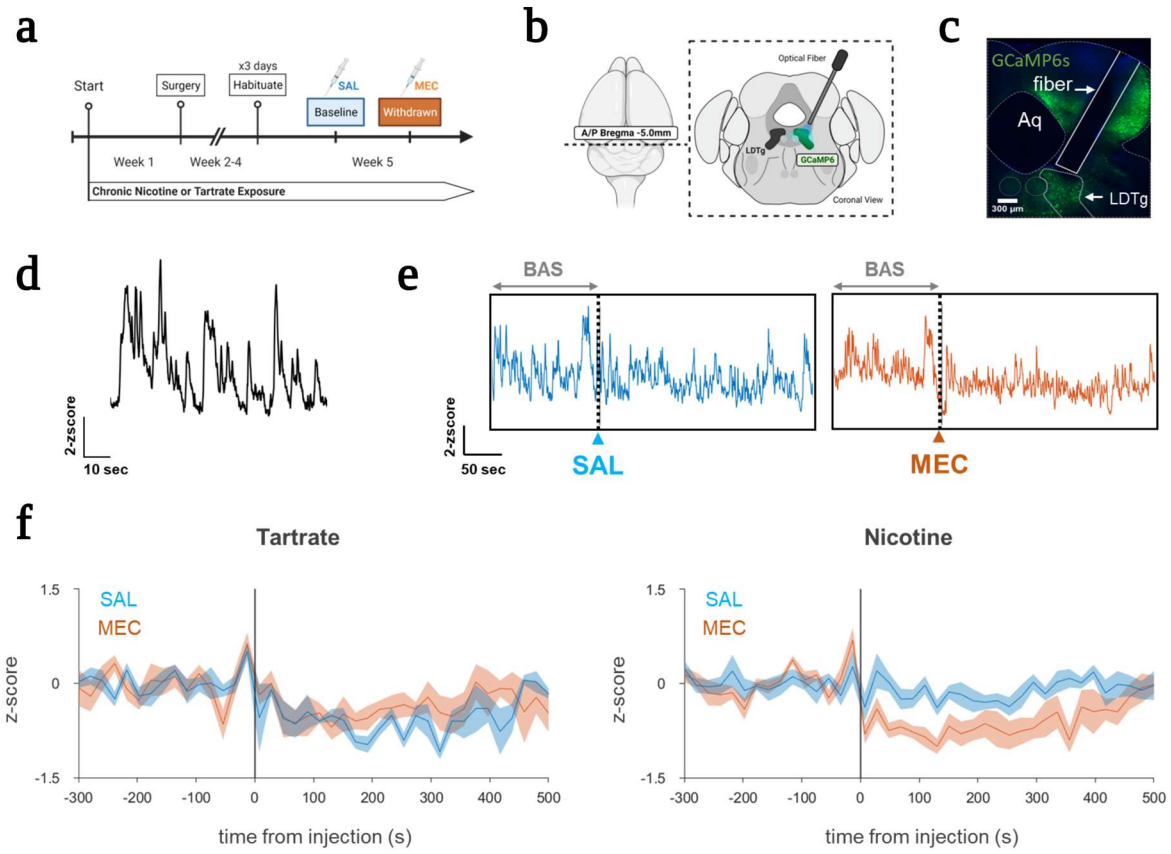

Figure 4. LDTg is spontaneously active and attenuates activity after nicotine withdrawal

a. Schematic of experimental timeline including nicotine drinking, surgery, and experimentation days. **b.** Schematic of GCaMP6s viral injection into the LDTg and fiber placed above nucleus. **c.** Representative histological verification image illustrating fiberoptic placement adjacent to the LDTg. **d.** Spontaneous GCaMP6 signal in the LDTg. **e.** Representative traces of spontaneous GCaMP6s activity in nicotine drinking mouse after an injection of SAL (control, blue) and 2mg/kg MEC (orange). Post injection peaks are compared to the baseline period (BAS) before injection. **f.** Average signal of tartrate (N=5) and nicotine (N=6) LDTg signal after SAL and MEC injections shows a decrease in signal in the nicotine + MEC (withdrawal) group. SOURCE: Author, Schematics made with BioRender

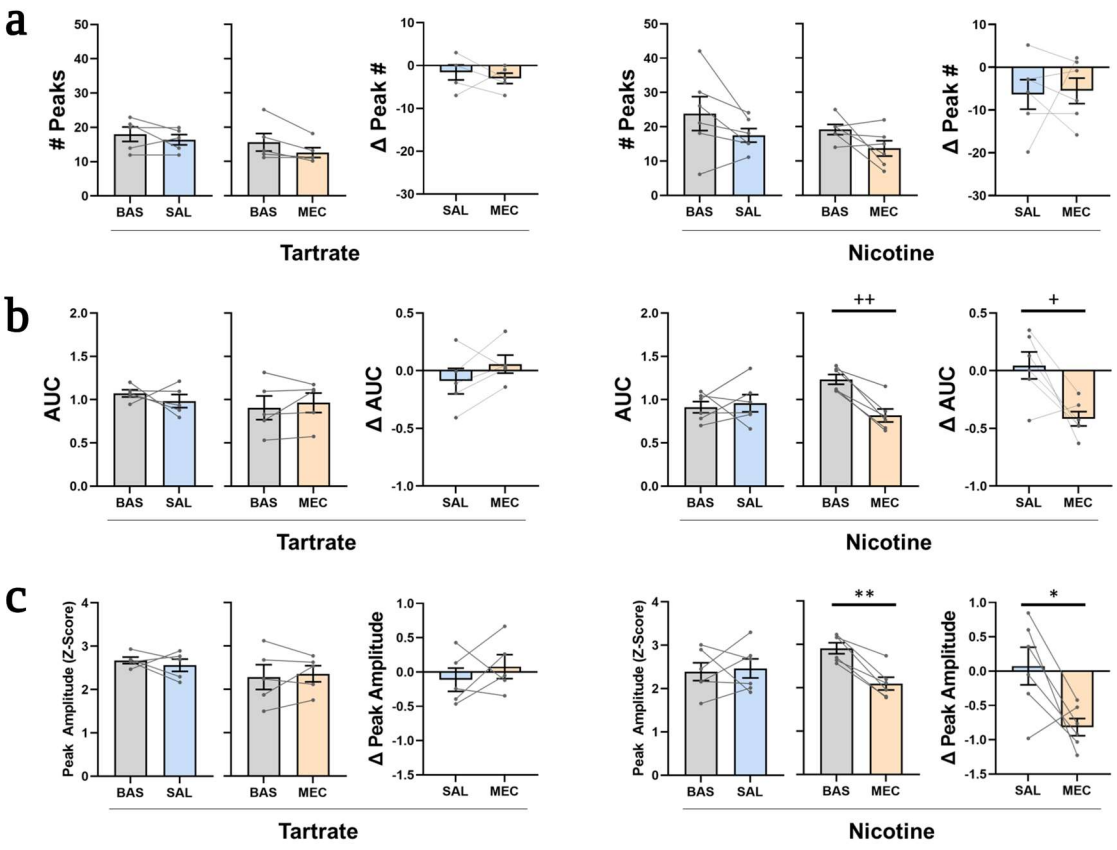

Figure 5. Mecamylamine decreases LDTg activity after chronic nicotine treatment

Measures of GCaMP6 signal in the LDTg 5-minutes post injection in comparison to the 5-minute baseline period before injection. **a.** SAL or MEC injection did not change frequency of peaks in chronic tartrate or nicotine drinking mice. **b.** MEC-precipitate nicotine withdrawal significantly decreased average AUC (in a 500ms window) of identified peaks but did not affect tartrate controls. **c.** MEC-precipitate nicotine withdrawal significantly decreased average amplitude of identified peaks but did not affect tartrate controls. SOURCE: Author

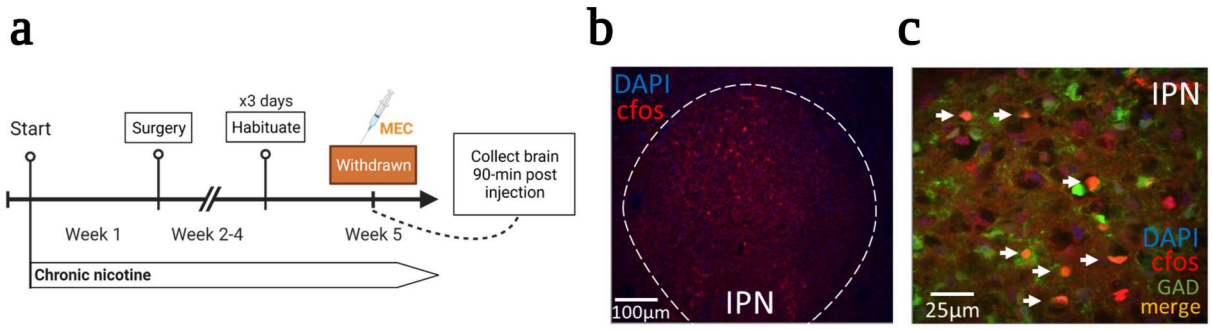

Figure 6. Nicotine withdrawal increases activity in IPN GABAergic neurons

Cfos expression increases in a nicotine withdrawal state. **a**. Schematic of nicotine drinking and withdrawal induction. 90-minutes post injection of 2mg/kg MEC, tissue was perfused and extracted for cfos staining. **b.** MEC injection in nicotine dependent mice increases IPN cfos expression. **c.** cfos activation co-localizes with cre-dependent viral expression in GAD-cre mice as indicated by the orange merged overlap (white arrows). SOURCE: Author, Schematic made with BioRender

lab previously showed that the inputs from IPN to LDTg are GABAergic using ex-vivo electrophysiology and that these connections are important in the aversive response to high acute doses of nicotine[46]. However, it is currently unknown which cell type within the LDTg the IPN is inhibiting. To determine this, we used rabies transsynaptic tracing to label monosynaptic functional GABAergic inputs from IPN to LDTg. We expressed cre-dependent helper virus in the LDTg of ChAT-cre, GAD-cre and Vglut-cre mice to target different LDTg cell types (Fig. 7A-D). The cre-driven virus expression is limited to the correct cells type as verified with IHC (Fig. 7D). Two weeks later, we introduced a g-deleted rabies virus in the same location (Fig. 7A-C). Starter cells populations were calculated as the number of cells positive for helper virus and rabies virus in the LDTg (Fig. 7C,E). Rabies positive cells that lacked staining for helper virus are indicative of LDTg local connections (Fig. 7E). Our data suggests there is a large portion (~50.8%) of LDTg rabies+ cells are local connections to GABAergic neurons within the LDTg (Fig. 7E). Monosynaptic inputs to LDTg were stained for GAD to identify subpopulation of GABAergic inputs (Fig. 8A,C). To our surprise, we found GABAergic IPN neurons project to both GABAergic and glutamatergic LDTg neurons, with a higher convergence index (input cells proportional to starter cells) than cholinergic neurons (Fig. 8). Of these populations, IPN neurons are coming primarily from IPC/IPR to GABAergic LDTg cells, from IPDM/IPDL to cholinergic LDTg cells, and from all IPN regions to glutamatertic LDTg cells (Fig 8E,F). In addition to IPN, we analyzed whole brain mapping to LDTg and our results show differential connections to GABAergic and cholinergic LDTg neurons (Fig 9). We know that nicotine withdrawal increases activity within the IPN[121] (Fig. 6A-C). This suggests that increased IPN GABAergic activity during nicotine withdrawal may contribute to the observed attenuation of LDTg activity and this inhibition occurs

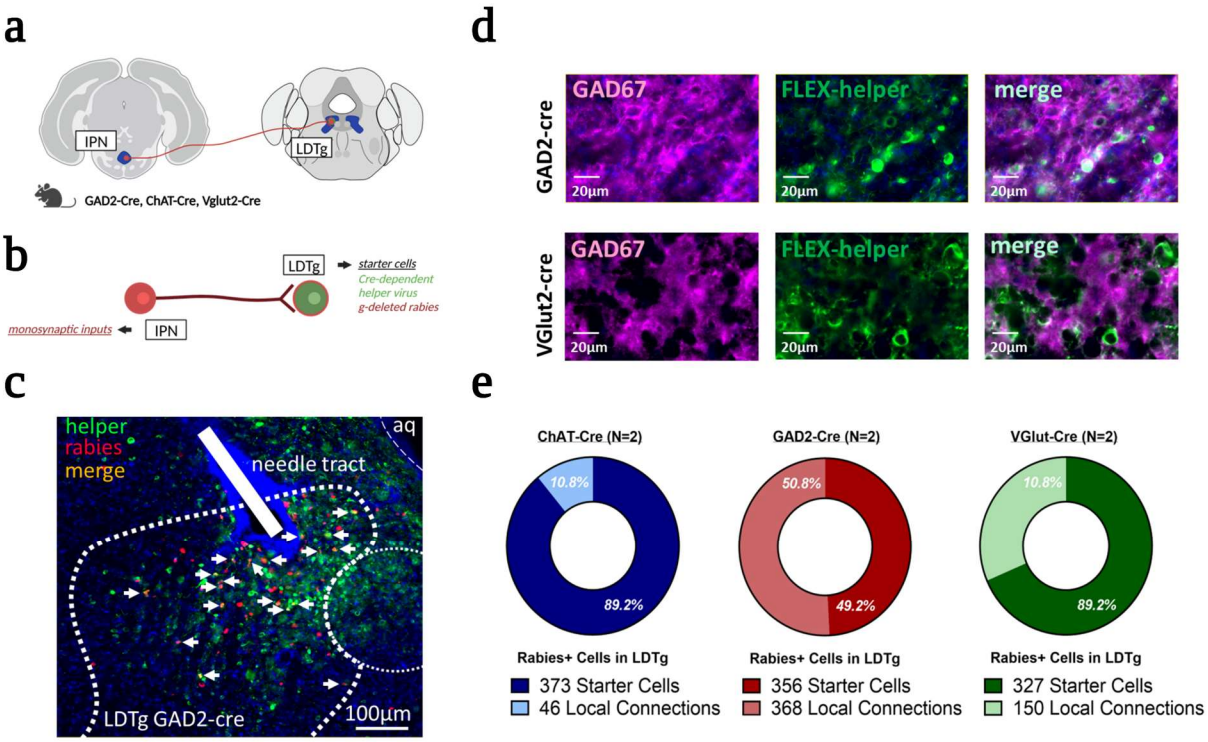

Figure 7. Starter cells in LDTg label monosynaptic inputs in a cell type specific manner

Rabies transsynaptic tracing identifies IPN cells synapsing onto LDTg neurons with cell type specificity. **a**. Schematic of circuitry targeted by rabies transsynaptic tracing experiment. **b.** A cre-dependent helper virus (GFP) is injected into the LDTg. 14-days after helper virus injection, a g-deleted rabies virus is injected into the LDTg to retrogradely label monosynaptic inputs (mCherry). **c.** Starter cell populations are identified with overlap between the helper and rabies virus contained within the LDTg (white arrows). **d.** Cre-dependent helper virus is localized within the appropriate cell type targeted by the transgenic strain. **e.** LDTg cholinergic, GABAergic and glutamatergic neurons have similar starter cell populations. GABAergic and glutamatergic LDTg neurons receive a large proportion of local circuit connections. SOURCE: Author, Schematics made with BioRender

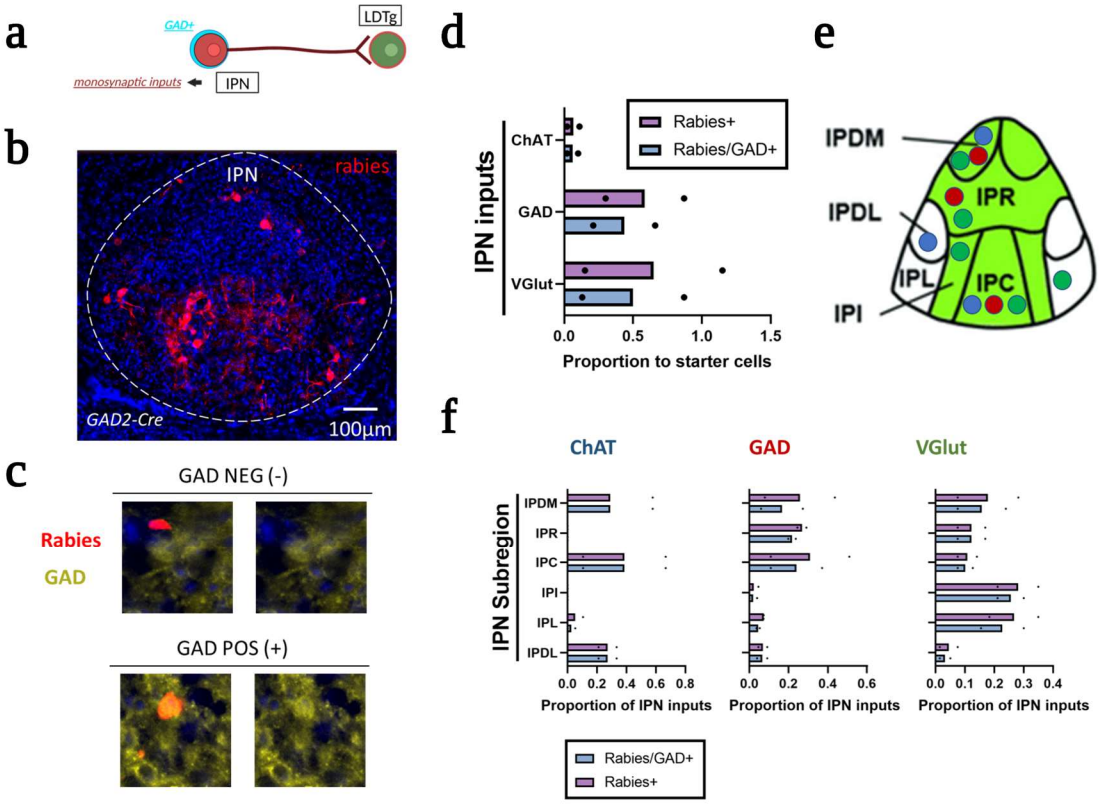

Figure 8. IPN subregions connect to different LDTg cell types

a. Schematic showing identification of monosynaptic inputs from IPN as GABAergic using the marker, GAD. **b.** Monosynaptic inputs within IPN (red) synapsing onto to GABAergic LDTg neurons **c.** Rabies back-labeled cells in IPN are identified as GAD positive or GAD negative using a secondary stain. **d.** IPN sends GABAergic projections to GABAergic and glutamatergic LDTg neurons more than cholinergic LDTg cells. **e.** IPN subregions project to different LDTg cell types (blue = LDTg cholinergic projections, red = LDTg GABAergic projections, green = glutmatergic LDTg projections). Bright green IPN regions receive ventral MHb input. **f.** GABAergic LDTg neurons receive connections primarily from central IPN regions, cholinergic LDTg neurons receive connection primarily from lateral IPN regions, and glutamatergic LDTg neurons receive central and lateral IPN inputs. SOURCE: Author, Schematics made with BioRender

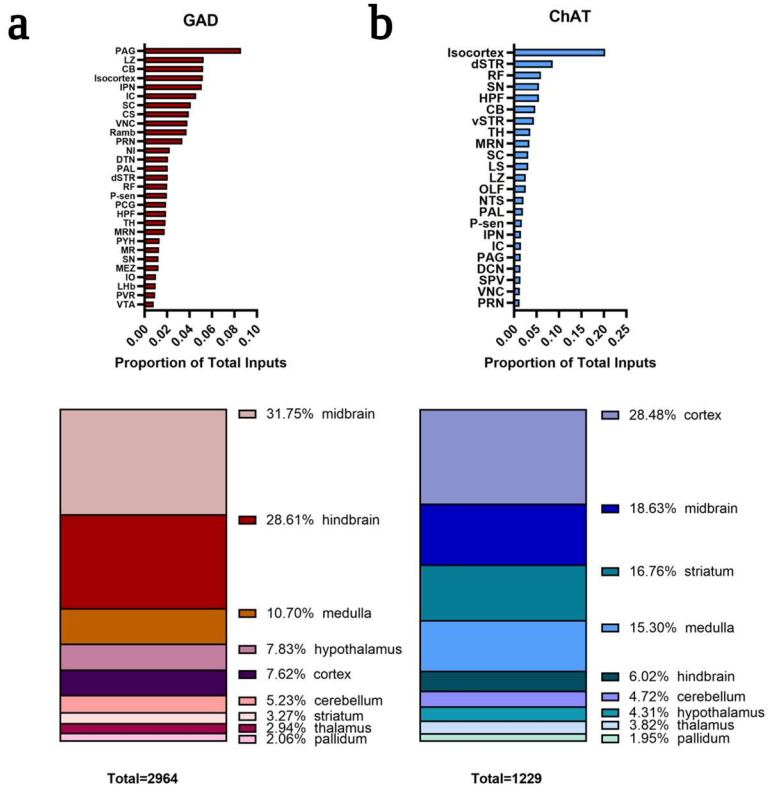

Figure 9. Whole brain inputs to LDTg GABAergic and cholinergic cells

a. GABAergic LDTg neurons receive connection from across the entire brain but largest input fractions from midbrain and hindbrain. **b.** Cholinergic LDTg neurons receive connections from across the entire brain but the largest input fractions from cortex and midbrain.
SOURCE: Author

mainly on the GABAergic LDTg neurons. We next aimed to test how blocking GABAergic inhibitory input from IPN to LDTg impact nicotine withdrawal behavior.

Blocking inhibitory inputs from IPN to LDTg is preferred in nicotine withdrawal

Our data suggests that the GABAergic drive from IPN to LDTg mediates withdrawal from chronic nicotine exposure. We hypothesized that by preventing this inhibitory transmission we can alleviate the severity of nicotine withdrawal. To test the role of the IPN to LDTg GABAergic connection in nicotine withdrawal affective behavior, we used a real-time place preference test (Fig. 12A,B). Nicotine or tartrate water was introduced to cages of GAD-Cre mice for 4 weeks (Fig. 12A). Within the IPN, either EGFP or NpHR was virally expressed in a cre-dependent manner and a fiber was placed above the LDTg for photo-inhibition of the GABAergic terminals (Fig. 10D-G). Electrophysiology was used to verify opsin function within the IPN, showing light stimulated hyperpolarization and inhibitory currents (Fig. 10A-C). After 20-minutes of photo-inhibition, cfos reveals an activation of LDTg neurons in cells surrounded by NpHR terminal expression (Fig. 11A,B), suggesting a disinhibition of LDTg. Activation of NpHR in this region does not impair locomotion under our experimental conditions (Fig. 12C). Terminal inhibition resulted in place preference only during nicotine withdrawal and not nicotine naïve or dependent conditions (Fig. 12D,E). This effect is observable over repeated testing (Fig. 13A). The real-time boxes had distinct patterned walls and textured floors (Fig. 12B). Three days of real-time testing was used as conditioning days where light inhibition was paired with a specific chamber as described[109]. During all conditioning days, the nicotine withdrawal group + NpHR inhibition maintained a preference for the light paired chamber (Fig. 13A). After the three conditioning days, a posttest day was used to observe conditioned preference to the previously light-paired chambers.

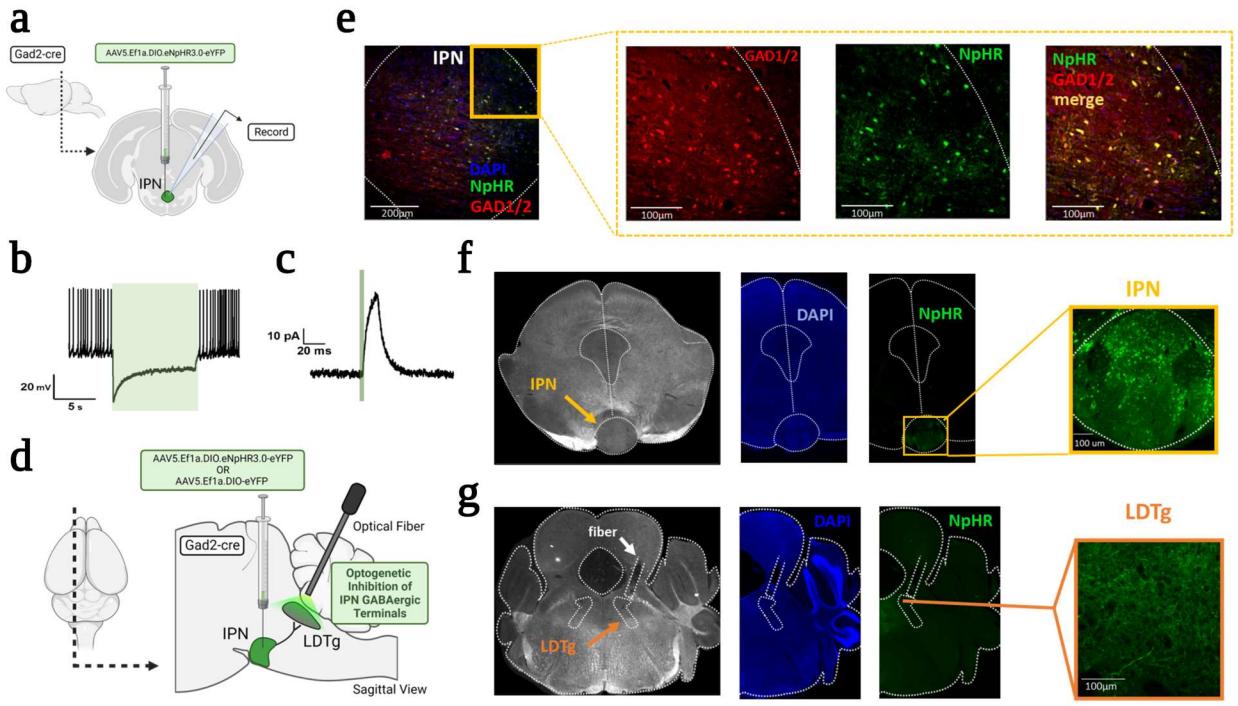

Figure 10. Optogenetic inhibition of IPN GABAergic terminals in LDTg

a. Schematic illustrating cre-mediated expression of NpHR in GAD2-cre mice. **b.** Light evoked hyperpolarization of the membrane in *ex vivo* slices. **c.** Light evoked inhibitory currents. **d.** Viral vector cre-mediated expression of NpHR or EGFP in the IPIN of GAD2-cre mice and fiber optic placement in the LDTg for light inhibition of the terminals. **e.** Restriction of viral expression within GAD positive neurons in IPN. **f.** Viral targeting of NpHR within the IPN. **g.** Fiber targeting of LDTg and expression of virus within LDTg terminals.
SOURCE: Author, Schematics made with BioRender

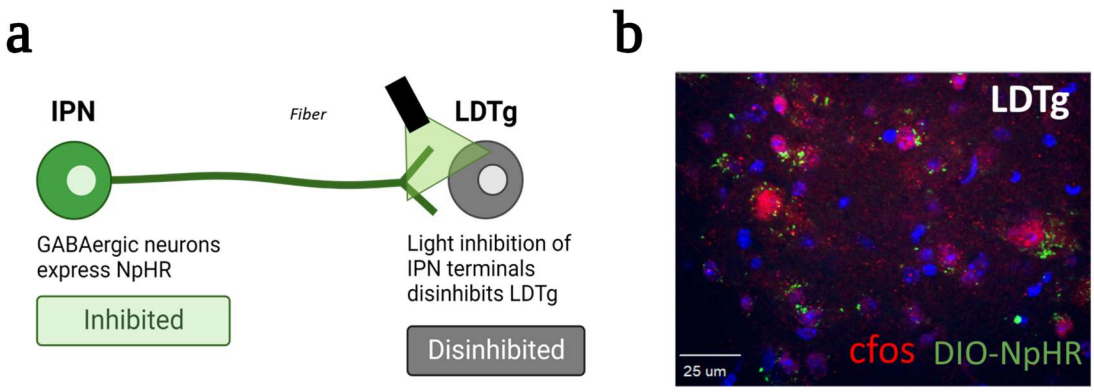

Figure 11. cfos expression in LDTg after photoinhibition of IPN GABAergic terminals

Mice underwent nicotine drinking for 4-weeks. Immediately after an injection of MEC, a light was turned on for photoinhibition of IPN GABAergic neurons in LDTg for 20-minutes. **a.** Schematic of optogenetic inhibition surgical protocol. **b.** cfos expression in LDTg after 20-minute photoinhibition of IPN GABAergic terminals shows cfos activation in neurons surrounded by NpHR expressing terminals. SOURCE: Author, Schematics made with BioRender

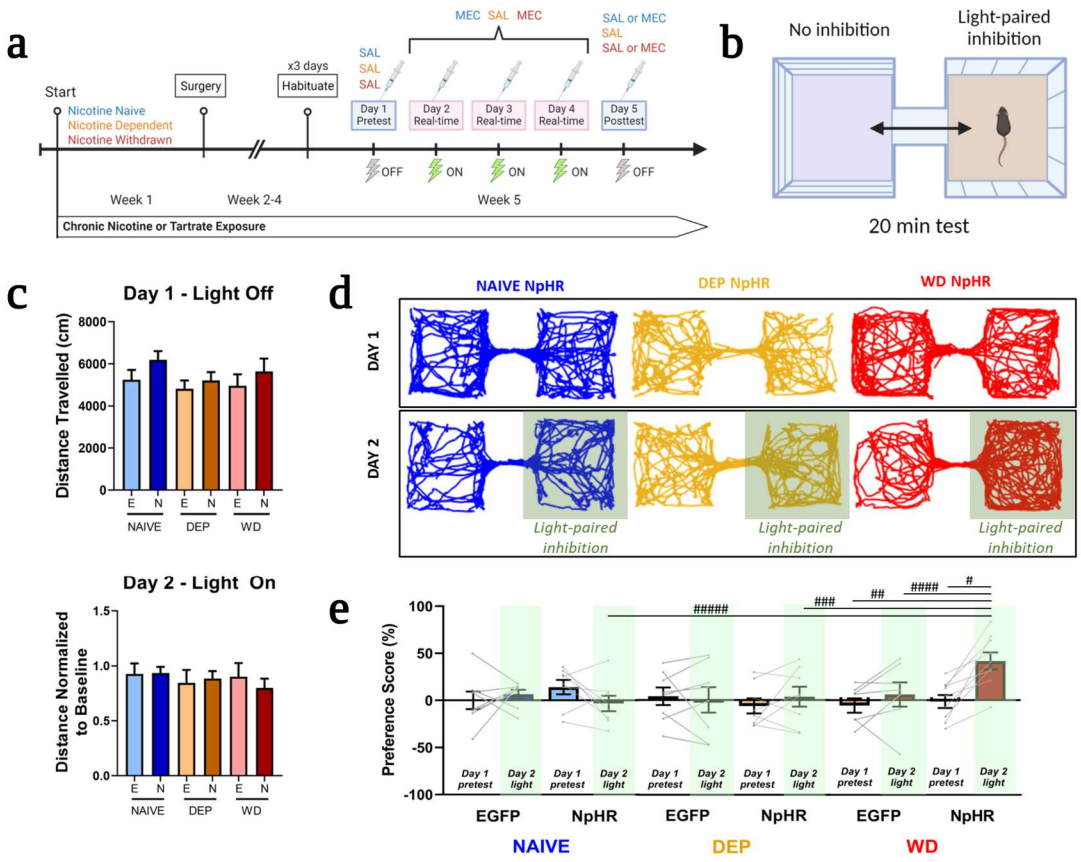

Figure 12. Inhibition of IPN-LDTg GABAergic terminals during nicotine withdrawal results in place preference

a. Timeline of nicotine drinking, surgery and behavior **b.** Real-time place preference behavioral apparatus with different patterned walls and textured floors for conditioning **c.** Distance travelled over 20-minutes on pretest day (baseline) and distance traveled on Day 2 (light on) proportional to baseline average (distance travelled/avg baseline distance) **d.** Positional traces (first 10-minutes) of representative trials on Day 1 (pretest) and Day 2 (light inhibition) **e.** Photo-inhibition of IPN GABAergic terminals in LDTg is preferred (preference score=%time spent in light-paired chamber - %time spent in non-paired chamber) only in MEC-precipitated nicotine withdrawal state. SOURCE: Author, Schematics made with BioRender

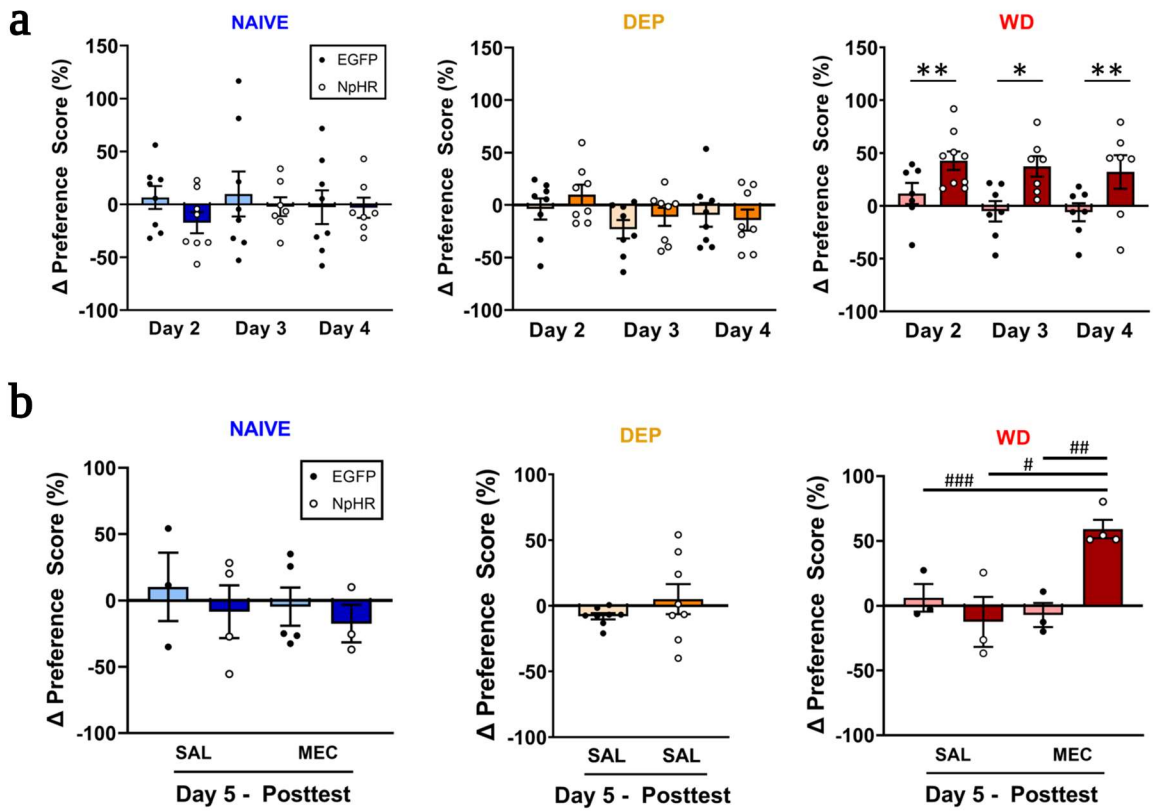

is

Figure 13. Context dependent conditioning for photoinhibition in nicotine withdrawal

Real-time test was repeated over the course of 3 days for conditioning of the light-paired side. **a.** The light-paired chamber is consistently preferred (Δpreference score = preference score – pretest preference score) during MEC-precipitated withdrawal, but not in nicotine naïve or dependent states. **b.** On posttest day (light off) the mice maintain preference for the light paired chamber only in nicotine withdrawal context. SOURCE: Author

We observed that preference to the chamber conditioned with optogenetic inhibition was maintained in a withdrawal context but not a dependent one (Fig. 13B).

Inhibition of IPN-LDTg GABAergic terminals alleviates nicotine withdrawal somatic signs

Previous literature reports an important role of the IPN in the induction of somatic signs during nicotine withdrawal[121,122]. Using MEC to induce nicotine withdrawal, we observed no change in the number of somatic signs (Fig. 14A,D), contradictory to data collected by other labs[152,153]. However, we did see an increase in the duration of time spent performing somatic behaviors (Fig. 14B,E). There is an inconsistency of reported somatic signs across the literature, with different labs scoring different behaviors[153,154]. For our experiments, we pooled the somatic signs reported across the literature for analysis and scored those that were observable by camera. Paw licking, shaking, and grooming had the longest time per bout of the observed somatic signs. When pooled and analyzed by time per bout, we see a significant elevation in the nicotine withdrawal state (Fig. 14C), which contributes to the lack of elevation in overall somatic sign number. Of the observable somatic behaviors, shaking and paw licking were the most indicative of a withdrawal state (Fig. 14E). After optogenetic inhibition of the GABAergic projections from IPN to LDTg, the duration of time spent performing somatic signs returned to levels consistent with tartrate control groups, and total number of signs remained unchanged across groups (Fig. 14).

LDTg mediates nicotine withdrawal behavioral response to novelty

In addition to somatic signs, IPN has been shown to mediate the affective symptoms of nicotine withdrawal[123,124,155]. To test if the IPN mediates these behaviors through its connection to

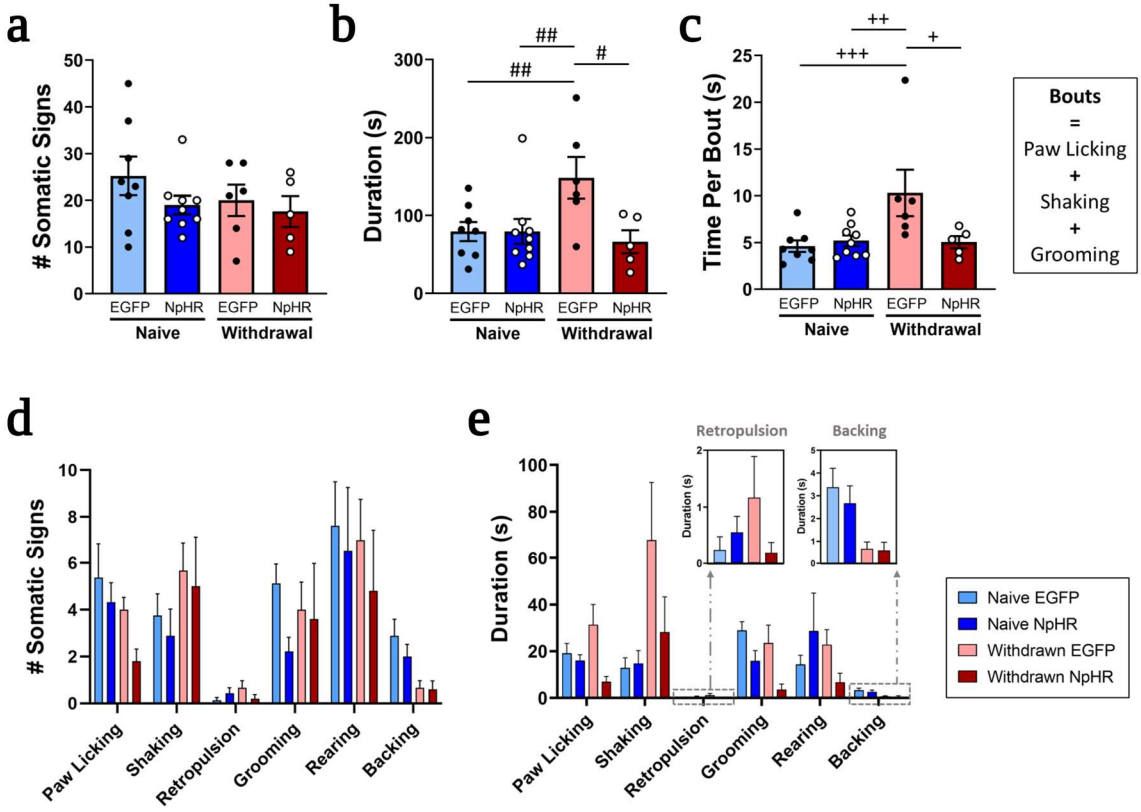

Figure 14. Silencing GABAergic IPN projections to LDTg decreases somatic sign duration

a. Total number of somatic signs show no change between nicotine treatment or optogenetic group. **b.** Duration of somatic signs increased during nicotine withdrawal and photo-inhibition during attenuated signs, consistent with tartrate control group durations. **c.** Combining signs that have extended bout time (paw licking, shaking, grooming), we see the average time per bout is increase in nicotine withdrawal. The bout time per sign decreases with optogenetic inhibition. **d.** Individual somatic sign numbers are not dependent on withdrawal state or optogenetic group **e.** Signs showing the greatest increase during nicotine withdrawal include paw licking and shaking. All somatic sign durations decrease with optogenetic inhibition during nicotine withdrawal. SOURCE: Author

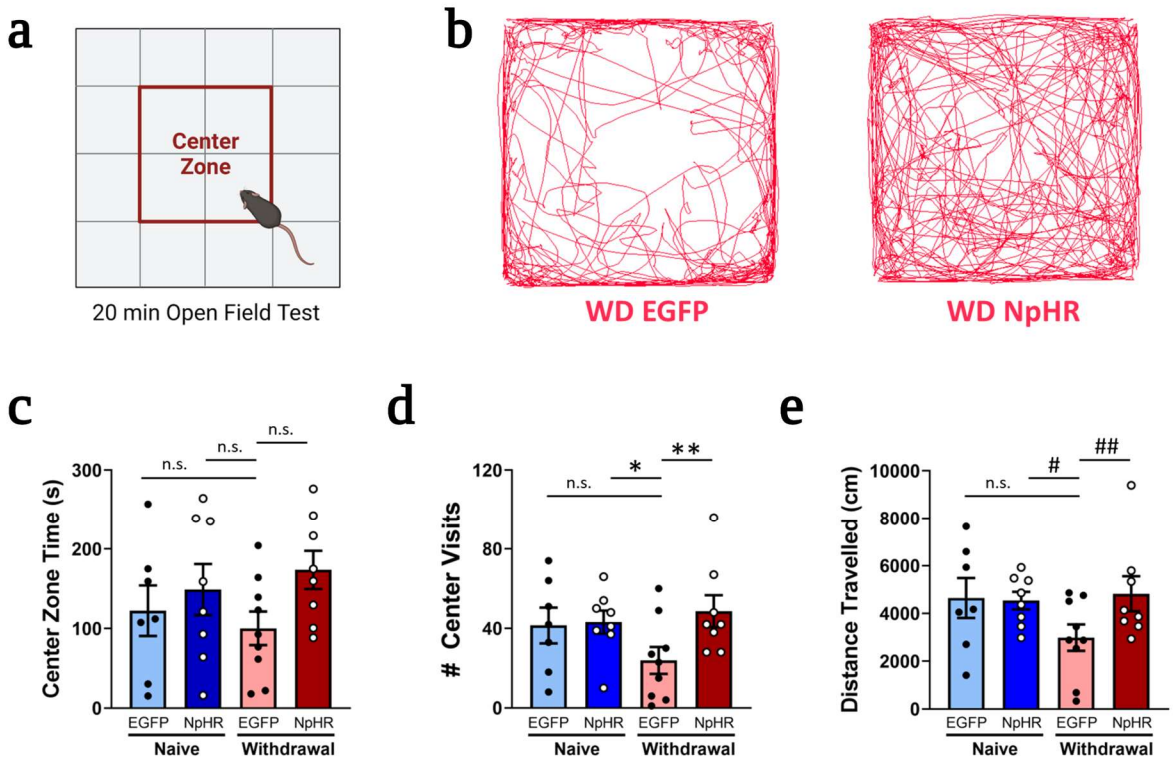

Figure 15. Silencing GABAergic IPN-LDTg projections increases open-field exploration

a. Schematic of open field test box with center zone outlined in red **b.** Representative position traces of a control withdrawal state (EGFP) and withdrawal state with optogenetic inhibition (NpHR) **c.** No change in center zone time across nicotine state and optogenetic groups **d.** Number of center visits decreases in a withdrawal state, and center visits increases to levels of naïve controls with optogenetic inhibition **e.** Distance travelled decreases in a withdrawal state, and distance increases to levels of naïve controls with optogenetic inhibition. SOURCE: Author, Schematics made with BioRender

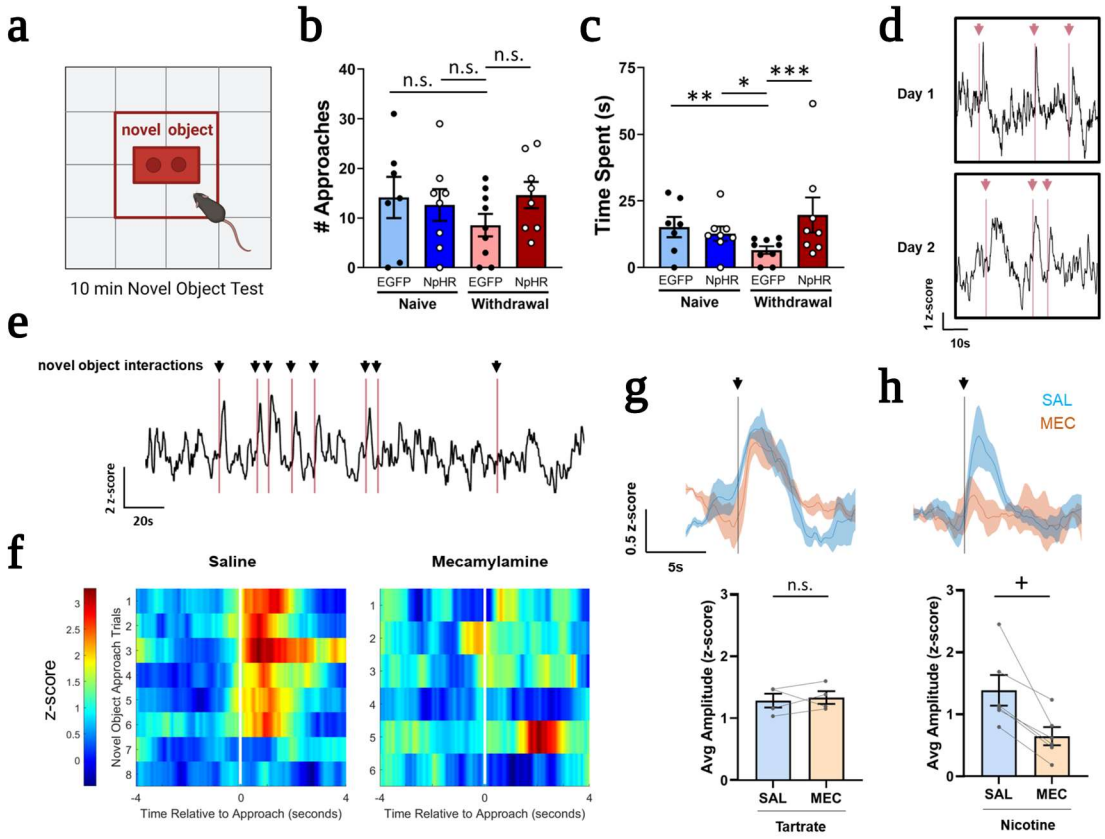

Figure 16. LDTg activity during novel object interaction

a. Schematic of novel object interaction test **b.** Novel object number of approaches remains unchanged across nicotine treatment and optogenetic group **c.** Time spent interacting with novel object decreases during withdrawal and optogenetic inhibition increases time spent back to control levels. **d.** LDTg GCaMP6 fluorescence increases to novel object approach. Top trace is response to one novel object and bottom trace is response to a second novel object on a separate recording. **e.** Occasionally, the LDTg does not response to novel object **f.** Heat maps of GCaMP6 signal to novel object of a mouse before (SAL) and after (MEC) nicotine withdrawal **g.** MEC injection does not alter novel object response in nicotine naive animals **h.** MEC-precipitated withdrawal decreases GCaMP6 signal to novel object.
SOURCE: Author, Schematics made with BioRender

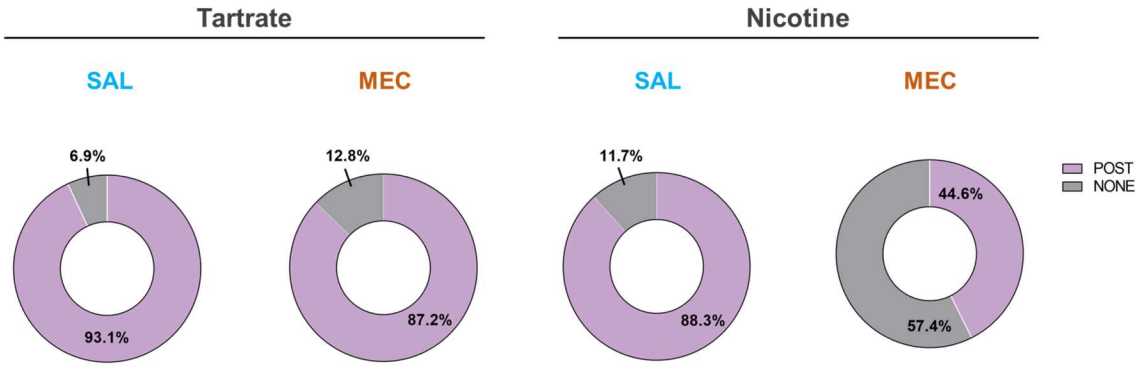

Figure 17. Nicotine withdrawal decreases LDTg responsiveness to novel object interaction

During novel object interaction, LDTg increases activity immediately to the onset of the interaction with a peak directly after completed approach. Novel object elicits a response from LDTg in ~87-93% of novel object approaches. After induction of nicotine withdrawal, there are an increased percentage of novel object interactions that elicit no response within LDTg, from around 10% to 57%. SOURCE: Author

LDTg, we tested our optogenetic inhibition in three tests of affective behavior, open field, novel object exploration, and anhedonia. Open field test and novel object test for exploration of novelty. During our open field test, we saw a decreased distance traveled and decrease in number of visits to the center zone (Fig. 15A-E), as observed previously[153]. After optogenetic inhibition of IPN-LDTg GABAergic terminals, mice increased their distance traveled and the number of visits to the center zone to levels consistent with tartrate controls (Fig. 15D,E). After presentation of a novel object within the open field arena, nicotine withdrawn mice spent less time interacting with the novel object, and this is recovered to baseline levels with optogenetic inhibition (Fig. 16A-C). We did not see any change in number of novel object approaches or time spent within the center zone (Fig. 15C & Fig 16B). All together, these results suggest an anxiolytic effect of our manipulation.

Interestingly, GCaMP6s signal in the LDTg (Fig. 4B,C) responds strongly to novelty and this response is reliable in about 90% of interactions (Fig. 16D-F & Fig. 17). After nicotine withdrawal, the LDTg no longer shows a robust response to novel object interaction with a significant decrease in the average amplitude of the peak immediately following novel object interaction (Fig. 16F-H). Individual novel object analysis reveals most interactions are immediately followed with an increase in LDTg activity However, in a small percentage of interactions there was no LDTg response (~6-13%) (Fig. 17). During nicotine withdrawal, the proportion of responses increases to almost 60% (Fig. 17).

LDTg mediates nicotine withdrawal behavioral response to hedonic stimuli

Anhedonia is another symptom of nicotine withdrawal. To measure the role of LDTg in anhedonia symptoms of withdrawal, we used a social odor preference test. In this test, mice are

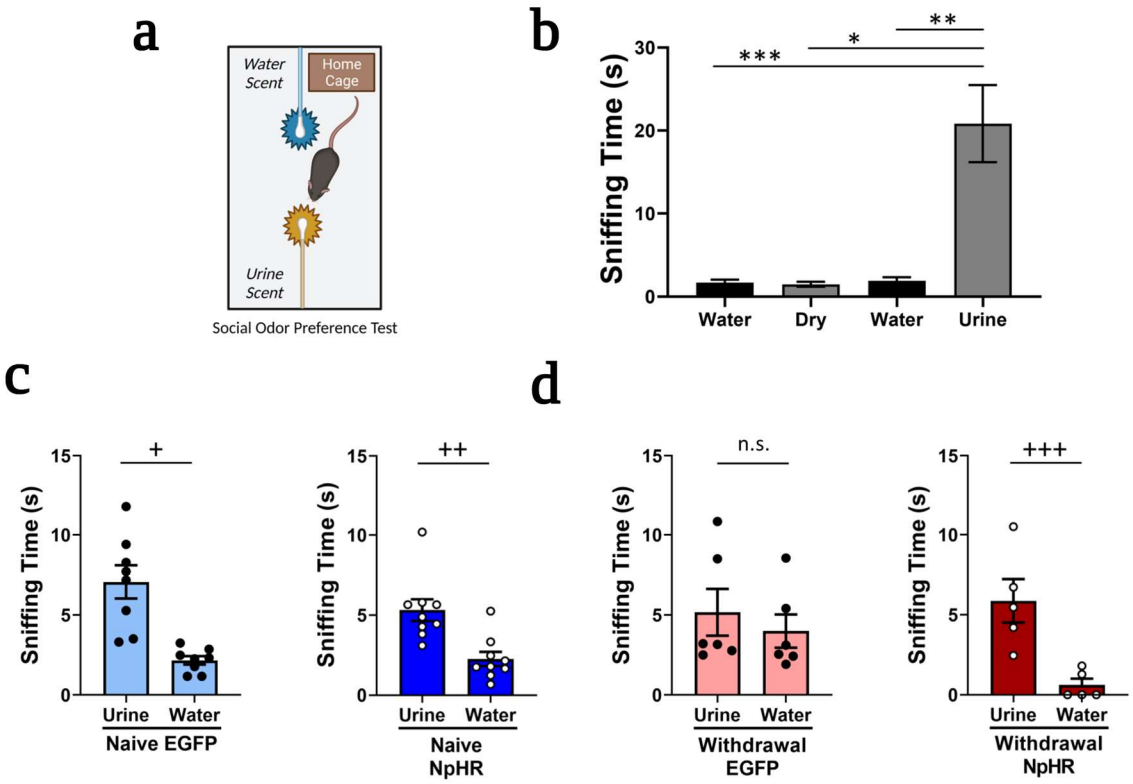

Figure 18. IPN-LDTg inhibition prevents nicotine withdrawal anhedonia to social odor

a. Schematic of social odor test with presentation of 2 swabs (water vs. urine of mouse of opposite sex) in the home cage **b.** In wild type mice, urine sniffing is preferred to water or dry swab **c.** Urine is preferred to water swab under baseline conditions. **d.** During nicotine withdrawal, preference for social odor is attenuated and photo-inhibition of IPN-LDTg GABAergic terminals recovers normal preference for social odor. SOURCE: Author, Schematics made with BioRender

presented with 2 swabs in the home cage dipped in either urine of a mouse of the opposite sex or water (Fig. 18A). Urine sniffing is preferred in mice and increases DA levels within the NAc[156] and be sniffed for higher duration than water, or extracts of other odors such as vanilla or almond[156,157]. We observed greater sniffing time of the urine over water or dry swab as previously reported (Fig. 18B,C). During nicotine withdrawal, mice lose their preference for the social odor. However, this response is recovered in mice that receive optogenetic inhibition of the IPN GABAergic terminals in LDTg (Fig. 18D). This data suggests that LDTg plays a role in hedonic response during nicotine withdrawal.

Dopamine in the NAc lateral shell aligns with LDTg activity

Nicotine withdrawal leads to attenuated DA release within the NAc as measured by microdialysis in rat and mouse[71,158-160]. Using a dopamine sensor, GRAB-DA, within the NAc lateral shell (NAcLat) (Fig. 19A-D) we measured DA transmission before and after nicotine withdrawal (Fig 19E,F). We observed a decrease in DA release after an injection of 2mg/kg MEC in nicotine dependent mice (Fig 19E,F). The peaks during nicotine withdrawal have decreased average peak amplitude and AUC in the 5-minutes after injection, compared to a baseline period (Fig 20B,C), similar to LDTg GCaMP response (Fig.5B,C). We do not see this response in tartrate controls after MEC of SAL injection (Fig 19F & Fig 20B,C). To compare responsiveness to salient stimuli within the LDTg and DA release within the NAc, we measured DA release to novel object before and after nicotine withdrawal (Fig. 21). DA dynamics reveal 4 types of responses to novel object (Fig. 21). Similar to LDTg activity, we saw a DA increase immediately following interaction, which we designated as “POST” and no response designated as “NONE” (Fig. 21). Additionally, we observed cases with a DA increase immediately before interaction, “PRE”, and

a suppression of DA when the signal was already elevated, “DEC” (Fig. 21). Interestingly, after withdrawal the frequency of “POST” responses decreases and “PRE” responses increased (Fig. 22). Overall, we saw a reduction in the number of novel object approaches (Fig. 22).

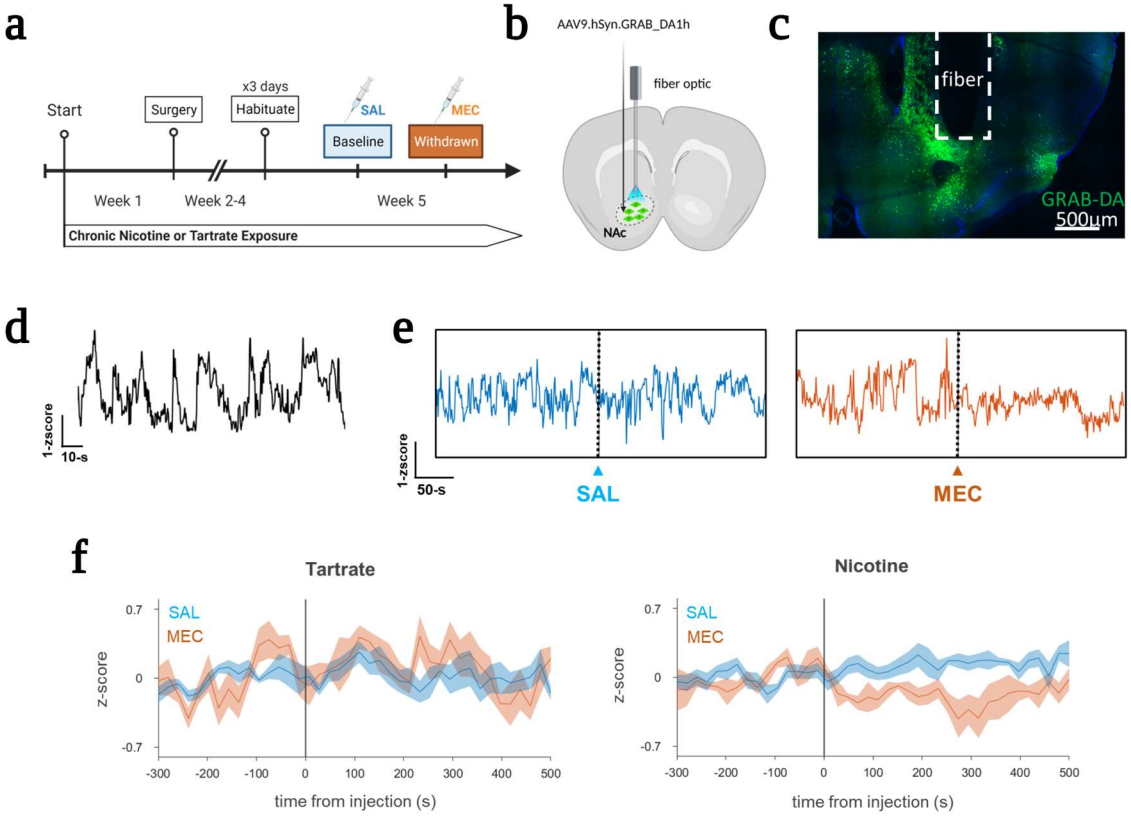

Figure 19. Spontaneous DA release in the NAc lateral shell to SAL and MEC injections

a. Schematic of experimental timeline. **b.** Schematic of viral surgery and implant into NAc Lat Shell. **c.** Histological verification. **d.** Spontaneous DA transients measured by GRAB-DA. **e.** DA release before and after and injection of SAL or MEC in a nicotine dependent mouse. **f.** Averaged traces of DA release in chronic tartrate and nicotine drinking animals after injection of SAL or MEC. SOURCE: Author, Schematics made with BioRender

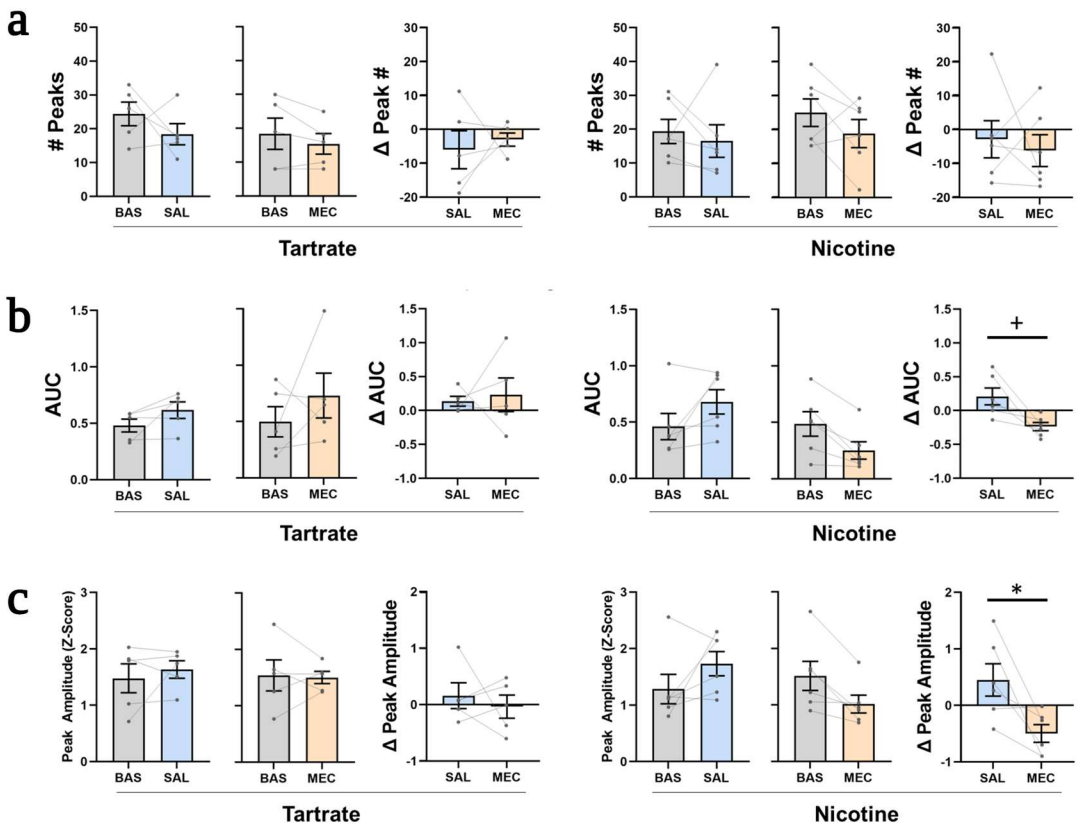

Figure 20. DA release in the NAc lateral shell is depressed after nicotine withdrawal

Measures of DA release signal in the NAc lateral shell 5-minutes post injection in comparison to the 5-minute baseline period before injection. **a.** SAL or MEC injection did not change frequency of peaks in chronic tartrate or nicotine drinking mice. **b.** MEC-precipitated nicotine withdrawal significantly decreased average AUC (in a 500ms window) of identified peaks but did not affect tartrate controls. **c.** MEC-precipitated nicotine withdrawal significantly decreased average amplitude of identified peaks but did not affect tartrate controls. SOURCE: Author

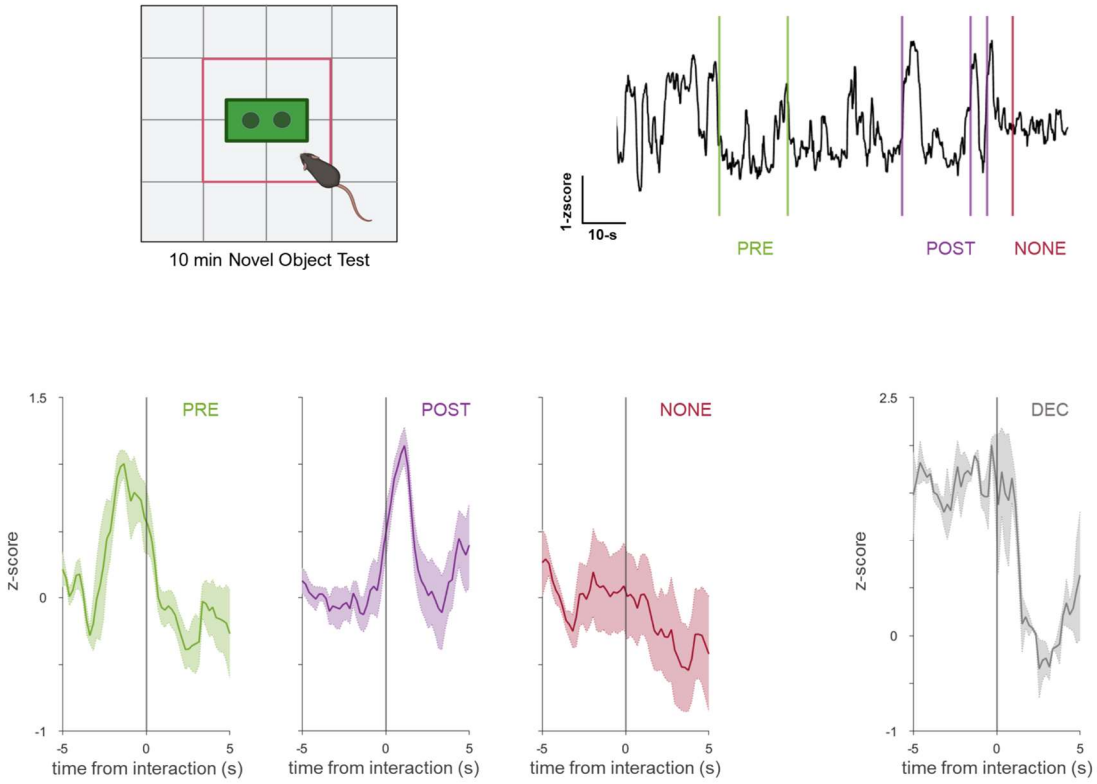

Figure 21. DA dynamics to novel object interaction in NAc lateral shell

Novel object interaction either induces DA release on approach (PRE), on interaction (POST), has no response (NONE), or suppresses release (DEC). SOURCE: Author, Schematics made with BioRender

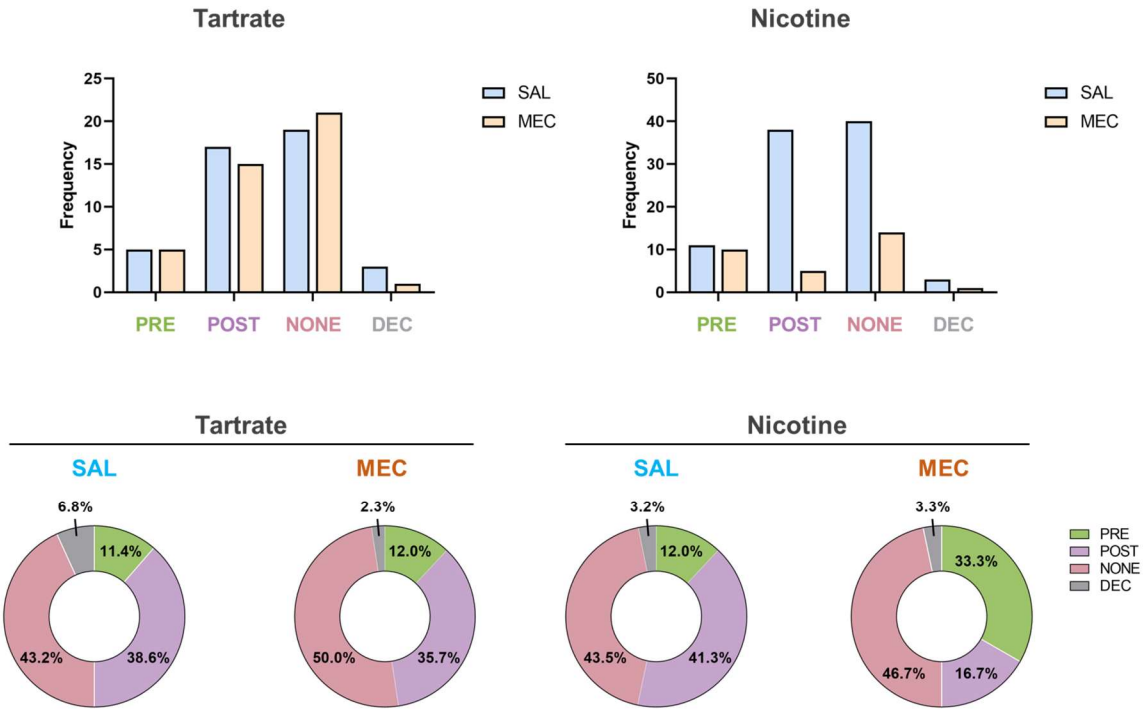

Figure 22. Nicotine withdrawal alters DA dynamics to novel object response

Proportions of "PRE", "POST", "NONE" and "DEC" responses remains relatively stable in chronic tartrate mice after SAL or MEC exposure. After MEC injection in nicotine dependent mice, the number of novel object interactions decreased, and the proportion of those interactions shifted from the SAL controls. After nicotine withdrawal the relative proportion of "POST" responses shifts from ~40% to ~16% and the proportion of "PRE" responses increased from about 12% to 33%. SOURCE: Author

P-VALUES BY FIGURE		
FIGURE	**SYMBOL**	**P-VALUE**
Fig. 3	*	0.0419
Fig. 3	**	0.0149
Fig. 3	***	0.0005
Fig. 5	*	0.0184
Fig. 5	**	0.0014
Fig. 5	+	0.0088
Fig. 5	++	0.0066
Fig. 12	#	0.0401
Fig. 12	##	0.0332
Fig. 12	###	0.0191
Fig. 12	####	0.0031
Fig. 12	#####	0.0026
Fig. 13	*	0.0384
Fig. 13	**	0.0287
Fig. 13	#	0.0126
Fig. 13	##	0.0038
Fig. 13	##	0.0026
Fig. 14	+	0.0428
Fig. 14	++	0.0254
Fig. 14	+++	0.0160
Fig. 14	#	0.0500
Fig. 14	##	0.0477
Fig. 15	*	0.0499
Fig. 15	**	0.0318
Fig. 15	#	0.0380
Fig. 15	##	0.0302
Fig. 16	*	0.0463
Fig. 16	**	0.0220
Fig. 16	***	0.0156
Fig. 16	+	0.0030
Fig. 18	*	0.0213
Fig. 18	**	0.0199
Fig. 18	***	0.0162
Fig. 18	+	0.0308
Fig. 18	++	0.0138
Fig. 18	+++	0.0065
Fig. 20	*	0.0304
Fig. 20	+	0.0355

Table 3. Statistical Significance. Data with statistical p-values <0.05 are listed with corresponding figures and graphical symbol. Additional p-values are provided in Table 4. SOURCE: Author

STATISTICAL TESTS AND OUTPUTS BY FIGURE				
Data	**Mean±SEM**	**Statistical Test(s)**	**N**	**Parameters and Outputs**
ELISA, Fig. 3	NV = 0.408±0.3536 DEP = 216.738±16.63 WD = 9.7918±2.07	Shapiro-Wilk, normality Kruskal-Wallis, Dunn's multiple comparisons	N = 4, NV N = 7, DEP N = 7, WD	W = 0.6298, p = 0.0012, fail W = 0.9406, p = 0.6438, pass W = 0.7337, p = 0.0085, fail H = 14.92, p<0.0001 NV vs DEP, MRD = -12.5, p = 0.0005 NV vs WD, MRD = -5.5, p = 0.2986 DEP vs WD, MRD = 7, p = 0.0419
Δ weight, Fig. 3	*TART* D3 = 0.9724±0.0099 D7 = 1.0127±0.0065 D10 = 1.0247±0.0062 D14 = 1.0169±0.0096 D17 = 1.0356±0.0192 D21 = 1.0562±0.0186 D24 = 1.0779±0.0109 D28 = 1.1440±0.0221 *NIC* D3 = 0.9862±0.0084 D7 = 1.0029±0.0104 D10 = 1.0089±0.0107 D14 = 1.0407±0.0131 D17 = 1.0428±0.0142 D21 = 1.0578±0.0164 D24 = 1.0511±0.0193 D28 = 1.0716±0.0190	Shapiro-Wilk, normality …if failed, Mann Whitney test …if passed, unpaired t-test, Welch's correction	N = 43, TART N = 54, NIC	*TART* D3, W=0.7638, p<0.0001, fail D7, W=0.9740, p=0.4305, pass D10, W=0.7638, p=0.6979, pass D14, W=0.9719, p=0.5522, pass D17, W=0.9237, p=0.1029, pass D21, W=0.8554, p=0.0066, fail D24, W=0.9292, p=0.0468, fail D28, W=0.9499, p=0.2702, pass *NIC* D3, W=0.7885, p<0.0001, fail ... p=0,8779, U=1140 D7, W=0.8712, p<0.0001, fail ... p=0.6140, U=1071 D10, W=0.9439, p=0.0148, fail ... p=0.4758, U=1017 D14, W=0.9548, p=0.0891, pass ... p=0.2085, U=570 D17, W=0.9185, p=0.0280, fail ... p=0.4949, U=269 D21, W=0.9765, p=0.7429, pass ... p=0.6502, U=267 D24, W=0.9538, p=0.2290, pass ... p=0.5994, U=413 D28, W=0.9566, p=0.2704, pass ... p=0.0149, t=2.482, df=88.73

Table 4. Statistical tests and outputs. Data is listed by figure with corresponding means±SEM, statistical tests, sample sizes (N), and statistical parameters with test outputs. SOURCE: Author

STATISTICAL TESTS AND OUTPUTS BY FIGURE, CONTINUED				
LDTg Peak #, Fig. 5	*Baseline* TART_SAL=18.0±1.90 TART_MEC=15.6±2.29 NIC_SAL=23.8±4.51 NIC_MEC=19.2±1.34 *Injection* TART_SAL=16.4±1.34 TART_MEC=12.6±1.28 NIC_SAL=17.5±1.80 NIC_MEC=13.7±2.05	Shapiro-Wilk, normality Two-Way RM ANOVA, Sidak's multiple comparisons, F1:NS, F2:WIN	N=5, TART N=6, NIC	all groups pass normality test (W=0.8422-0.9916 ... p=0.1711-0.9927) F1:NS, SS=91.22, df=1, MS= 91.22, ... F=1.164, p=0.3086 F2:WIN, SS=331.7, df=3, MS=110.6, … F=4.461, p=0.0273 INT, SS=42.68, df=3, MS=14.23, … F=0.5741, p=0.6370 no sig main effect no sig simple effect
LDTg Δ Peak #, Fig. 5	TART_SAL=-1.6±1.56 TART_MEC=-3.0±1.10 NIC_SAL=-6.3±3.16 NIC_MEC=--5.5±2.71	Shapiro-Wilk, normality Two-Way RM ANOVA, Sidak's multiple comparisons, F1:NS, F2:INJ	N=5, TART N=6, NIC	all groups pass normality test (W=0.9079-0.9682 ... p=0.4553-0.8800) F1:NS, SS=71.35, df=1, MS= 71.35, ... F=1.784, p=0.2145 F2:INJ, SS=0.4379, df=1, MS=0.4379, … F=0.01107, p=0.9185 INT, SS=6.802, df=1, MS=6.802, … F=0.1719, p=0.6881, no sig MC
LDTg Peak Amp, Fig. 5	*Baseline* TART_SAL=2.67±0.07 TART_MEC=2.28±0.26 NIC_SAL=2.39±0.19 NIC_MEC=2.91±0.12 *Injection* TART_SAL=2.56±0.13 TART_MEC=2.36±0.17 NIC_SAL=2.46±0.20 NIC_MEC=2.09±0.13	Shapiro-Wilk, normality Two-Way RM ANOVA, Sidak's multiple comparisons, F1:NS, F2:WIN	N=5, TART N=6, NIC	all groups pass normality test (W=0.8074-0.9855 ... p=0.0684-0.9616) F1:NS, SS=0.0001569, df=1, MS= 0.0001569, ... F=0.0003777, p=0.9849 F2:WIN, SS=0.8780, df=3, MS=0.2927, … F=2.650, p=0.0690 INT, SS=1.515, df=3, MS=0.5051, … F=4.573, p=0.0103 no sig main effect simple effect, ... nic baseline vs nic mec, p=0.0014

Table 4, continued. Data is listed by figure with corresponding means±SEM, statistical tests, sample sizes (N), and statistical parameters with test outputs. SOURCE: Author

STATISTICAL TESTS AND OUTPUTS BY FIGURE, CONTINUED				
LDTg Δ Peak Amp, Fig. 5	TART_SAL=-0.11±0.15 TART_MEC=0.08±0.16 NIC_SAL=0.07±0.25 NIC_MEC=-0.82±0.11	Shapiro-Wilk, normality Two-Way RM ANOVA, Sidak's multiple comparisons, F1:NS, F2:INJ	N=5, TART N=6, NIC	all groups pass normality test (W=0.9079-0.9682 ... p=0.4553-0.8800) F1:NS, SS=0.6801, df=1, MS= 0.6801, ... F=0,9827, p=0.5101 F2:INJ, SS=0.6682, df=1, MS=0.6682, … F=3.056, p=0.1144 INT, SS=1.593, df=1, MS=1.593, … F=7.284, p=0.0244 MC, … SAL-MEC, NIC, p=0.0184 … TART-NIC, MEC, p=0.0106
LDTg Peak AUC, Fig. 5	*Baseline* TART_SAL=1.07±0.04 TART_MEC=0.91±0.12 NIC_SAL=0.91±0.06 NIC_MEC=1.23±0.05 *Injection* TART_SAL=0.98±0.07 TART_MEC=0.96±0.10 NIC_SAL=0.96±0.09 NIC_MEC=0.82±0.07	Shapiro-Wilk, normality Two-Way RM ANOVA, Sidak's multiple comparisons, F1:NS, F2:WIN	N=5, TART N=6, NIC	all groups pass normality test (W=0.7934-0.9868 ... p=0.0512-0.9673) F1:NS, SS=0.0000045, df=1, MS= 0.0000045, ... F=0.000059, p=0.9940 F2:WIN, SS=0.1786, df=3, MS=0.05954, … F=2.110, p=0.1435 INT, SS=0.4234, df=3, MS=0.1411, … F=5.001, p=0.0069 no sig main effect MC, ... baseline vs mec, NIC, p=0.0066
LDTg Δ Peak AUC, Fig. 5	TART_SAL=-0.09±0.10 TART_MEC=0.06±0.07 NIC_SAL=0.05±0.11 NIC_MEC=-0.42±0.05	Shapiro-Wilk, normality Two-Way RM ANOVA, Sidak's multiple comparisons, F1:NS, F2:INJ	N=5, TART N=6, NIC	all groups pass normality test (W=0.9079-0.9682 ... p=0.4553-0.8800) F1:NS, SS=0.1559, df=1, MS= 0.1559, ... F=2.905, p=0.1225 F2:INJ, SS=0.1358, df=1, MS=0.1358, … F=3.003, p=0.1172 INT, SS=0.5075, df=1, MS=0.5075, … F=11.22, p=0.0085 MC, … SAL-MEC, NIC, p=0.0088 … TART-NIC, MEC, p=0.0049

Table 4, continued. Data is listed by figure with corresponding means±SEM, statistical tests, sample sizes (N), and statistical parameters with test outputs. SOURCE: Author

STATISTICAL TESTS AND OUTPUTS BY FIGURE, CONTINUED				
Distance travelled, Fig. 12	*D1* NV_E=5242.3±437.9 NV_N=6190.4±387.9 DEP_E=4817.4±368.2 DEP_N=5214.3±368.8 WD_E=4954.9±506.3 WD_N=5639.4±575.4	Shapiro-Wilk, normality Two-Way ANOVA, Tukey's HSD multiple comparisons, F1:NS, F2:VE	N=8, NV_E N=8, NV_N N=8, DEP_E N=8, DEP_N N=7, WD_E N=9, WD_N	*D1* all groups pass normality test (W=0.8882-0.9742 ... p=0.2252-0.9267) F1:NS, SS=3975653, df=2, MS= 1987827, ... F=1.061, p=0.3551 F2:VE, SS=5462832, df=1, MS=5462832, … F=2.916, p=0.0951 INT, SS=607939, df=2, MS=303969, … F=0.1623, p=0.8507, no sig MC
Distance normalized to baseline, Fig. 12	*D2* NV_E=0.926±0.091 NV_N=0.934±0.052 DEP_E=0.846±0.109 DEP_N=0.886±0.062 WD_E=0.901±0.115 WD_N=0.798±0.081	Shapiro-Wilk, normality Two-Way ANOVA, Tukey's HSD multiple comparisons, F1:NS, F2:VE	N=8, NV_E N=8, NV_N N=8, DEP_E N=8, DEP_N N=7, WD_E N=9, WD_N	*D2* all groups pass normality test (W=0.8818-0.9822 ... p=0.3317-0.9696) F1:NS, SS=0.05808, df=2, MS= 0.02904, ... F=0.4204, p=0.6595 F2:VE, SS=0.003905, df=1, MS=0.003905, … F=0.05653, p=0.8132 INT, SS=0.04470, df=2, MS=0.02235, … F=0.3235, p=0.7254, no sig MC

Table 4, continued. Data is listed by figure with corresponding means±SEM, statistical tests, sample sizes (N), and statistical parameters with test outputs. SOURCE: Author

STATISTICAL TESTS AND OUTPUTS BY FIGURE, CONTINUED				
Preference Score, %, Fig. 12	*D1* NV_E=0.078±8.68 NV_N=14.040±7.17 DEP_E=4.019±8.71 DEP_N=-6.167±7.35 WD_E=-5.642±6.97 WD_N=-1.426±6.38 *D2* NV_E=6.566±4.36 NV_N=-3.250±7.67 DEP_E=0.202±12.53 DEP_N=3.605±9.85 WD_E=6.011±11.86 WD_N=41.274±8.56	D'Agostino & Pearson, normality Shapiro-Wilk, normality Two-Way RM ANOVA, Holm-Sidak's multiple comparisons, F1:LO, F2:VE	N=8, NV_E N=8, NV_N N=8, DEP_E N=8, DEP_N N=7, WD_E N=9, WD_N	*NV* all groups pass normality test (K2=1.721-4.459, ... p=0.1076-0.4229) F1:LO, SS=70.93, df=1, MS=70.93, ... F=0.09234, p=0.7635 F2:VE, SS=92.04, df=1, MS=92.04, … F=0.1198, p=0.7318 INT, SS=369.4, df=1, MS=369.4, … F=0.4808, p=0.4938, no sig MC *DEP* all groups pass normality test (K2=0.4358-1.574, ... p=0.4552-0.8042) F1:LO, SS=233.4, df=1, MS=233.4, ... F=0.5703, p=0.4564 F2:VE, SS=34.39, df=1, MS=34.39, … F=0.0840, p=0.1076 INT, SS=1131, df=1, MS=1131, … F=2.763, p=0.1076, no sig MC *WD* all groups pass normality test (W=0.8871-9816, ... p=0.2599-0.9721) F1:LO, SS=5816, df=1, MS=5816, ... F=10.08, p=0.0036 F2:VE, SS=3068, df=1, MS=3068, … F=5.318, p=0.0287 INT, SS=1898, df=1, MS=1898, … F=3.289, p=0.0805 MC, ...EGFP:D1 vs NpHR:D2, p=0.0031 ...EGFP:D2 vs NpHR:D2, p=0.0332 ...NpHR:D1 vs NpHR:D2, p=0.0041
		Three-Way RM ANOVA, Holm-Sidak's multiple comparisons, F1:LO, F2:VE, F3:NS		F1:LO vs F2:VE vs F3:NS ... SS=3120, df=2, MS=1560, F=4.010, p=0.0255 F1:LO vs F3:NS ... SS=4534, df=2, MS=2267, F=5.828, p=0.0058 F1:LO ... SS=1625, df=1, MS=1625, F=4.178, p=0.0473 MC, ... NV_N:D2 vs WD_N:D2, p=0.0401 ... DEP_N:D2 vs WD_N:D2, p=0.0191 ... WD_E:D1 vs WD_N:D2, p=0.0338 ... WD_N:D1 vs WD_N:D2, p=0.0026 all other comparisons not sig

Table 4, continued. Data is listed by figure with corresponding means±SEM, statistical tests, sample sizes (N), and statistical parameters with test outputs. SOURCE: Author

STATISTICAL TESTS AND OUTPUTS BY FIGURE, CONTINUED				
Δ Preference Score, %, Fig 13	*D2* NV_E=6.488±10.12 NV_N=-17.291±9.33 DEP_E=-3.817±9.40 DEP_N=9.772±8.98 WD_E=11.652±9.27 WD_N=42.700±8.26 *D3* NV_E=9.835±19.86 NV_N=-2.219±8.25 DEP_E=-23.133±8.20 DEP_N=-11.230±8.03 WD_E=-5.230±8.93 WD_N=37.257±8.96 *D4* NV_E=-2.738±14.87 NV_N=-3.169±8.80 DEP_E=-9.462±10.51 DEP_N=-14.323±9.39 WD_E=-6.135±7.86 WD_N=32.015±14.68	D'Agostino & Pearson, normality Shapiro-Wilk, normality Two-Way RM ANOVA, Holm-Sidak's multiple comparisons, F1:LO, F2:VE RM Mixed-effects model, Holm-Sidak's multiple comparisons, F1:LO, F2:VE	N=8, NV_E N=8, NV_N N=8, DEP_E N=8, DEP_N N=7, WD_E N=7-9, WD_N	*NV* all groups pass normality test (K2=0.3468-1.823, ... p=0.4019-0.8408) F1:LO, SS=728.1, df=2, MS=364.1, ... F=0.2872, p=0.7518 F2:VE, SS=1753, df=1, MS=1753, … F=1.383, p=0.2462 INT, SS=1090, df=2, MS=545.1, … F=0.4300, p=0.6533, no sig MC *DEP* all groups pass normality test (K2=1.066-2.935, ... p=0.2305-0.5868) F1:LO, SS=3496, df=2, MS=1748, ... F=2.626, p=0.0843 F2:VE, SS=567.6, df=1, MS=567.6, … F=0.8525, p=0.3611 INT, SS=832.4, df=2, MS=416.2, … F=0.6251, p=0.5401, no sig MC *WD* all groups pass normality test (W=0.8748-0.9497, ... p=0.1954-0.5065) F1:LO, F=1.264, p=0.3008 F2:VE, F=14.12, p=0.0021 INT, F=0.1494, p=0.8620 MC, ... WD_E:D2 vs WD_N:D2, p=0.0384 ... WD_E:D3 vs WD_N:D3, p=0.0287 ... WD_E:D4 vs WD_N:D4, p=0.0384

Table 4, continued. Data is listed by figure with corresponding means±SEM, statistical tests, sample sizes (N), and statistical parameters with test outputs. SOURCE: Author

STATISTICAL TESTS AND OUTPUTS BY FIGURE, CONTINUED				
Δ Preference Score, %, Fig 13	*D5* NV_E_SAL= 10.264±21.04 NV_E_MEC= -4.675±12.91 NV_N_SAL= -8.522±17.21 NV_N_MEC= -17.46±11.54 DEP_E_SAL= -8.052±2.21 DEP_N_SAL= 5.015±10.71 WD_E_SAL= 6.103±8.71 WD_E_MEC= -7.211±7.58 WD_N_SAL= -12.505±15.72 WD_N_MEC= 59.181±6.12	Shapiro-Wilk, normality Two-Way ANOVA, Holm-Sidak's multiple comparisons, F1:INJ, F2:VE Unpaired parametric t-test	N=3, NV_E_SAL N=5, NV_E_MEC N=4, NV_N_SAL N=3, NV_N_MEC N=8, DEP_E_SAL N=8, DEP_N_SAL N=3, WD_E_SAL N=3, WD_E_MEC N=3, WD_N_SAL N=4, WD_N_MEC	*NV* all groups pass normality test (W=0.7941-0.9994, ... p=0.0725-0.9536) F1:INJ, SS=510.5, df=1, MS=510.5, ... F=0.5430, p=0.4766 F2:VE, SS=892.5, df=1, MS=892.5, … F=0.9492, p=0.3509 INT, SS=32.27, df=1, MS=32.27, … F=0.0343, p=0.85643, no sig MC *DEP* all groups pass normality test (W=2.448, 0.4841, ... p=0.2940, 0.7850) p=0.2823, two-tailed, t=1.118, df=14 *WD* all groups pass normality test (W=0.8272-9.139, ... p=0.1813-0.4311) F1:INJ, SS=2726, df=1, MS=2726, ... F=8.971, p=0.0151 F2:VE, SS=1827, df=1, MS=1827, ... F=6.012, p=0.0151 INT, SS=5780, df=1, MS=5780, ... F=19.02, p=0.0018 MC, ... WD_E_SAL vs WD_N_MEC, p=0.0126 ... WD_E_MEC vs WD_N_MEC, p=0.0038 ... WD_N_SAL vs WD_N_MEC, p=0.0026

Table 4, continued. Data is listed by figure with corresponding means±SEM, statistical tests, sample sizes (N), and statistical parameters with test outputs. SOURCE: Author

STATISTICAL TESTS AND OUTPUTS BY FIGURE, CONTINUED				
Somatic Signs Number, Fig. 14	NV_E = 25.25±3.85 NV_N= 19.00±1.88 WD_E= 20.00±3.06 WD_N=17.60±2.95	Shapiro-Wilk, normality Two-Way ANOVA, Holm-Sidak's multiple comparisons, F1:NS, F2:VE	N=8, NV_E N=9, NV_N N=6, WD_E N=5, WD_N	all groups pass normality test (W=0.8379-0.9622 ... p=0.0548-0.8307) F1:NS, SS=73.36, df=1, MS= 73.36, ... F=0.9833, p=0.3313 F2:VE, SS=124.1, df=1, MS=124.1, … F=1.664, p=0.2094 INT, SS=24.59, df=1, MS=24.59, … F=0.3296, p=0.5713, no sig MC
Somatic Signs Duration, Fig. 14	NV_E = 79.38±11.48 NV_N= 79.44±15.11 WD_E= 148±24.42 WD_N=66.40±13.19	Shapiro-Wilk, normality Two-Way ANOVA, Holm-Sidak's multiple comparisons, F1:NS, F2:VE	N=8, NV_E N=9, NV_N N=6, WD_E N=5, WD_N	all groups pass normality test (W=0.7242-0.9683 ... p=0.3148-0.8641) F1:NS, SS=11118, df=1, MS= 11118, ... F=5.059, p=0.0339 F2:VE, SS=5187, df=1, MS=5187, … F=2.360, p=0.1376 INT, SS=11156, df=1, MS=11156, … F=5.076, p=0.0337 MC, ... NV_E vs WD_E, p=0.0500 ... NV_N vs WD_E, p=0.0500 ... WD_N vs WD_E, p=0.0477

Table 4, continued. Data is listed by figure with corresponding means±SEM, statistical tests, sample sizes (N), and statistical parameters with test outputs. SOURCE: Author

STATISTICAL TESTS AND OUTPUTS BY FIGURE, CONTINUED				
Grooming/Paw Licking/Shaking Time Per Bout, Fig. 14	NV_E = 4.61±0.57 NV_N= 5.20±0.54 WD_E= 10.31±2.27 WD_N=5.04±0.58	Shapiro-Wilk, normality Two-Way ANOVA, Holm-Sidak's multiple comparisons, F1:NS, F2:VE	N=8, NV_E N=9, NV_N N=6, WD_E N=5, WD_N	all groups pass normality test (W=0.7388-0.9726 ... p=0.05243-0.9097) F1:NS, SS=50.99, df=1, MS= 50.99, ... F=5.134, p=0.0328 F2:VE, SS=36.43, df=1, MS=36.43, … F=3.668, p=0.0675 INT, SS=56.81, df=1, MS=56.81, … F=5.720, p=0.0250 MC, ... NV_E vs WD_E, p=0.0160 ... NV_N vs WD_E, p=0.0254 ... WD_N vs WD_E, p=0.0428
Social Odor (Wild Type), Fig. 18	*WATER VS DRY* water = 1.68±0.35 dry = 1.48±0.28 *WATER VS URINE* water =1.92±0.39 urine=20.84±4.34	Shapiro-Wilk, normality One-Way RM ANOVA, Tukey's HSD multiple comparisons	water vs dry N=8 water vs urine N=8	all groups pass normality test (W=0.8913-0.9797 ... p=0.2404-0.9613) SS=2201, df=3, MS=733.7, F=16.39, ...p=0.0045 MC, ... water vs urine, p=0.0199 … dry vs urine, p=0.0213 … water vs urine, p=0.0162

Table 4, continued. Data is listed by figure with corresponding means±SEM, statistical tests, sample sizes (N), and statistical parameters with test outputs. SOURCE: Author

STATISTICAL TESTS AND OUTPUTS BY FIGURE, CONTINUED				
Social Odor, Fig. 18	*URINE* NV_E = 7.06±0.97 NV_N= 5.31±0.64 WD_E= 5.17±1.33 WD_N=5.87±1.21 *WATER* NV_E = 2.16±0.25 NV_N= 2.25±0.42 WD_E= 3.99±0.95 WD_N=0.62±0.35	Shapiro-Wilk, normality Three-Way RM ANOVA, Holm-Sidak's multiple comparisons, F1:NS, F2:VE, F3:SC	N=8, NV_E N=9, NV_N N=6, WD_E N=5, WD_N	all groups pass normality test (W=0.8931-0.9797, ... p=0.2402-0.9613) F1:NS, SS=1.078, df=1, MS= 1.078, ... F=0.2101, p=0.6508 F2:VE, SS=15.58, df=1, MS=15.58, … F=3.036, p=0.0942 F3:SC, SS=171.5, df=1, MS=171.5, … F=32.95, p<0.0001 F1:NS vs F2:VE vs F3:SC, SS=29.09, … MS=29.09, F=5.591, p=0.0265 MC, urine vs water: NV_E vs NV_E, p=0.0065 NV_N vs NV_N, p=0.0138 WD_N vs WD_N, p=0.0308
Open Field Test, Center Time, Fig. 15	NV_E = 122.39±29.46 NV_N= 148.95±30.04 WD_E= 100.19±19.85 WD_N=173.58±22.33	Shapiro-Wilk, normality Two-Way ANOVA, Holm-Sidak's multiple comparisons, F1:NS, F2:VE	N=7, NV_E N=8, NV_N N=9, WD_E N=8, WD_N	all groups pass normality test (W=0.9370-0.9653 ... p=0.5817-0.8515) F1:NS, SS=11.77, df=1, MS= 11.77, ... F=0.002, p=0.9646 F2:VE, SS=19823, df=1, MS=19823, … F=3.382, p=0.0765 INT, SS=4352, df=1, MS=4352, … F=0.7425, p=0.3962, no sig MC

Table 4, continued. Data is listed by figure with corresponding means±SEM, statistical tests, sample sizes (N), and statistical parameters with test outputs. SOURCE: Author

STATISTICAL TESTS AND OUTPUTS BY FIGURE, CONTINUED				
Open Field Test, Center Visits, Fig. 15	NV_E =41.43±8.33 NV_N=43.13±5.40 WD_E= 23.89±6.38 WD_N=48.63±7.54	Shapiro-Wilk, normality Two-Way ANOVA, Holm-Sidak's multiple comparisons, F1:NS, F2:VE	N=7, NV_E N=8, NV_N N=9, WD_E N=8, WD_N	all groups pass normality test (W=0.8395-0.9760 ... p=0.0744-0.9382) F1:NS, SS=287.6, df=1, MS=287.6, ... F=2.417, p=0.1313 F2:VE, SS=1830, df=1, MS=1830, … F=4.411, p=0.0448 INT, SS=1053, df=1, MS=1053, … F=2.417, p=0.1313 MC, NV_N vs WD_E, p=0.0499 WD_N vs WD_E, p=0.0318
Open Field Test, Distance Travelled, Fig. 15	NV_E =4643.35±772.32 NV_N=4534.47±346.71 WD_E=2986.28±517.92 WD_N=4822.83±686.88	Shapiro-Wilk, normality Two-Way ANOVA, Holm-Sidak's multiple comparisons, F1:NS, F2:VE	N=7, NV_E N=8, NV_N N=9, WD_E N=8, WD_N	all groups pass normality test (W=0.8303-0.9704 ... p=0.0656-0.9011) F1:NS, SS=3717305, df=1, MS=3717305, ... F=1.172, p=0.2883 F2:VE, SS=13320241, df=1, MS=13320241, … F=4.198, p=0.0499 INT, SS=7509801, df=1, MS=7509801, ... F=2.367, p=0.1352 MC, NV_N vs WD_E, p=0.0302 WD_N vs WD_E, p=0.0380
Novel object, #Approaches, Fig 16	NV_E = 122.39±29.46 NV_N= 148.95±30.04 WD_E= 100.19±19.85 WD_N=173.58±22.33	Shapiro-Wilk, normality Two-Way ANOVA, Holm-Sidak's multiple comparisons, F1:NS, F2:VE	N=7, NV_E N=8, NV_N N=9, WD_E N=8, WD_N	all groups pass normality test (W=0.9279-0.9614 ... p=0.4620-0.8234) F1:NS, SS=25.53, df=1, MS= 25.53, ... F=0.3463, p=0.5610 F2:VE, SS=41.11, df=1, MS=41.11, … F=0.5574, p=0.4615 INT, SS=114.2, df=1, MS=114.2, … F=1.549, p=0.2236, no sig MC

Table 4, continued. Data is listed by figure with corresponding means±SEM, statistical tests, sample sizes (N), and statistical parameters with test outputs. SOURCE: Author

STATISTICAL TESTS AND OUTPUTS BY FIGURE, CONTINUED				
Novel object, Time Spent, Fig. 16	NV_E = 14.14±3.86 NV_N= 12.72±2.51 WD_E= 6.57±1.37 WD_N=19.73±6.16	Shapiro-Wilk, normality Kruskal-Wallis, Dunn's multiple comparisons	N=7, NV_E N=8, NV_N N=9, WD_E N=8, WD_N	all groups pass normality test … NV_E=pass, W=0.9566, p=0.7892 … NV_N=pass, W=0.8832, p=0.8657 …WD_E=pass, W=0.8657, p=0.1106 …WD_N=fail, W=0.7596, p=0.104 H=7.987, p=0.463 NV_E vs WD_E, MRD=10.82, p=0.0220 NV_N vs WD_E, MRD=9.076, p=0.0463 WD_E vs WD_N, MRD=-11.01, p=0.0156
LDTg Novel Object Amplitude, Fig. 16	TART_SAL=1.28±0.10 TART_MEC=1.33±0.09 NIC_SAL=1.38±0.64 NIC_MEC=0.64±0.13	Shapiro-Wilk, normality Two-Way RM ANOVA, Holm Sidak's multiple comparisons, F1:NS, F2:INJ	N=4, TART N=5, NIC	all groups pass normality test (W=0.8443-0.9590 … p=0.2082-0.8121) F1:NS, SS=0.4146, df=1, MS= 0.4146, ... F=1.538, p=0.2501 F2:INJ, SS=0.5676, df=1, MS=0.5676, … F=7.794, p=0.0235 INT, SS=0.7435, df=1, MS=0.7435, … F=10.21, p=0.0127 MC, ... TART-NIC, MEC, p=0,0404 … SAL-MEC, NIC, p=0.0030
GRAB-DA Peak #, Fig. 20	*Baseline* TART_SAL=24.4±3.13 TART_MEC=18.4±4.12 NIC_SAL=19.3±3.25 NIC_MEC=25.0±3.72 *Injection* TART_SAL=18.4±2.80 TART_MEC=15.4±2.71 NIC_SAL=16.5±4.38 NIC_MEC=18.8±3.77	Shapiro-Wilk, normality Two-Way RM ANOVA, Sidak's multiple comparisons, F1:NS, F2:WIN	N=5, TART N=6, NIC	all groups pass normality test (W=0.7989-0.9554 ... p=0.0575-0.7755) F1:NS, SS=6.412, df=1, MS= 6.412, ... F=2.510, p=0.8450 F2:WIN, SS=221.7, df=3, MS=73.89, … F=1.171, p=0.3371 INT, SS=224.4, df=3, MS=74.80, … F=1.185, p=0.3340 no sig main effect no sig simple effect

Table 4, continued. Data is listed by figure with corresponding means±SEM, statistical tests, sample sizes (N), and statistical parameters with test outputs. SOURCE: Author

STATISTICAL TESTS AND OUTPUTS BY FIGURE, CONTINUED				
GRAB-DA Δ Peak #, Fig. 20	TART_SAL=-1.6±1.56 TART_MEC=-6.0±5.0 NIC_SAL=-6.3±3.16 NIC_MEC=-2.8±4.99	Shapiro-Wilk, normality Two-Way RM ANOVA, Sidak's multiple comparisons, F1:NS, F2:INJ	N=5, TART N=6, NIC	all groups pass normality test (W=0.8535-0.9805 ... p=0.1679-0.9370) F1:NS, SS=0.000, df=1, MS= 0.000, ... F=0.000, p=0.9999 F2:INJ, SS=0.1515, df=1, MS=0.1515, … F=0.0009771, p=0.9757 INT, SS=54.70, df=1, MS=54.70, … F=0.3527, p=0.5672, no sig MC
GRAB-DA Peak Amp, Fig. 20	*Baseline* TART_SAL=1.48±0.23 TART_MEC=1.54±0.25 NIC_SAL=1.28±0.24 NIC_MEC=1.51±0.24 *Injection* TART_SAL=1.63±0.14 TART_MEC=1.50±0.10 NIC_SAL=1.73±0.19 NIC_MEC=1.02±0.14	Shapiro-Wilk, normality Friedman RM, Dunn's multiple comparison's	N=5, TART N=6, NIC	all groups did not pass normality test Friedman statistic = 9.800 p=0.0130 MC, … NIC_SAL vs NIC_MEC (injection), p=0.0219
GRAB-DA Δ Peak Amp, Fig. 20	TART_SAL=0.16±0.20 TART_MEC=-0.04±0.18 NIC_SAL=0.45±0.26 NIC_MEC=-0.50±0.14	Shapiro-Wilk, normality Two-Way RM ANOVA, Sidak's multiple comparisons, F1:NS, F2:INJ	N=5, TART N=6, NIC	all groups pass normality test (W=0.8253-0.9671 ... p=0.1282-0.8727) F1:NS, SS=0.03873, df=1, MS= 0.03873, ... F=0.8725, p=0.5789 F2:INJ, SS=1.774, df=1, MS=1.774, … F=5.873, p=0.0384 INT, SS=0.7747, df=1, MS=0.7747, … F=2.565, p=0.1437 MC, … SAL-MEC, NIC, p=0.0304
GRAB-DA Peak AUC. Fig. 20	*Baseline* TART_SAL=0.48±0.05 TART_MEC=0.50±0.12 NIC_SAL=0.46±0.10 NIC_MEC=0.49±0.10 *Injection* TART_SAL=0.62±0.065 TART_MEC=0.73±0.18 NIC_SAL=0.68±0.10 NIC_MEC=0.30±0.08	Shapiro-Wilk, normality Friedman RM, Dunn's multiple comparison's	N=5, TART N=6, NIC	all groups did not pass normality test Friedman statistic = 12.80 p=0.0009 MC, … NIC_SAL vs NIC_MEC (injection), p=0.0021

Table 4, continued. Data is listed by figure with corresponding means±SEM, statistical tests, sample sizes (N), and statistical parameters with test outputs. SOURCE: Author

STATISTICAL TESTS AND OUTPUTS BY FIGURE, CONTINUED				
GRAB-DA Δ Peak AUC	TART_SAL=0.16±0.20 TART_MEC=-0.04±0.18 NIC_SAL=0.45±0.26 NIC_MEC=-0.50±0.14	Shapiro-Wilk, normality Two-Way RM ANOVA, Sidak's multiple comparisons, F1:NS, F2:INJ	N=5, TART N=6, NIC	all groups pass normality test (W=0.8912-0.9826 ... p=0.3632-0.9639) F1:NS, SS=0.2029, df=1, MS=0.2029, ... F=2.954, p=0.1198 F2:INJ, SS=0.8633, df=1, MS=1.774, … F=6.125, p=0.0384 INT, SS=0.4139, df=1, MS=0.4139, … F=2.970, p=0.1189 MC, … SAL-MEC, NIC, p=0.0355

Table 4, continued. Data is listed by figure with corresponding means±SEM, statistical tests, sample sizes (N), and statistical parameters with test outputs. SOURCE: Author

STATISTICAL ABBREVIATIONS IN TABLE 4	
ABBREVIATION	**DEFINITION**
D1-D28	day 1 - day 28
DEP	nicotine dependent
DEP_E	nicotine dependent + EGFP
DEP_N	nicotine dependent + NpHR
df	degrees of freedom
F	F test
F1	Factor 1
F2	Factor 2
F3	Factor 3
H	Kruskal-Wallis statistic
INJ	injection
INT	interaction
K2	higher is more significant
K2	D'Agostino & Pearson statistic
LO	light on/off (days 1-5)
MC	multiple comparisons
MRD	mean rank difference
MS	mean square
NIC	nicotine
NS	nicotine state
NV	nicotine naïve
NV_E	nicotine naïve + EGFP
NV_N	nicotine naïve + NpHR
SC	scent
sig	significant
SS	type III sum of squares
TART	tartrate
U	Mann-Whitney statistic
VE	viral expression
W	Shapiro-Wilk statistic
WD	nicotine withdrawn
WD_E	nicotine withdrawal + EGFP
WD_N	nicotine withdrawal + NpHR
WIN	recording window

Table 5. Statistical abbreviations

Abbreviation meanings for Table 3.

DISCUSSION

Translatability of nicotine dependence and withdrawal in mice

Translation of animal model findings to human disease is an important goal of research. While we cannot perfectly mimic human nicotine addiction, we can take several methods under consideration to produce meaningful results.

Nicotine Exposure

To establish nicotine dependence within our experiments, we subjected the mice to forced nicotine drinking for 4-weeks. Under these conditions, mice exhibit elevated serum cotinine levels (consistent with concentrations exhibited by heavy human smokers) and demonstrate both spontaneous and mecamylamine-precipitated withdrawal symptoms[147,151,161]. This confirms that mice are consuming relevant levels of nicotine and developing dependence that causes withdrawal symptoms when access to nicotine is removed. Nicotine is an appetite suppressant, and we see lower body weight of nicotine drinking animals compared to tartrate controls on the tail end of our 4-week exposure, consistent with the expectation that nicotine is causing decreased food consumption compared to controls. While the mice gained less weight over time due to consuming nicotine solution, this method of nicotine exposure does not cause weight loss, allowing us to perform behavioral tests on mice at a biologically healthy weight. If mice had body weight reduction of >20% they would have been removed from the study. However, none of our mice exhibited weight loss with the given nicotine concentration. Any difference in weight did not impair general activity level or baseline behavior as seen in our saline controls.

This method of nicotine exposure models the intermittent nicotine intake of human smokers. The mice consume nicotine during the waking hours and decline in nicotine intake during sleep cycles. This method of chronic nicotine exposure has advantages over daily nicotine injections or osmotic minipumps that deliver nicotine at experimenter-determined time points or continuously. While these other methods allow for precise measurement of nicotine dose, they lack the natural kinetics of nicotine exposure experienced by smokers which impacts receptor dynamics and circuit plasticity[162,163]. A limitation of nicotine drinking water is the lack of conditioned cue associations and operant responding during nicotine consumption, they must drink the water for hydration. Intravenous self-administration (IVSA) is the best model for human drug taking behavior, as it includes operant cue associations and quantitative measure of drug pursuit. However, IVSA requires food restriction and extensive training which lessen the clinical significance[164]. An additional option for nicotine exposure is 2-bottle choice. While this method would provide additional details about nicotine seeking, there is evidence from our lab and others that suggest oral nicotine is not consumed at higher levels than control water in mice which may limit nicotine consumption by choice[165]. While this limits experiments in studies of nicotine reinforcement, oral nicotine administration remains a great method of studying withdrawal behaviors. Additionally, we chose forced nicotine drinking over 2-bottle choice to avoid water restriction or co-exposure to ethanol[165,166]. Further complications with 2-bottle choice include side preference of one water bottle over another[161]. Side preference can be minimized by switching the relative positions of the bottles. However, this method creates an even higher barrier for mice to learn which bottle contains nicotine, a substance that won't readily be consumed in solution to begin with. Additionally, during 2-bottle choice, mice are traditionally single-housed which introduces stress to the animals[161]. This has been known to impact metabolism and

neurotransmitter signaling, reducing clinical significance[167]. While IVSA and 2-bottle choice provide a way to study drug seeking, cue associations, and relapse, it is not the best method for our questions surrounding withdrawal, which require a reliable induction of nicotine dependence.

While some nicotine consumption in humans occurs through oral or nasal administration (smokeless tobacco), most is inhaled. The route of nicotine intake in our mice is gastrointestinal and not respiratory. A limitation of oral administration is that nicotine will be metabolized in the liver, leading to lower quantities of nicotine levels in the brain[161]. Studies have suggested that cotinine levels are about 1/3 for the same dose of oral nicotine vs injected nicotine[161]. The 4-week drinking timeline was chosen to combat this limitation, allowing more nicotine to accumulate in the system, as seen by cotinine levels. Our data and that from other labs have reported clinically relevant levels of nicotine within the brain using this protocol[147,151]. More recent models of vaporized nicotine operant self-administration have been established[168]. Studies are currently validating withdrawal behaviors and nicotine serum concentrations to see if this can be an improved model of nicotine dependence and withdrawal[168]. Future studies should observe the effects of IPN and LDTg using this method of nicotine delivery.

Nicotine is known for its bitter taste and irritant properties[161]. Nicotine activates chorda tympani neurons that are sensitive to bitter tastes such as quinine[161]. Elimination of the bitter taste receptor, TRPM5, in mice reduces chorda tympani response to nicotine and additional administration of mecamylamine further reduces this response[161]. This suggests that nAChRs independently modulate the bitter taste to nicotine[161]. Interestingly, smokers have on average higher taste thresholds than non-smokers[161]. The aversive taste of nicotine is also observed in mice[161]. To combat the bitter taste of nicotine, we added saccharin sweetener to the solution for palatability.

Induction of withdrawal

After nicotine exposure for 4-weeks, we precipitated withdrawal using 2 mg/kg mecamylamine (MEC), a non-selective, non-competitive nAChR antagonist. This antagonist readily crosses blood brain barrier[169]. MEC is primarily used as an experimental tool but also was the first orally available antihypertensive drug approved in humans as a parasympathetic ganglionic blocker[169]. Therapeutically, it is not prescribed in most cases due to its severe side effects. MEC-precipitated withdrawal in rodents has been used consistently in the field since the 1990s and has been verified by many other labs to induce a withdrawal-like state in nicotine dependent mice but not in control mice[150,153]. The dose we used minimizes the adverse side effects of MEC administration while inducing robust withdrawal symptoms in nicotine dependent subjects. While this method of nicotine withdrawal is less comparable to human nicotine cessation, antagonist-induced withdrawal produces a quick, reliable, and robust withdrawal state. Of note, precipitated withdrawal is a phenomenon that we see in humans addicted to other drugs of abuse including opioids. Buprenorphine is a high affinity partial agonist of the mu-receptor, weak antagonist of the kappa receptor, and weak agonist of the delta receptor[170]. Buprenorphine replaces heroin molecules attached to opioid receptors and produces a significantly reduced opioid reaction also triggering withdrawal symptoms[170]. Mecamylamine administration in humans does not elicit a major withdrawal state but does reduce subjective and reinforcing effects of cigarettes influencing smoking behavior[171].

Spontaneous withdrawal (removal of nicotine water for 24-hours) mimics human nicotine cessation but is variable in timing and severity of symptoms[150]. Behavioral experiments already have a great deal of variability, so it is important that the severity of withdrawal symptoms is comparable across groups. We have repeated our experiments in spontaneous withdrawal and seen

similar behavioral results in many measures (data not shown). MEC-precipitated withdrawal standardizes the timing of withdrawal for more interpretable and reproducible results. Importantly, MEC injection elicits a withdrawal state similar to spontaneous withdrawal including circuit level activation of the GABAergic neurons in the IPN and withdrawal behavior in nicotine dependent, but not control mice[121,123,150]. All of these factors make MEC-precipitated withdrawal a very useful tool in studying withdrawal-based questions. A strength of combining oral nicotine administration with MEC-precipitate withdrawal, is that previous studies have shown somatic, affective, and cognitive symptoms induced in both male and female mice[153,161].

MEC-precipitated withdrawal in rodents is likely a complex version of a withdrawal state that is not completely understood. Because administration of the antagonist is systemic, nicotinic receptors everywhere within the CNS and PNS are targeted. More specifically, nicotinic antagonism selectively with MEC within the MHb or IPN, but not the VTA, hippocampus or cortex, triggers nicotine withdrawal in nicotine exposed mice[122]. One interpretation being nicotine dependence involves sensitization of nicotinic signaling. Within the IPN, it has been hypothesized that chronic nicotine exposure potentiates the signaling from SSt GABA interneurons onto MHb glutamatergic terminals in the IPN through β3 and β4 nAChR upregulation[121]. The activation of GABAergic interneurons silences the IPN GABA projection neurons, by blocking the glutamatergic input[121]. After MEC exposure (or nicotine cessation), β3 and β4 receptors are blocked (or no longer activated by nicotine), silencing SSt GABA interneurons and allowing glutamatergic signaling from MHb and activation of IPN GABAergic projection neurons[121]. Taken together, chronic exposure of nicotine combined with MEC-precipitated withdrawal is an experimental approach to study nicotine withdrawal behavior and circuit level questions in mice.

LDTg activity is suppressed during nicotine withdrawal

Originally, the LDTg was defined as a center for attention and REM sleep[172,173]. More recently, the nucleus has been implicated in locomotion, reward, and mood[172,174]. While the contribution of LDTg to drug research is relatively new, there are several studies implicating the LDTg in the sensitizing effects of psychostimulants and reward from drugs of abuse[172]. For example, LDTg-lesioned rats show attenuation of amphetamine and morphine-induced locomotor behaviors and dopamine release[175,176]. In addition to drug locomotor effects, LDTg has been shown to play a role in drug seeking and acute drug exposure[172]. AMPA/kainate receptor blockade in LDTg decreases cocaine reinstatement[95]. A single injection of nicotine increases cfos in the LDTg and these cells were non-cholinergic[177]. LDTg cholinergic cells do co-express α7 and β2, arguing for a direct effect of nicotine on this cell type despite cfos data[172]. Patch clamp studies show nicotine excitatory action on LDTg cholinergic cells with large inward currents[178]. These nicotine-mediated inward currents are the result of α7, β2, and other non-α7 subunits[178]. The subunit expression of GABAergic and glutamatergic LDTg neurons are not known, however, α4 is present on non-cholinergic neurons[172]. Glutamatergic EPSC on cholinergic cells are sensitive to MEC and not sensitive to MLA (α7 antagonist) or DHBE (β2 antagonist)[172]. GABAergic IPSCs were sensitive to MEC, MLA and DHBE[172].

So far, LDTg literature surrounding drugs of abuse have failed to capture its role in the progression of drug addiction. Studies have captured aspects of withdrawal such as lesion-induced changes in behavior and effects of single or minimal repeated dose exposure on cellular activation. There are no studies characterizing the role of LDTg in nicotine (or other drug) withdrawal. In our studies, we observed a depression of LDTg activity with pan-neuronal GCaMP6s during MEC-precipitated nicotine withdrawal *in vivo*. LDTg is spontaneously active and after an injection of

MEC in nicotine dependent animals there is a depression of average peak amplitude and AUC (within a 500-ms window). Of note, average AUC is still decreased when you analyze the entire peak and not within a specific window (data not shown). We did not see a significant change in the number of peaks after MEC injection. A change in the size of peaks without a change in the number can indicate a decrease in the number of active neurons being recorded or a decrease in the coordinated activity of the same population of neurons.

Method considerations

Fiber photometry recordings measure fast calcium dynamics after a relatively non-invasive surgery, in freely moving mice. However, this method does have limitations. This method records "bulk" signal from a population of neurons and does not allow for spatial information that can be obtained with single cell resolution[179]. However, for our studies, behavior readouts were an important endpoint of nicotine withdrawal. This method allows for correlation of animal behavior to neuronal activity without head restriction and has minimal tissue damage[179].

Summary

Up until this study, there was no evidence for a role of the LDTg in nicotine withdrawal or withdrawal from any drugs of abuse. These results propose that MEC-precipitated nicotine withdrawal broadly suppresses LDTg activity. We hypothesize this suppression may come from long-range GABAergic inputs, including the IPN. Future studies should observe cre-dependent activity within the GABAergic, cholinergic, and glutamatergic populations for increased resolution of the important cell types in the effect of decreased cellular activity associated with nicotine withdrawal. Additionally, pharmacological blockade of different receptors may provide

insight about the mechanism of suppressed activity either during *in vivo* photometry recordings or during *in vivo, or ex vivo,* electrophysiology.

The IPN sends GABAergic synaptic connections differentially to cell types in LDTg

The LDTg contains GABAergic, glutamatergic, and cholinergic cell types that are largely distinct with very little evidence for neurotransmitter co-expression[81]. While the IPN is largely a GABAergic nucleus, it does contain small amounts of glutamate[133]. During development, the IPN undergoes complex migratory events along a rostral-caudal axis, driven by key transcription factors[180]. Deficits or variations of transcription factors have been linked to various psychiatric disorders, indicating that the organization of brain nuclei is important in function. In this study, we observed the IPN subregion-specific connections to the LDTg through rabies-mediated monosynaptic tracing and identified the GABAergic nature of these inputs using IHC staining.

Local LDTg connectivity

Within the LDTg, we see relatively equal expression of starter cells in GAD, ChAT and Vglut cre-expressing mouse lines. Interestingly, we see greater number of local synaptic connections to GABAergic and glutamatrgic LDTg neurons than to cholinergic neurons. The local synaptic inputs to GABAergic LDTg neurons are almost equally proportional to the number of starter cells. One interpretation of this result is that GABAergic cells receive more synaptic connections from local interneurons. Alternatively, we are not able to conclude if a starter cell is also providing local connections. Another interpretation is that cholinergic local connections are coming from other cholinergic neurons, while GABAergic and glutamatergic cells receive local

synaptic connections from cell types different than the starter cell population and this effect was masked by the helper virus expression.

IPN presynaptic targets and subregions

There is strong topological organization of MHb to IPN connections. Ventral MHb (vMHb) innervates the majority of IPN with glutamatergic/cholinergic connections to the most central and dorsal regions (IPR, IPC, IPI, IPDM) while the dorsal MHb (dMHb) innervates the most lateral region (IPL,IPDL) with glutamatergic/SP/NKB signaling[181]. Overall, dMHB seems to regulate exercise motivation, hedonic state, and primary reinforcement; while vMHB regulates drug addiction, withdrawal, anxiety, and depression through cholinergic projections[133]. There has not been a strong case for MHb innervation of IPA subregion. While a few studies have examined which IPN subregions project to LDTg, this is the first to classify by the three LDTg cell types and with use of RV. Previous tracing studies using CBt, and other conventional tracers, have many limitations. For example, they are taken up by fibers of passage, may have non-specific labeling, do not rely on functional connectivity, and may not be exclusively retrograde axonal transport[182].

We observed GABAergic drive from the IPN to LDTg GABAergic neurons most strongly from the central regions of IPN (IPR, IPC) and to LDTg glutamatergic neurons from both the central and lateral regions of IPN. In comparison to cholinergic neurons, GABAergic and glutamatergic LDTg neurons received more IPN input in proportion to the number of starter cells (convergence index). A pitfall of this analysis is that you cannot assume that starter cells do not share presynaptic input cells[183]. Regardless of if cholinergic neurons are receiving less input from the IPN or if they are receiving divergent input from a small set of IPN cells, the input cells are localized to the periphery of the IPN (IPL, IPDL, IPDM). An interesting future direction would be

to design the experiment with a range of starter cell numbers within the LDTg cholinergic neurons and see how the relative number of IPN input cells changes or remains the same. For all LDTg starter cells, the IPN inputs were largely GABAergic.

Function of the IPN, seems to vary by IPN subregion and the subregions of input cells to LDTg are likely important to behavior. Cfos activation studies show nicotine withdrawal activation specifically within the more central regions (IPC/IPI), and within the IPN in general[121,123,184]. This suggests that projections to GABAergic and glutamatergic neurons may be recruited more during nicotine withdrawal. Additionally, there are region specific difference in nicotinic receptor composition in the MHb-IPN projections that have differing contributions to withdrawal behavior. vMHb inferior portion is the only vMHb region expressing α6 (in addition to α3, β2, β3, and β4) that largely projects to IPC/IPI regions[185]. vMHb central portion contains α3, β2, β3, and β4 and largely projects to IPR/IPC/IPI regions[185]. vMHb lateral portion is the only vMHb region expressing α4 (in addition to α3, β2, β3, and β4) that largely projects to IPR/IPDM[185]. In all regions α3 and β4 were expressed at very high levels[185]. IPN expresses α5 (lower in IPDL/IPL) and α2 throughout the entirety of IPN[117]. IPR/IPDM express α4, IPR/IPC express α6[117]. IPN expresses β2 throughout but lowest in IPR/IPC[117]. IPN expresses β3 uniformly but lowest in IPDM/IPR[117].

Most of the studies showing receptor contribution to nicotine withdrawal come from global receptor KOs[14,117].

- α2 KO have decreased somatic withdrawal signs
- α3 KO have developmental abnormalities, but pharmacological inhibition blocks somatic withdrawal and hyperalgesia.
- α5 KO have decreased somatic withdrawal, hyperalgesia, conditioned place aversion (CPA), and anxiety but no change in withdrawal-induced shifts in intercranial self-

stimulation (ICSS). ICSS is delivery of electrical pulses into the medial forebrain bundle (also lateral hypothalamus, VTA, and pons).

- No α6 KO, but pharmacological blockade shows decreased CPA and anxiety with no change in somatic signs
- α7 KO have delayed hyperalgesia, reduced ICSS, and reduced somatic signs (does not persist at longer withdrawal timepoints)
- β2 KO mice have no change in somatic signs or hyperalgesia, or ICSS

Together with previous literature, the results of this subregion analysis may suggest that GABAergic and glutamatergic neurons to LDTg are involved in nicotine withdrawal. GABAergic IPN neurons originating from central IPN project to GABAergic and glutamatergic LDTg neurons. IPR and IPC have shown cfos activation to nicotine withdrawal[121,123,184]. This is contradictory to previous studies that identified IPR connections to LDTg as glutamatergic, while IPDL connections are GABAergic[133]. These studies are not easily comparable due to differences in retrograde labeling techniques (CBt vs RV). Our studies show an overwhelming majority of IPN-LDTg connections to all cell types are GABAergic. Interestingly, there is evidence that LDTg sends reciprocal connections to the IPN that are largely GABAergic[132]. This may provide evidence for IPN-LDTg GABAergic loop[132], which have been proposed to have an overall disinhibition and temporally coordinated oscillatory activity[186]. On the other hand, cholinergic LDTg neurons receive connections from the IPL and IPDL, which are less implicated in nicotine withdrawal.

Method considerations

Rabies virus (RV) spreads exclusively in the retrograde direction in central nervous system neurons[187]. In our experiments, the glycoprotein ("G" protein) has been deleted, without which

RV is incapable of spreading to presynaptic neurons. The RV is also coated with an envelope of the avian-endemic retrovirus ("EnvA"), rendering the virus incapable of infecting the mammalian neurons. With these RV modifications, a second helper virus can be used to selectively express the rabies virus within experimentally designed neuronal targets. The helper virus contains the receptor for EnvA ("TVA receptor") to allow for infection of starter cells and the "G" protein to allow for synaptic transport. We used a cre-dependent AAV helper virus that introduced both helper proteins in our cre-mouse lines (ChAT-cre or GAD-cre).

Cre-mice are genetically modified to express cre recombinase in specific cell types. Throughout this study we introduced a variety of cre-dependent AAVs containing gene cassettes that rely on recombination for genetic expression. Cre-dependent AAVs utilize the Cre/Lox system for protein expression. Transgenes are surrounded with 2 pairs of lox recombinant sites and the gene cassette is inverted relative to the promoter between these sites (DIO or FLEX). When the lox sites (viral injection) contacts cre recombinase (mouse line), two steps happen. First, the open reading frame of the gene cassette is reverted, and the transgene is now in the correct orientation to be transcribed and expressed. Second, the recombination orients one of each lox site pairs in position to be excised. The excision ensures the transgene is no longer able to flip back to the inverted orientation, leaving only two pairs of mismatched lox sites behind. This allows for restriction of protein expression within specific cell types and regions of the brain.

A limitation of this technique is that high concentrations of "G" proteins and relatively low levels of TVA must be present to have successful transsynaptic spread[187]. While you can inject two separate AAVs for each helper protein, this decreases the chance of successful infection of starter cells with the three substates needed for tracing. To ensure expression of TVA and "G" protein in the same cell we used an AAV containing both proteins to be expressed under the same

promoter, which increases chances of success. However, high concentrations of AAV can lead to "leak" (spontaneous recombination of virion's genomes leading to non-specific AAV expression)[188]. We controlled for leaky expression by injecting our viruses in wild type mice. We saw no AAV-helper or RV expression in these mice. Additionally, we used secondary stains to verify that the AAV is restricted within the expected cell type.

Successful cell body staining for GABAergic neurons using GAD varies widely based on the region. GAD67 stains cell bodies better than GAD65, which labels synapses strongly[189]. GAD67 primarily forms homodimers with itself and stays in the cell bodies but it will form heterodimers with GAD65 and be transported to the synapses[190]. With the high density of GABAergic cell bodies within the IPN, the cell body stain is not always identifiable from the surrounding tissue and may overinflate the number of GAD+ neurons reported. While this method does stain for protein expression, studies using RNAscope for mRNA may provide improved colocalization analysis in future studies. Another consideration for future studies should be to quantify ipsilateral vs contralateral projections. For analysis, projections from both sides were counted and combined.

Whole brain mapping reveals differential inputs to LDTg cholinergic and GABAergic cells

While the primary goal of our RV tracing experiment was to observe subregion specific information from IPN inputs, we also were able to obtain whole brain mapping of all inputs to LDTg. One other study has utilized rabies transsynaptic tracing from LDTg glutamatergic, cholinergic, PV-positive, and SOM-positive cells to label long-range inputs[82] and another from cholinergic only[191]. Our study differs by the number of slices sampled (every other vs every fourth

slice), looking at GAD-cre starter cells instead of PV or SOM cre starter cells, and identification of presynaptic inputs as GAD+.

Cholinergic LDTg starter cells

Cholinergic LDTg neurons receive presynaptic inputs from across the entirety of the brain with the largest proportion coming from cortex, midbrain, and striatum. Very few inputs came from thalamus and pallidum.

Cortical projections to LDTg have been identified by other tracing studies[82,97,191]. However, a role for these projections has not been identified other than PL for top-down control[192]. We observed high cortical labeling from SS, MO, AUD, RSP, and PL. Other notable connections include presynaptic inputs from striatum (dorsal, ventral and lateral septal complex), reticular formation, substantia nigra, hippocampus, cerebellum, midbrain reticular nucleus, superior and inferior colliculus, hypothalamus (lateral zone), NTS, pons, IPN, PAG, dorsal column nuclei, spinal nucleus of the trigeminal, vestibular nuclei, and pontine reticular nuclei.

GABAergic LDTg starter cells

GABAergic LDTg neurons receive presynaptic inputs from across the entirety of the brain with the largest proportion coming from midbrain, hindbrain, and medulla. Very few inputs came from thalamus and pallidum.

PAG innervation to LDTg has been reported by several tracing studies, yet a clearly defined role for this circuit has not been identified[82,97,191]. There are reciprocal connections between these two nuclei.

Other notable presynaptic inputs to LDTg GABAergic neurons include, hypothalamus (lateral and medial zone and periventricular region), cerebellum, cortex, IPN, inferior and superior colliculus, pontine reticular nucleus, nucleus incertus, dorsal tegmental nucleus, dorsal striatum, reticular formation, pons, pontine central gray, hippocampus, midbrain reticular nucleus, vestibular nuclei, perihypoglossal nucleus, raphe nuclei, substantia nigra, inferior olive, lateral habenula, and VTA.

Methodological considerations

A limitation of our experiment includes under sampling from some specific regions due to preparation: small portion of cortical/hippocampal regions, most posterior sections of brainstem, most anterior sections of cortex, and all of the olfactory bulb. While this may slightly skew our results, we had a relatively high sampling rate (every other slice at 40μm) and are likely capturing a highly representative summary of the mouse brain. Additionally, while we combined visual anatomical landmarks (aqueducts, ventricles, high density vs. low density, etc.), comparison of serial sections, and spatial distances from midline or identifiable structures, precise delineations obtained by tissue specific markers were not utilized. When a precise structure could not be identified with certainty, the cell was grouped into a broader category still being as specific as possible.

The habenulo-peduncular system regulates nicotine withdrawal through LDTg

The dorsal diencephalic conduction system (DDC) is heavily conserved and is important in the regulation of mood and motivation[193]. Within this system is the MHb that sends dense projections to the IPN through the fasciculus retroflexus fiber bundle[193]. These projections are

largely excitatory cholinergic, with glutamate co-expression[118]. These neurons have pacemaker activity (controlled by HCN channels)[118]. Short photo stimulation produces fast excitatory post synaptic currents, while tonic stimulation produces slow inward currents in IPN neurons[185]. Additionally, substance P, GABA, norepinephrine, serotonin, ATP, interleukin-18, and other neuropeptides have been identified within this pathway[118]. Fear, stress, anxiety and depression have all been linked with the MHb-IPN pathway in rodents and several studies corroborate the role of this pathway in mood disorders in humans[185].

In addition to mood disorders, this circuit broadly modulates effects of drugs of abuse and psychostimulants, notably alcohol, opiates, and nicotine[118]. The most studied drug of abuse in the MHb-IPN circuit is nicotine. Together, the MHb and IPN express the highest density of nAChRs in the mammalian brain, with >90% of MHb neurons expressing nAChRs[118]. During nicotine addiction, the drug interacts with the high density of receptors here to limit drug intake and mediate withdrawal symptoms.

It is likely that somatic and affective nicotine withdrawal symptoms are regulated through MHb excitatory drive to IPN GABAergic neurons[14]. During nicotine withdrawal, GABAergic neurons in the IPN are activated[121]. Opto-activation of these neurons stimulates somatic withdrawal symptoms in nicotine dependent mice and NMDA inhibition in IPN reduces withdrawal symptoms[121]. Opto-inhibition of MHB cholinergic neurons alleviates nicotine withdrawal anxiety[123,124]. While this paints a picture of MHb-IPN control of nicotine withdrawal behaviors, it is still unknown how IPN mediates this withdrawal behavior to the limbic system. Previously our lab demonstrated that connections from the IPN to the LDTg are GABAergic. In this study, we show that the IPN-LDTg GABAergic circuit mediates both somatic and affective nicotine withdrawal symptoms.

Using optogenetics, we blocked GABAergic input from IPN terminals in LDTg during nicotine naïve, dependent, and withdrawn conditions. Both IPN and LDTg have been connected to locomotor behaviors. To verify our manipulation had no effect on baseline locomotion, we monitored distance traveled with and without optogenetic inhibition and saw no significant effect of opto-inhibition. We observed a preference for light inhibition only during nicotine withdrawn conditions, suggesting that blockade of this circuit reduces the negative affective state experienced during nicotine withdrawal. Importantly, nicotine naïve and dependent conditions showed no significant preference, indicating inhibition of this circuit alone was not rewarding to baseline MEC injections or chronic nicotine exposure alone. Over 3 consecutive days of testing, nicotine withdrawn mice maintained a preference for IPN-LDTg GABAergic terminal inhibition. Smokers typically require more than one quit attempt to successfully abstain from nicotine[79], and the persistence of our optogenetic treatment suggests that a therapeutic developed to target this same endpoint would work even after multiple relapse events. Environmental context is an important driver of smoking cues and conditioned smoking behavior and relapse[194]. Our data shows evidence of context dependent conditioning to inhibition of the IPN-LDTg GABAergic terminals. After 3 conditioning days, a posttest day (the light is turned off) reveals that the group of nicotine withdrawn mice stop preferring the light-paired chamber. This is likely because the mice are experiencing their normal baseline, nicotine dependent state. However, if they are injected with MEC and are actively experiencing an aversive withdrawal response, they maintain their preference for the previously light-paired side. This also has positive therapeutic potential, as it suggests that smokers may seek out this treatment when they are experience aversive withdrawal symptoms but will not seek out the treatment in a baseline state. Together these data suggest a

treatment that blocks IPN-LDTg GABAergic circuitry would have high attenuation of nicotine withdrawal and low abuse liability.

Inhibition of IPN-LDTg GABAergic terminals relieves somatic nicotine withdrawal

Nicotine withdrawal is comprised of somatic, affective and cognitive symptoms[195]. While we demonstrated the relief of withdrawal aversive state with IPN-LDTg GABAergic inhibition, it was still unclear what withdrawal symptoms were targeted by this manipulation. To test this, we applied our optogenetic manipulation during several nicotine withdrawal behavioral tests. We investigated both somatic and affective withdrawal symptoms, as there are previous studies that implicate the IPN in these behaviors[121,123]. While cognitive deficits that occur during nicotine withdrawal are important drivers of relapse, previous studies have not yet implicated IPN in these cognitive symptoms. Hippocampus, VTA, and substantia nigra have all been connected to nicotine withdrawal cognitive deficits[195,196]. While it was not the focus of this study, future studies should investigate the IPN's role (if any) in the cognitive symptoms of nicotine withdrawal. IPN has connections to hippocampus, so there is reason to suspect it may regulate some of the withdrawal cognitive symptoms surrounding learning and memory[197]. Additionally, a potential confound in our data is that nicotine withdrawal induces memory impairments, which may affect the ability of the mice to form conditioned association to the light-paired chamber. On our posttest day, we see an effect in our NpHR group but not our EGFP control mice. While learning deficits may play a role in this context dependent memory formation, typical nicotine withdrawal cognitive memory impairments show up in tests such as radial arm maze task, Morris water maze, contextual fear conditioning and spatial object recognition task[153]. Additionally, studies have shown that learned contextual aversion to the nicotine withdrawal state is possible in CPA test[198,199], indicating our

observed conditioned results are likely unaffected by the withdrawal-induced memory impairments.

To test alteration of specific withdrawal behaviors with optogenetic inhibition of GABAergic IPN-LDTg terminals, we applied this protocol in separate groups of animals to observe changes in somatic signs and affective behavior. Affective state is encompassed by a wide variety of symptoms, so we chose three separate measures of affective state that encompassed symptoms of anxiety and anhedonia – open field test, novel object test, and social odor preference test.

We measured somatic signs in an elevated plexiglass box with an angled mirror beneath to observe physical behaviors from multiple angles. Scored signs included grooming, paw licking, straub tail, shaking, rearing, backing, retropulsion, head nodding, abdominal gasps, and jumping. Signs were chosen as a compilation of reported signs across various studies. Videos were scored by a blinded experimenter. Some reported signs were excluded from analysis if they were unable to be reliably detected on video (yawns, chewing, facial fasciculations, cage scratching, ptosis, and piloerection). We noticed that across various publications, the somatic sign behaviors reported were inconsistent. We chose to comprehensively score all reported withdrawal somatic signs and we did not see any withdrawal-associated difference in the overall number of somatic signs as reported by other labs[153,200]. We did observe an increase in the duration of time spent performing somatic signs during a withdrawal state. This is likely due to 1) some signs being more indicative of a withdrawal state and 2) counting number of somatic signs skews results to signs with short durations. For example, mice can "rear" many times in one minute and in our experiment rearing was more prevalent in a control state than a withdrawn state. In contrast, a "grooming" bout may only happen a few times within a minute but it lasts for a long time and in that aspect, is more

indicative of a withdrawn state than a control state. Indeed, when we pool signs with typically longer duration (paw licking, shaking, and grooming), we see an elevation in the time per bout during nicotine withdrawal. With optogenetic inhibition, the duration of all somatic signs and time per bout (paw licking, shaking and grooming) during withdrawal decreased to levels observed in control mice. Paw licking and shaking showed the greatest duration increase during withdrawal that is recovered with optogenetic inhibition.

Previous studies revealed that IPN is activated during MEC-precipitated nicotine withdrawal and that IPN opto-activation elicits withdrawal signs similar to those seen in MEC-precipitated withdrawal[121]. Glutamatergic drive from the MHb to IPN is necessary for development of these somatic signs[121]. Conversely, opto-inhibition of IPN GABAergic neurons decreases nicotine withdrawal somatic signs[201]. Interestingly, somatic signs seem to decrease IPN activity[201]. It is likely that during nicotine withdrawal, the IPN is highly active and performing somatic behaviors may reduce IPN activity and thereby alleviate the aversive withdrawal state. With optogenetic silencing of IPN, these behaviors are no longer necessary, decreasing the number of signs (or duration of these signs) performed. This theory is supported by evidence that mice increase grooming during novel object presentation, indicating a stress relief response[202]. We have good reason to suspect that the MEC injection is mediating the somatic withdrawal symptoms through IPN because local injection of MEC into IPN or MHb elicits somatic withdrawal, but not within the VTA, hippocampus or cortex[122]. Additionally, KO of α2, α5, or β4, subunits in high density in the MHb/IPN, abolishes nicotine withdrawal somatic signs, but not in β2 KO, which are in high density in the VTA[14,117]. Our data suggests that the IPN control of physical signs of nicotine dependence is mediated downstream through the LDTg.

Inhibition of IPN-LDTg GABAergic terminals relieves affective nicotine withdrawal

Exploratory behavior in mice has been used to explore anxiety-like phenotypes. A symptom of nicotine withdrawal in mice in decreased exploration of novel apparatuses and open spaces[153]. To test the effect of IPN-LDTg optogenetic inhibition on anxiety-like affective nicotine withdrawal behavior, we used an open field test. During this test we saw a decrease in the number of visits to the center zone and distance traveled in the chamber during nicotine withdrawal. This exploratory depression was recovered with optogenetic inhibition of IPN-LDTg terminals. We did not see any change in the time spent in the center zone across groups, suggesting that while nicotine withdrawn mice are choosing to enter the center zone less frequently, all mice do not choose to spend longer periods of time in the center of the chamber (averages about 100-200s of a 1200s test). After chronic nicotine exposure, there is upregulation of the α6 receptor into MHb neurons that seem to incorporate into an α4β2 receptors[195]. Increased signaling through α4 receptors on MHB cholinergic neurons through overexpression increases anxiety behavior, and this effect is blocked by local or systemic blockade of the receptor and by optogenetic inhibition[124]. β2 KO mice blunts the effect of the anxiety-inducing effects of high doses of nicotine while β2 agonists are anxiogenic[152]. Antagonists alone have little effect on anxiety in nicotine naïve mice suggesting baseline signaling through these receptors is low, compared to direct infusion into the adjacent LHb which has anxiolytic effects regardless of nicotine exposure. Blockade of α3β4 receptors has no effect on anxiety – suggesting a strong role for somatic but not affective role of these receptors. Downstream of the habenula, the IPN has also been shown to a neuroanatomical substrate of nicotine withdrawal anxiety. Local infusions of mecamylamine induces anxiety behavior in marble burying and EPM only after chronic nicotine exposure, and this effect is mediated through CRF input from VTA and glutamatergic signaling from MHb within the IPI[123]. Together with our

results, increased sensitivity to acetylcholine during nicotine withdrawal drives activation of the MHb-IPN pathway during withdrawal induced anxiety and these effects are relayed to the limbic system through connections to the LDTg. Future studies should study anxiety response of this circuit in other measures of anxiety including elevated plus maze, marble burying test, and light-dark box.

To further probe the affective state of the mice during nicotine withdrawal, we looked at anhedonia – a common symptom of depression. Anhedonia is characterized as the reduced ability to experience pleasure[203]. In mice this may manifest as losing preference for an experience that under normal conditions is preferred or elevation in ICSS threshold[204]. Previous studies have shown that sucrose preference is reduced during nicotine withdrawal and that this response is recovered with KO of β2 or α6[205]. Sucrose preference test was not chosen for this assay as nicotine was paired with saccharin for 4-weeks. Studies show that nicotine produces a taste aversion to saccharin similar to levels seen with lithium chloride[155]. While a study has shown sucrose preference attenuation during nicotine withdrawal, this study used a mini-osmotic pump that did not pair nicotine with saccharin. Instead, we used a newer measure of hedonic preference for social odor. The social odor preference test observes the sniffing time for the scent of the urine of the mouse of the opposite sex[156,157]. During this test mice prefer to sniff the urine over no scent (dry swab), neutral scent (water swab), or sweet scent (vanilla swab)[156]. This is the first study to demonstrate nicotine withdrawal anhedonia using social odor preference test. We observed a preference for the urine swab over water in all control groups. In nicotine withdrawal this preference was lost, demonstrating anhedonia. During optogenetic inhibition of IPN-LDTg GABAergic terminals normal preference was recovered. Future studies should repeat this experiment in more traditional measure of anhedonia, such as ICSS.

Nicotine withdrawal alters normal LDTg response and dopamine release to novel object

Novel object exploration is an experimental method used to assess behavioral state (such as anxiety or depression) and recognition memory[202]. Animals will naturally explore novelty (environment, social interactions, novel objects) and repeated exposure will lead to decreased exploration (i.e., habituation)[202]. Animals can be dishabituated with spatial movement or substitution of the stimuli, enhancing preference compared to familiar context[202]. Internal psychological factors and external environmental conditions can alter the degree of novelty exploration[202].

This is the first record of LDTg activity during novel object interaction. We see a rapid rise in LDTg GCaMP6s signal immediately to novel object interaction (nose contacts object). Notably, we do not see this increase to failed approaches (stopped approach midway) or to interactions with the walls of the apparatus (nose contacts the wall) even though locomotor behavior looks very similar across these contexts. Interestingly, occasionally (~10% of interactions) result in no LDTg response to novel object interaction. Recently, the Tapper lab showed the IPN GABAergic neurons have low activity to novel stimuli and progressively increase activity with repeated exposures as an object becomes more familiar[206]. This response is mediated by MHb cholinergic/glutamatergic terminals in IPN as activation of these terminals decreases novel interaction and inhibition increases familiar interaction[206]. It is possible, that as an object becomes more familiar, the IPN GABAergic activation is preventing an increase in LDTg cell body firing. Importantly, the IPN appears to be controlling saliency over novel vs familiar interactions as IPN inhibition increases CPP for familiar social encounter[206]. Discrimination of novel vs familiar contexts is likely from cortical and hippocampal control[206].

Interestingly, during nicotine withdrawal, the durations of novel object exploration is decreased, suggesting an anxiety-like state similar to what we see in open field explorations. Additionally, nicotine withdrawal reduces responsiveness of LDTg to novel object interaction shifting the percentage of no response to novel object to be almost 60% of interactions. With IPN-LDTg optogenetic inhibition, the effect of nicotine withdrawal is reversed, and novel object interaction is increased. This supports the idea that IPN GABAergic control of LDTg mediates response to novelty.

A limitation of our study is the use of a single novel object. Our study can be strengthened in the future by examining the response to a novel object in comparison to a familiar object the mice had been previously habituated to[207]. It is out of experimenter control how often the mice choose to interact with the novel object and is therefore difficult to assess when the object switched to familiarity. In one particularly active experimental mouse that was not in our nicotine/tartrate drinking study, there were 34 novel object approaches and the LDTg completely stopped responding at 18 novel object interactions. However, in most mice we observed an average of 9-10 interactions within our 10-minute testing period. Future studies of novelty in LDTg should observe changes over longer periods of time to assess if transitions to familiarity is encoded in the LDTg in addition to withdrawal-mediated changes in learned object recognition. It is hard to dissociate measures of stress/anxiety and locomotion in a lot of novelty tests, another test in the future that may isolate the LDTg response to neophilia would be the hole-board test[207].

In the Tapper study, they also identified VTA DA projections to IPN as an important modulator of the novelty response through D1 receptors[206]. A subset of IPN neurons are activated by novel stimuli, through VTA DA activation[206]. Activation of this circuit enhances exploration of a familiar stimuli, mimicking novelty-like exploration and this effect is prevented by IPN D1

antagonism[206]. This circuit is active during novel contexts, potentially to reduce familiarity encoding IPN neurons and increase novelty salience[206].

While this role of the IPN has been more recently identified as an important mediator of novelty, much of the previous research in novelty has implicated regulation from the VTA, NAc, PFC and hippocampus[207]. High novelty seeking is a risk factor for addiction through higher sensitivity to drugs of abuse including, amphetamine, cocaine, nicotine, and alcohol[207]. High novelty seekers tend to have high response to reward despite potential punishment, leading to earlier and more varied drug use[207]. In animals, high novelty seeking groups self-administer lower concentrations of nicotine, seek nicotine more frequently, perform more work to acquire nicotine, and have a greater drug response to DA than low novelty seekers[207]. This may be due to lower basal firing of DA neurons in high novelty seekers increasing sensitivity and a lower concentration of D2R in the SN and VTA[207]. Interestingly, high novelty seekers have low serotonin responsiveness[207]. Maladaptive novelty seeking may also be a consequence of other psychological disorders such as depression, anxiety, or panic disorders that may use drugs for symptom mitigation[207]. The connection between novelty seeking and addiction is likely mediated through the mesolimbic DA system[207]. Novelty and drugs of abuse activate VTA-NAc DA release[207].

To monitor extracellular DA levels, we introduced GRAB-DA, a dopamine sensor, into the NAc lateral shell (NAcLat) and recorded changes in dopamine release to novel object interaction using fiber photometry. Our results show that dopamine release in the NAcLat is highly variable but can be categorized into 4 types of responses. Dopamine release to novel object interaction, similar to LDTg GCaMP6s response (POST) is seen as well as no response (NONE). However, there is also an observed increase before novel object interaction during the approach (PRE), and very occasionally, a suppression of activity when the DA levels were already elevated (DEC). The

proportion of these responses is very stable across control groups for PRE (~12%), POST (~38%), NONE (~45%), and DEC (~5%). However, during nicotine withdrawal there is a shift in the proportion of these responses with an increase in the PRE responses to 33% and a decrease in the POST responses to 17%. While we cannot directly attribute the DA release to LDTg activity, it is possible that LDTg suppression of novel object response during nicotine withdrawal contributes to the decreased POST responses observed with GRAB-DA. Further investigations are needed to see LDTg necessity in DA response to novel object.

Method considerations

This method uses a modified D2R to measure endogenous DA release[208]. When DA binds to the receptor, a conformational change causes increases in fluorescence. While this receptor also binds NE, the sensor is much more sensitive to DA and physiological concentrations (10-100nM, EC_{50} DA =10nM vs EC_{50} NE = 97nM) [208]. There is no evidence that expression of this receptor on neurons triggers G-protein receptor (GPR) or β-arrestin signaling pathways[208]. For example, DA application to wild type D2R-expressing neurons reduces forskolin (adenylate cyclase agonist) - induced cAMP increases through GPRi coupled adenylate cyclase inhibition[208]. However, the same DA application to GRAB-DA expressing neurons did not alter cAMP levels[208]. Additionally, blockade of GPR coupling with pertussis toxin or activation with GTPγS (a poorly hydrolysable GTP analogue) did not alter the EC_{50} (half maximal effective concentration) to DA for the GRAB-DA sensor[208]. Together, this data implies that introduction of GRAB-DA to neurons will not lead to GPR intracellular signaling. GRAB-DA also seems to have negligible β-arrestin induced internalization. Wild type D2R expressing neurons undergo rapid β-arrestin mediated internalization within 10-minutes of continuous agonist (DA) exposure[208]. GRAB-DA expressing

cells show stable expression throughout a 2-hour DA exposure[208]. Additionally, TANGO-assay revealed lower β-arrestin-dependent signaling in GRAB-DA expressing neurons that D2R expressing neurons[208]. Therefore, GRAB-DA allows us to visualize endogenous DA release within the NAc, without altering endogenous activity of DA receptors or altering our fluorescent signal through receptor mediated changes in intracellular signaling.

Coordination of LDTg activity and dopamine release in NAc lateral shell

The LDTg is uniquely positioned to both receive information from the habenulo-peduncular system and to modulate the limbic system through afferent connections. The LDTg may modulate the striatal part of the limbic system in a variety of ways, 1) innervation of midbrain dopamine neurons, 2) innervation of intralaminar and midline thalamus and 3) direct innervation of the striatum itself[172]. Collateralization of thalamic and VTA projections from LDTg have been shown to be very minimal, creating two distinct populations of LDTg efferents[209]. Of these, innervation of midbrain dopamine neurons is particularly intriguing due to the selective connectivity to VTA neurons projecting to the NAc[98]. Broadly, activation of LDTg increases VTA DA cell body firing, decreases VTA GABAergic firing, and produces place preference[172]. Optical activation of LDTg terminal in VTA enhances food reward value and inhibition decreases value (same results seen for LDTg-NAc stimulation /inhibition)[86,174]. More specifically, several labs have studied the cell type connections between the LDTg and the VTA, where the LDTg sends glutamatergic, cholinergic and GABAergic projections[85,107,109,172]. It has been shown that glutamatergic neurons to the VTA produces burst firing and place preference[172]. Cholinergic neurons to VTA cause depolarization, burst firing and place preference[172]. Pharmacologic activation of n/m nAChRs in VTA elevates DA in NAc and selective ablation of LDTg prevents

DA release[172]. Interestingly, baseline activation of LDTg does not change locomotion, anxiety, or open field exploration[172].

Using the same protocol as we did in the LDTg to measure activity before and after nicotine withdrawal, we observed a decrease in DAergic signaling within the NAcLat. We observed a decrease in peak amplitude and peak AUC without a change in peak number. Decreases in NAc DA during withdrawal has been observed using microdialysis[210]. Many microdialysis studies take samples with minute resolution (10-30 min sampling frequency)[71,158]. These studies were largely done in rat with mecamylamine and spontaneous withdrawal[210]. In these studies, the DA decrease was documented 10-60 min post injection and can last a duration of > 5 hours[210]. Mecamylamine has a half-life of 1-2 hours in rats[211], so the dopamine decrease is seen long after peak effects of mecamylamine in the system. Spontaneous withdrawal shows depressed DA levels 24 hours after nicotine cessation and these effects are largely dependent on mode and length of nicotine dependence[71]. There does not seem to be a strong correlation between accumbal DA levels and severity of withdrawal symptoms[159]. There is evidence in ethanol withdrawal from electrophysiology of DA neurons that activity is reduced longer than the behavioral manifestations of the withdrawal, suggesting that the cellular consequence of withdrawal have actions outside of dictating behavior.

We are the first to demonstrate immediate action of mecamylamine-precipitated withdrawal on DA levels (within 10 min of injection) with 10s of ms resolution, elucidating patterns in phasic dopamine release using fiber photometry. Most behavioral tests observe withdrawal symptoms within the first 5-20-minutes post mecamylamine injection, with peak symptoms happening from 5-10-minutes[201]. We observed peak decrease in DA 5-minutes after dopamine injection, in line with behavioral manifestations. Additionally, fiber photometry allows

for more specific targeting of the NAc than large microdialysis probes. Our recordings were taken from NAcLat. Traditionally, the core is associated with motor function and the shell is associated with emotion[212]. There is evidence that DA is involved in psychostimulant reinforcement preferentially within the NAc Shell and not the NAc core[212,213]. Notably, even with the differences in temporal resolution, there is a handling effect of increase in DA levels in both microdialysis and fiber photometry[158]. While it is well documented that nicotine withdrawal decreases dopamine release the exact mechanism for this decrease is not known. It has been hypothesized to come from increased inhibitory drive to the VTA DA neurons, but we propose an alternative theory of a converging withdrawal signal from IPN to VTA through the LDTg.

CONCLUSIONS

Until the present study, no role for the LDT in nicotine withdrawal behavior had been identified. Our data outlines the importance of GABAergic IPN neuronal connections to LDTg in mediating nicotine withdrawal somatic and affective states. Selective optogenetic inhibition of this pathway reveals alleviation of nicotine withdrawal somatic behaviors (primarily paw licking and shaking) and affective state (novelty exploration and anhedonia) through LDTg disinhibition. This optogenetic inhibition is preferred by mice in a real time place preference test and after repeated conditioning, mice seek out this treatment during a nicotine withdrawal state even when the opot-inhibition is no longer available to them.

We hypothesize that increased GABAergic drive from IPN to LDTg leads to the nicotine withdrawal induced suppression in LDTg activity. We observed selective LDTg reduction in activity during GCaMP6 fiber photometry recordings only during the nicotine withdrawal state. Rabies virus mediated monosynaptic tracing suggests IPN GABAergic inhibition is primarily suppressing GABAergic LDTg neurons. One explanation is LDTg GABAergic neurons increase VTA DA neuronal activity through suppression of local VTA GABAergic neurons. With increased IPN inhibition of LDTg GABA neurons, the net result would be increased VTA DA suppression. We observe evidence for DA suppression during nicotine withdrawal through our GRAB-DA recordings and coordinated decrease in LDTg increase to novel object and DA release following nicotine withdrawal, in line with this hypothesis.

Further studies should be done to dissect the precise mechanisms of LDTg control over nicotine addiction and withdrawal, in addition to other drugs of abuse. LDTg may provide novel therapeutic targets to increase cessation rate and improve withdrawal symptomology.

FUTURE DIRECTIONS

To further dissect the complex circuitry encompassing nicotine withdrawal, further testing within these various nuclei should be pursued. While there are many follow up questions to be answered, the present study leaves us with two major points of intrigue.

1) **Do LDTg cell types play specific roles in nicotine withdrawal?**

   While we have identified the key cell types within the LDTg receiving specific IPN inputs, it is of interest how these cell types respond to nicotine withdrawal. Using cre-dependent GCaMP signal within glutamatergic, cholinergic, and GABAergic populations will elucidate the source of nicotine withdrawal suppression of LDTg activity and cell type specific mediators of novel object interaction.

2) **Does IPN activity modulate DA release dynamics in the NAc through LDTg?**

   Additionally, a concrete connection between IPN activity and VTA DA suppression during nicotine withdrawal has not been demonstrated. It is of interest how IPN-LDTg inhibition and excitation modulates VTA DA neuronal activation and DA release within the NAc. While methodologically complicated due to degree of separation between the nuclei, combining optogenetic modulation of IPN-LDTg terminals with VTA DA cell body or DA release monitoring with fiber photometry could demonstrate bi-directional control over dopamine dynamics. IPN-LDTg inhibition during nicotine withdrawal could potentially prevent withdrawal-induced DA suppression or alteration of novel object response.

While our study demonstrates novel findings surrounding the role of LDTg in nicotine withdrawal there is still much work to be done in understanding the neurobiological underpinnings of nicotine addiction. Continued work in this area should assess the following points:

- Additional behavioral tests regulated by IPN-LDTg in nicotine withdrawal such as hyperalgesia, ICSS, EPM, marble burying, etc.
- IPN control of withdrawal through other downstream targets such as the raphe nuclei
- Nicotine withdrawal effects in other NAc subregions (medial shell and core)
- Input control over diverse novel object response within the NAcLat Shell
- Effect of acute and chronic nicotine exposure on LDTg neurons and nAChR subunits present on the different cell types

REFERENCES

1. Pan, B., et al., *The relationship between smoking and stroke: A meta-analysis.* Medicine (Baltimore), 2019. **98**(12): p. e14872.

2. Samet, J.M., *Tobacco smoking: the leading cause of preventable disease worldwide.* Thorac Surg Clin, 2013. **23**(2): p. 103-12.

3. *Tobacco*. July 26 2019; World Health Organization:[Available from: https://www.who.int/en/news-room/fact-sheets/detail/tobacco.

4. *Tobacco, Nicotine, and E-Cigarettes Research Report*. 2022: National Institute on Drug Abuse.

5. Benowitz, N.L., *Pharmacology of nicotine: addiction, smoking-induced disease, and therapeutics.* Annu Rev Pharmacol Toxicol, 2009. **49**: p. 57-71.

6. Henningfield, J.E., K. Miyasato, and D.R. Jasinski, *Cigarette smokers self-administer intravenous nicotine.* Pharmacol Biochem Behav, 1983. **19**(5): p. 887-90.

7. Rose, J.E. and W.A. Corrigall, *Nicotine self-administration in animals and humans: similarities and differences.* Psychopharmacology (Berl), 1997. **130**(1): p. 28-40.

8. Lopez-Quintero, C., et al., *Probability and predictors of transition from first use to dependence on nicotine, alcohol, cannabis, and cocaine: results of the National Epidemiologic Survey on Alcohol and Related Conditions (NESARC).* Drug Alcohol Depend, 2011. **115**(1-2): p. 120-30.

9. Zheng, Y.L., et al., *Updated Role of Neuropeptide Y in Nicotine-Induced Endothelial Dysfunction and Atherosclerosis.* Front Cardiovasc Med, 2021. **8**: p. 630968.

10. Chaiton, M., et al., *Estimating the number of quit attempts it takes to quit smoking successfully in a longitudinal cohort of smokers.* BMJ Open, 2016. **6**(6): p. e011045.

11. Polosa, R. and N.L. Benowitz, *Treatment of nicotine addiction: present therapeutic options and pipeline developments.* Trends Pharmacol Sci, 2011. **32**(5): p. 281-9.

12. Jackson, K.J., et al., *New mechanisms and perspectives in nicotine withdrawal.* Neuropharmacology, 2015. **96**(Pt B): p. 223-34.

13. Uhl, G.R., G.F. Koob, and J. Cable, *The neurobiology of addiction.* Ann N Y Acad Sci, 2019. **1451**(1): p. 5-28.

14. McLaughlin, I., J.A. Dani, and M. De Biasi, *Nicotine withdrawal.* The Neuropharmacology of Nicotine Dependence, 2015: p. 99-123.

15. Henningfield, J.E., C. Cohen, and J.D. Slade, *Is nicotine more addictive than cocaine?* Br J Addict, 1991. **86**(5): p. 565-9.

16. Hughes, J.R., S.T. Higgins, and W.K. Bickel, *Nicotine withdrawal versus other drug withdrawal syndromes: similarities and dissimilarities.* Addiction, 1994. **89**(11): p. 1461-70.

17. Kenny, P.J. and A. Markou, *Neurobiology of the nicotine withdrawal syndrome.* Pharmacology Biochemistry and Behavior, 2001. **70**(4): p. 531-549.

18. Goldman, D.P., et al., *The benefits of risk factor prevention in Americans aged 51 years and older.* Am J Public Health, 2009. **99**(11): p. 2096-101.

19. Dai, H.D. and A.M. Leventhal, *Use of Traditional Smokeless, Snus, and Dissolvable Tobacco Among U.S. Youth.* Am J Prev Med, 2023. **64**(2): p. 204-212.

20. Simonavicius, E., et al., *Heat-not-burn tobacco products: a systematic literature review.* Tob Control, 2019. **28**(5): p. 582-594.

21. *The Health Consequences of Smoking—50 Years of Progress: A Report of the Surgeon General*, in *National Center for Chronic Disease Prevention and Health Promotion (US) Office on Smoking and Health*. 2014.

22. Durazzo, T.C., N. Mattsson, and M.W. Weiner, *Smoking and increased Alzheimer's disease risk: a review of potential mechanisms.* Alzheimers Dement, 2014. **10**(3 Suppl): p. S122-45.

23. National Academies of Sciences, E., et al., in *Public Health Consequences of E-Cigarettes*, D.L. Eaton, L.Y. Kwan, and K. Stratton, Editors. 2018, National Academies Press (US)
Copyright 2018 by the National Academy of Sciences. All rights reserved.: Washington (DC).
24. Cooper, M., et al., *Notes from the Field: E-cigarette Use Among Middle and High School Students - United States, 2022.* MMWR Morb Mortal Wkly Rep, 2022. **71**(40): p. 1283-1285.

25. CDC, *About Electronic Cigarettes*, in *Smoking and Tobacco Use*. 2023.

26. Moheimani, R.S., et al., *Sympathomimetic Effects of Acute E-Cigarette Use: Role of Nicotine and Non-Nicotine Constituents.* J Am Heart Assoc, 2017. **6**(9).

27. Haustein, K.O., et al., *Effects of cigarette smoking or nicotine replacement on cardiovascular risk factors and parameters of haemorheology.* J Intern Med, 2002. **252**(2): p. 130-9.

28. Struik, L.L., et al., *Tactics for Drawing Youth to Vaping: Content Analysis of Electronic Cigarette Advertisements.* J Med Internet Res, 2020. **22**(8): p. e18943.

29. Sargent, J.D., et al., *Adolescent smoking experimentation as a predictor of daily cigarette smoking.* Drug Alcohol Depend, 2017. **175**: p. 55-59.

30. Kowitt, S.D., et al., *E-Cigarette Use Among Adolescents Not Susceptible to Using Cigarettes.* Prev Chronic Dis, 2018. **15**: p. E18.

31. Groom, A.L., et al., *The Influence of Friends on Teen Vaping: A Mixed-Methods Approach.* Int J Environ Res Public Health, 2021. **18**(13).

32. Liu, J., S.M. Gaiha, and B. Halpern-Felsher, *A Breath of Knowledge: Overview of Current Adolescent E-cigarette Prevention and Cessation Programs.* Curr Addict Rep, 2020. **7**(4): p. 520-532.

33. Barrett, S.P., *The effects of nicotine, denicotinized tobacco, and nicotine-containing tobacco on cigarette craving, withdrawal, and self-administration in male and female smokers.* Behav Pharmacol, 2010. **21**(2): p. 144-52.

34. Smith, P.H., et al., *Sex Differences in Smoking Cessation Pharmacotherapy Comparative Efficacy: A Network Meta-analysis.* Nicotine Tob Res, 2017. **19**(3): p. 273-281.

35. Datta, U., et al., *Prospects for finding the mechanisms of sex differences in addiction with human and model organism genetic analysis.* Genes Brain Behav, 2020. **19**(3): p. e12645.

36. Quigley, H. and J.H. MacCabe, *The relationship between nicotine and psychosis.* Ther Adv Psychopharmacol, 2019. **9**: p. 2045125319859969.

37. Smucny, J. and J.R. Tregellas, *Targeting neuronal dysfunction in schizophrenia with nicotine: Evidence from neurophysiology to neuroimaging.* J Psychopharmacol, 2017. **31**(7): p. 801-811.

38. Keřková, B., et al., *Smoking and attention in schizophrenia spectrum disorders: What are we neglecting?* Front Psychol, 2023. **14**: p. 1114473.

39. Sved, A.F., et al., *Monoamine oxidase inhibition in cigarette smokers: From preclinical studies to tobacco product regulation.* Front Neurosci, 2022. **16**: p. 886496.

40. Cather, C., et al., *Achieving Smoking Cessation in Individuals with Schizophrenia: Special Considerations.* CNS Drugs, 2017. **31**(6): p. 471-481.

41. Taylor, G.M., et al., *Smoking cessation for improving mental health.* Cochrane Database Syst Rev, 2021. **3**(3): p. Cd013522.

42. CDC, *Declines in Cigarette Smoking During Pregnancy in the United States, 2016–2021*. 2023.

43. Jensen, K.P., E.E. DeVito, and M. Sofuoglu, *How Intravenous Nicotine Administration in Smokers Can Inform Tobacco Regulatory Science.* Tob Regul Sci, 2016. **2**(4): p. 452-463.

44. Quattrocki, E., A. Baird, and D. Yurgelun-Todd, *Biological aspects of the link between smoking and depression.* Harv Rev Psychiatry, 2000. **8**(3): p. 99-110.

45. Picciotto, M.R. and P.J. Kenny, *Molecular mechanisms underlying behaviors related to nicotine addiction.* Cold Spring Harb Perspect Med, 2013. **3**(1): p. a012112.

46. Wolfman, S.L., et al., *Nicotine aversion is mediated by GABAergic interpeduncular nucleus inputs to laterodorsal tegmentum.* Nat Commun, 2018. **9**(1): p. 2710.

47. Zabor, E.C., et al., *Initial reactions to tobacco use and risk of future regular use.* Nicotine Tob Res, 2013. **15**(2): p. 509-17.

48. Benowitz, N.L., *Nicotine addiction.* N Engl J Med, 2010. **362**(24): p. 2295-303.

49. Pang, R.D., et al., *Subjective effects from the first cigarette of the day vary with precigarette affect in premenopausal female daily smokers.* Exp Clin Psychopharmacol, 2020. **28**(3): p. 299-305.

50. CDC, *Smoking Cessation: Fast Facts*, in *Smoking & Tobacco Use*. 2022.

51. Wise, R.A. and M.A. Robble, *Dopamine and Addiction.* Annu Rev Psychol, 2020. **71**: p. 79-106.

52. Corrigall, W.A., et al., *The mesolimbic dopaminergic system is implicated in the reinforcing effects of nicotine.* Psychopharmacology (Berl), 1992. **107**(2-3): p. 285-9.

53. Pontieri, F.E., et al., *Effects of nicotine on the nucleus accumbens and similarity to those of addictive drugs.* Nature, 1996. **382**(6588): p. 255-7.

54. Grenhoff, J., G. Aston-Jones, and T.H. Svensson, *Nicotinic effects on the firing pattern of midbrain dopamine neurons.* Acta Physiol Scand, 1986. **128**(3): p. 351-8.

55. Mao, D. and D.S. McGehee, *Nicotine and behavioral sensitization.* J Mol Neurosci, 2010. **40**(1-2): p. 154-63.

56. Szczypka, M.S., et al., *Feeding behavior in dopamine-deficient mice.* Proc Natl Acad Sci U S A, 1999. **96**(21): p. 12138-43.

57. Hamid, A.A., et al., *Mesolimbic dopamine signals the value of work.* Nat Neurosci, 2016. **19**(1): p. 117-26.

58. Berke, J.D., *What does dopamine mean?* Nat Neurosci, 2018. **21**(6): p. 787-793.

59. Lerner, T.N., A.L. Holloway, and J.L. Seiler, *Dopamine, Updated: Reward Prediction Error and Beyond.* Curr Opin Neurobiol, 2021. **67**: p. 123-130.

60. Di Chiara, G. and A. Imperato, *Drugs abused by humans preferentially increase synaptic dopamine concentrations in the mesolimbic system of freely moving rats.* Proc Natl Acad Sci U S A, 1988. **85**(14): p. 5274-8.

61. Fu, Y., et al., *Local alpha-bungarotoxin-sensitive nicotinic receptors in the nucleus accumbens modulate nicotine-stimulated dopamine secretion in vivo.* Neuroscience, 2000. **101**(2): p. 369-75.

62. Mao, D., K. Gallagher, and D.S. McGehee, *Nicotine potentiation of excitatory inputs to ventral tegmental area dopamine neurons.* J Neurosci, 2011. **31**(18): p. 6710-20.

63. Clarke, P.B., et al., *Evidence that mesolimbic dopaminergic activation underlies the locomotor stimulant action of nicotine in rats.* J Pharmacol Exp Ther, 1988. **246**(2): p. 701-8.

64. Corrigall, W.A., et al., *The mesolimbic dopaminergic system is implicated in the reinforcing effects of nicotine.* Psychopharmacology, 1992. **107**: p. 285-289.

65. Corrigall, W.A., K.M. Coen, and K.L. Adamson, *Self-administered nicotine activates the mesolimbic dopamine system through the ventral tegmental area.* Brain research, 1994. **653**(1-2): p. 278-284.

66. Mansvelder, H.D., J.R. Keath, and D.S. McGehee, *Synaptic mechanisms underlie nicotine-induced excitability of brain reward areas.* Neuron, 2002. **33**(6): p. 905-19.

67. Govind, A.P., P. Vezina, and W.N. Green, *Nicotine-induced upregulation of nicotinic receptors: underlying mechanisms and relevance to nicotine addiction.* Biochem Pharmacol, 2009. **78**(7): p. 756-65.

68. Marks, M.J., J.B. Burch, and A.C. Collins, *Effects of chronic nicotine infusion on tolerance development and nicotinic receptors.* J Pharmacol Exp Ther, 1983. **226**(3): p. 817-25.

69. Marks, M.J., et al., *Increased nicotinic acetylcholine receptor protein underlies chronic nicotine-induced up-regulation of nicotinic agonist binding sites in mouse brain.* J Pharmacol Exp Ther, 2011. **337**(1): p. 187-200.

70. Perry, D.C., et al., *Increased nicotinic receptors in brains from smokers: membrane binding and autoradiography studies.* J Pharmacol Exp Ther, 1999. **289**(3): p. 1545-52.

71. Zhang, L., et al., *Withdrawal from chronic nicotine exposure alters dopamine signaling dynamics in the nucleus accumbens.* Biol Psychiatry, 2012. **71**(3): p. 184-91.

72. Grieder, T.E., et al., *Phasic D1 and tonic D2 dopamine receptor signaling double dissociate the motivational effects of acute nicotine and chronic nicotine withdrawal.* Proc Natl Acad Sci U S A, 2012. **109**(8): p. 3101-6.

73. Koranda, J.L., et al., *Nicotinic receptors regulate the dynamic range of dopamine release in vivo.* J Neurophysiol, 2014. **111**(1): p. 103-11.

74. Marks, M.J., S.R. Grady, and A.C. Collins, *Downregulation of nicotinic receptor function after chronic nicotine infusion.* J Pharmacol Exp Ther, 1993. **266**(3): p. 1268-76.

75. Dani, J.A. and M. De Biasi, *Mesolimbic dopamine and habenulo-interpeduncular pathways in nicotine withdrawal.* Cold Spring Harb Perspect Med, 2013. **3**(6).

76. Kenny, P.J. and A. Markou, *Nicotine self-administration acutely activates brain reward systems and induces a long-lasting increase in reward sensitivity.* Neuropsychopharmacology, 2006. **31**(6): p. 1203-11.

77. Epping-Jordan, M.P., et al., *Dramatic decreases in brain reward function during nicotine withdrawal.* Nature, 1998. **393**(6680): p. 76-9.

78. Baiamonte, B.A., et al., *Nicotine dependence produces hyperalgesia: role of corticotropin-releasing factor-1 receptors (CRF1Rs) in the central amygdala (CeA).* Neuropharmacology, 2014. **77**: p. 217-23.

79. Doherty, K., et al., *Urges to smoke during the first month of abstinence: relationship to relapse and predictors.* Psychopharmacology, 1995. **119**: p. 171-178.

80. Piasecki, T.M., M.C. Fiore, and T.B. Baker, *Profiles in discouragement: two studies of variability in the time course of smoking withdrawal symptoms.* Journal of abnormal psychology, 1998. **107**(2): p. 238.

81. Wang, H.L. and M. Morales, *Pedunculopontine and laterodorsal tegmental nuclei contain distinct populations of cholinergic, glutamatergic and GABAergic neurons in the rat.* Eur J Neurosci, 2009. **29**(2): p. 340-58.

82. Wang, X., et al., *Brain-wide Mapping of Mono-synaptic Afferents to Different Cell Types in the Laterodorsal Tegmentum.* Neurosci Bull, 2019. **35**(5): p. 781-790.

83. Lodge, D.J. and A.A. Grace, *The laterodorsal tegmentum is essential for burst firing of ventral tegmental area dopamine neurons.* Proc Natl Acad Sci U S A, 2006. **103**(13): p. 5167-72.

84. Liu, C., et al., *An inhibitory brainstem input to dopamine neurons encodes nicotine aversion.* Neuron, 2022. **110**(18): p. 3018-3035.e7.

85. Dautan, D., et al., *Segregated cholinergic transmission modulates dopamine neurons integrated in distinct functional circuits.* Nat Neurosci, 2016. **19**(8): p. 1025-33.

86. Coimbra, B., et al., *Role of laterodorsal tegmentum projections to nucleus accumbens in reward-related behaviors.* Nature Communications, 2019. **10**(1): p. 4138.

87. Steidl, S. and K. Veverka, *Optogenetic excitation of LDTg axons in the VTA reinforces operant responding in rats.* Brain Res, 2015. **1614**: p. 86-93.

88. Xiao, C., et al., *Cholinergic Mesopontine Signals Govern Locomotion and Reward through Dissociable Midbrain Pathways.* Neuron, 2016. **90**(2): p. 333-47.

89. Luquin, E., et al., *Stereological Estimates of Glutamatergic, GABAergic, and Cholinergic Neurons in the Pedunculopontine and Laterodorsal Tegmental Nuclei in the Rat.* Front Neuroanat, 2018. **12**: p. 34.

90. Fagen, Z.M., et al., *Short- and long-term modulation of synaptic inputs to brain reward areas by nicotine.* Ann N Y Acad Sci, 2003. **1003**: p. 185-95.

91. Ishibashi, M., C.S. Leonard, and K.A. Kohlmeier, *Nicotinic activation of laterodorsal tegmental neurons: implications for addiction to nicotine.* Neuropsychopharmacology, 2009. **34**(12): p. 2529-47.

92. Alderson, H.L., M.P. Latimer, and P. Winn, *Involvement of the laterodorsal tegmental nucleus in the locomotor response to repeated nicotine administration.* Neurosci Lett, 2005. **380**(3): p. 335-9.

93. Shinohara, F., et al., *Critical role of cholinergic transmission from the laterodorsal tegmental nucleus to the ventral tegmental area in cocaine-induced place preference.* Neuropharmacology, 2014. **79**: p. 573-9.

94. Steidl, S., K.M. Cardiff, and R.A. Wise, *Increased latencies to initiate cocaine self-administration following laterodorsal tegmental nucleus lesions.* Behav Brain Res, 2015. **287**: p. 82-8.

95. Schmidt, H.D., K.R. Famous, and R.C. Pierce, *The limbic circuitry underlying cocaine seeking encompasses the PPTg/LDT.* Eur J Neurosci, 2009. **30**(7): p. 1358-69.

96. Beier, K.T., et al., *Circuit Architecture of VTA Dopamine Neurons Revealed by Systematic Input-Output Mapping.* Cell, 2015. **162**(3): p. 622-34.

97. Cornwall, J., J.D. Cooper, and O.T. Phillipson, *Afferent and efferent connections of the laterodorsal tegmental nucleus in the rat.* Brain Res Bull, 1990. **25**(2): p. 271-84.

98. Oakman, S.A., et al., *Distribution of pontomesencephalic cholinergic neurons projecting to substantia nigra differs significantly from those projecting to ventral tegmental area.* J Neurosci, 1995. **15**(9): p. 5859-69.

99. Watabe-Uchida, M., et al., *Whole-brain mapping of direct inputs to midbrain dopamine neurons.* Neuron, 2012. **74**(5): p. 858-73.

100. Omelchenko, N. and S.R. Sesack, *Laterodorsal tegmental projections to identified cell populations in the rat ventral tegmental area.* J Comp Neurol, 2005. **483**(2): p. 217-35.

101. Faget, L., et al., *Afferent Inputs to Neurotransmitter-Defined Cell Types in the Ventral Tegmental Area.* Cell Rep, 2016. **15**(12): p. 2796-808.

102. Coimbra, B., et al., *Impairments in laterodorsal tegmentum to VTA projections underlie glucocorticoid-triggered reward deficits.* Elife, 2017. **6**.

103. Lammel, S., et al., *Input-specific control of reward and aversion in the ventral tegmental area.* Nature, 2012. **491**(7423): p. 212-7.

104. Lester, D.B., et al., *Midbrain acetylcholine and glutamate receptors modulate accumbal dopamine release.* Neuroreport, 2008. **19**(9): p. 991-5.

105. Chen, L. and D.J. Lodge, *The lateral mesopontine tegmentum regulates both tonic and phasic activity of VTA dopamine neurons.* J Neurophysiol, 2013. **110**(10): p. 2287-94.

106. Blaha, C.D., et al., *Modulation of dopamine efflux in the nucleus accumbens after cholinergic stimulation of the ventral tegmental area in intact, pedunculopontine*

tegmental nucleus-lesioned, and laterodorsal tegmental nucleus-lesioned rats. The Journal of neuroscience, 1996. **16**(2): p. 714.

107. Forster, G.L. and C.D. Blaha, *Laterodorsal tegmental stimulation elicits dopamine efflux in the rat nucleus accumbens by activation of acetylcholine and glutamate receptors in the ventral tegmental area.* Eur J Neurosci, 2000. **12**(10): p. 3596-604.

108. Mansvelder, H.D., et al., *Cholinergic modulation of dopaminergic reward areas: upstream and downstream targets of nicotine addiction.* Eur J Pharmacol, 2003. **480**(1-3): p. 117-23.

109. Steidl, S., et al., *Optogenetic excitation in the ventral tegmental area of glutamatergic or cholinergic inputs from the laterodorsal tegmental area drives reward.* Eur J Neurosci, 2017. **45**(4): p. 559-571.

110. Soden, M.E., et al., *Anatomic resolution of neurotransmitter-specific projections to the VTA reveals diversity of GABAergic inputs.* Nat Neurosci, 2020. **23**(8): p. 968-980.

111. Dautan, D., et al., *A major external source of cholinergic innervation of the striatum and nucleus accumbens originates in the brainstem.* Journal of Neuroscience, 2014. **34**(13): p. 4509-4518.

112. Broussot, L., et al., *A non-canonical GABAergic pathway to the VTA promotes unconditioned freezing.* Mol Psychiatry, 2022. **27**(12): p. 4905-4917.

113. Yang, H., et al., *Nucleus Accumbens Subnuclei Regulate Motivated Behavior via Direct Inhibition and Disinhibition of VTA Dopamine Subpopulations.* Neuron, 2018. **97**(2): p. 434-449.e4.

114. Bouarab, C., B. Thompson, and A.M. Polter, *VTA GABA Neurons at the Interface of Stress and Reward.* Front Neural Circuits, 2019. **13**: p. 78.

115. Hernandez, N.S., et al., *GLP-1 receptor signaling in the laterodorsal tegmental nucleus attenuates cocaine seeking by activating GABAergic circuits that project to the VTA.* Mol Psychiatry, 2021. **26**(8): p. 4394-4408.

116. de Jong, J.W., et al., *A Neural Circuit Mechanism for Encoding Aversive Stimuli in the Mesolimbic Dopamine System.* Neuron, 2019. **101**(1): p. 133-151.e7.

117. Wills, L., et al., *Neurobiological Mechanisms of Nicotine Reward and Aversion.* Pharmacol Rev, 2022. **74**(1): p. 271-310.

118. McLaughlin, I., J.A. Dani, and M. De Biasi, *The medial habenula and interpeduncular nucleus circuitry is critical in addiction, anxiety, and mood regulation.* J Neurochem, 2017. **142 Suppl 2**(Suppl 2): p. 130-143.

119. Antolin-Fontes, B., et al., *The habenulo-interpeduncular pathway in nicotine aversion and withdrawal.* Neuropharmacology, 2015. **96**(Pt B): p. 213-22.

120. Molas, S., et al., *Anxiety and Nicotine Dependence: Emerging Role of the Habenulo-Interpeduncular Axis.* Trends Pharmacol Sci, 2017. **38**(2): p. 169-180.

121. Zhao-Shea, R., et al., *Activation of GABAergic neurons in the interpeduncular nucleus triggers physical nicotine withdrawal symptoms.* Curr Biol, 2013. **23**(23): p. 2327-35.

122. Salas, R., et al., *Nicotinic receptors in the habenulo-interpeduncular system are necessary for nicotine withdrawal in mice.* Journal of Neuroscience, 2009. **29**(10): p. 3014-3018.

123. Zhao-Shea, R., et al., *Increased CRF signalling in a ventral tegmental area-interpeduncular nucleus-medial habenula circuit induces anxiety during nicotine withdrawal.* Nat Commun, 2015. **6**: p. 6770.

124. Pang, X., et al., *Habenula cholinergic neurons regulate anxiety during nicotine withdrawal via nicotinic acetylcholine receptors.* Neuropharmacology, 2016. **107**: p. 294-304.

125. Olale, F., et al., *Chronic nicotine exposure differentially affects the function of human alpha3, alpha4, and alpha7 neuronal nicotinic receptor subtypes.* J Pharmacol Exp Ther, 1997. **283**(2): p. 675-83.

126. Rasmussen, B.A. and D.C. Perry, *An autoradiographic analysis of [125I]alpha-bungarotoxin binding in rat brain after chronic nicotine exposure.* Neurosci Lett, 2006. **404**(1-2): p. 9-14.

127. Wang, F., et al., *Assembly of human neuronal nicotinic receptor alpha5 subunits with alpha3, beta2, and beta4 subunits.* J Biol Chem, 1996. **271**(30): p. 17656-65.

128. Wills, L. and P.J. Kenny, *Addiction-related neuroadaptations following chronic nicotine exposure.* J Neurochem, 2021. **157**(5): p. 1652-1673.

129. Loukola, A., et al., *Genome-wide association study on detailed profiles of smoking behavior and nicotine dependence in a twin sample.* Mol Psychiatry, 2014. **19**(5): p. 615-24.

130. Jordan, C.J. and Z.X. Xi, *Discovery and development of varenicline for smoking cessation.* Expert Opin Drug Discov, 2018. **13**(7): p. 671-683.

131. Ables, J.L., et al., *Retrograde inhibition by a specific subset of interpeduncular α5 nicotinic neurons regulates nicotine preference.* Proc Natl Acad Sci U S A, 2017. **114**(49): p. 13012-13017.

132. Bueno, D., et al., *Connections of the laterodorsal tegmental nucleus with the habenular-interpeduncular-raphe system.* J Comp Neurol, 2019. **527**(18): p. 3046-3072.

133. Quina, L.A., et al., *Specific connections of the interpeduncular subnuclei reveal distinct components of the habenulopeduncular pathway.* J Comp Neurol, 2017. **525**(12): p. 2632-2656.

134. Lima, L.B., et al., *Afferent and efferent connections of the interpeduncular nucleus with special reference to circuits involving the habenula and raphe nuclei.* J Comp Neurol, 2017. **525**(10): p. 2411-2442.

135. Risinger, F.O. and R.A. Oakes, *Nicotine-induced conditioned place preference and conditioned place aversion in mice.* Pharmacol Biochem Behav, 1995. **51**(2-3): p. 457-61.

136. Fowler, C.D., et al., *Habenular alpha5 nicotinic receptor subunit signalling controls nicotine intake.* Nature, 2011. **471**(7340): p. 597-601.

137. Le Foll, B., et al., *Tobacco and nicotine use.* Nat Rev Dis Primers, 2022. **8**(1): p. 19.

138. Wilkes, S., *The use of bupropion SR in cigarette smoking cessation.* Int J Chron Obstruct Pulmon Dis, 2008. **3**(1): p. 45-53.

139. Hays, J.T., D.D. McFadden, and J.O. Ebbert, *Pharmacologic agents for tobacco dependence treatment: 2011 update.* Curr Atheroscler Rep, 2012. **14**(1): p. 85-92.

140. García-Gómez, L., et al., *SMOKING CESSATION TREATMENTS: CURRENT PSYCHOLOGICAL AND PHARMACOLOGICAL OPTIONS.* Rev Invest Clin, 2019. **71**(1): p. 7-16.

141. Prochaska, J.J. and N.L. Benowitz, *The Past, Present, and Future of Nicotine Addiction Therapy.* Annu Rev Med, 2016. **67**: p. 467-86.

142. NIDA, *What are treatments for tobacco dependence?*, N.I.o.D. Abuse, Editor. 2021.

143. Cinciripini, P.M., et al., *Effects of varenicline and bupropion sustained-release use plus intensive smoking cessation counseling on prolonged abstinence from smoking and on*

depression, negative affect, and other symptoms of nicotine withdrawal. JAMA Psychiatry, 2013. **70**(5): p. 522-33.

144. Turner, J.R., et al., *Divergent functional effects of sazetidine-a and varenicline during nicotine withdrawal.* Neuropsychopharmacology, 2013. **38**(10): p. 2035-47.

145. Leone, F.T. and S. Evers-Casey, *Tobacco Use Disorder.* Med Clin North Am, 2022. **106**(1): p. 99-112.

146. Rigotti, N.A., et al., *Treatment of Tobacco Smoking: A Review.* Jama, 2022. **327**(6): p. 566-577.

147. Grabus, S.D., et al., *Nicotine physical dependence and tolerance in the mouse following chronic oral administration.* Psychopharmacology (Berl), 2005. **178**(2-3): p. 183-92.

148. Arany, I., et al., *Chronic nicotine exposure exacerbates acute renal ischemic injury.* Am J Physiol Renal Physiol, 2011. **301**(1): p. F125-33.

149. Hukkanen, J., P. Jacob, 3rd, and N.L. Benowitz, *Metabolism and disposition kinetics of nicotine.* Pharmacol Rev, 2005. **57**(1): p. 79-115.

150. Damaj, M.I., W. Kao, and B.R. Martin, *Characterization of spontaneous and precipitated nicotine withdrawal in the mouse.* J Pharmacol Exp Ther, 2003. **307**(2): p. 526-34.

151. Pekonen, K., et al., *Plasma nicotine and cotinine concentrations in mice after chronic oral nicotine administration and challenge doses.* European Journal of Pharmaceutical Sciences, 1993. **1**(1): p. 13-18.

152. Salas, R., F. Pieri, and M. De Biasi, *Decreased signs of nicotine withdrawal in mice null for the beta4 nicotinic acetylcholine receptor subunit.* J Neurosci, 2004. **24**(45): p. 10035-9.

153. Chellian, R., et al., *Rodent models for nicotine withdrawal.* J Psychopharmacol, 2021. **35**(10): p. 1169-1187.

154. Nishitani, N., et al., *Serotonin neurons in the median raphe nucleus bidirectionally regulate somatic signs of nicotine withdrawal in mice.* Biochem Biophys Res Commun, 2021. **562**: p. 62-68.

155. Fowler, C.D., L. Tuesta, and P.J. Kenny, *Role of α5* nicotinic acetylcholine receptors in the effects of acute and chronic nicotine treatment on brain reward function in mice.* Psychopharmacology (Berl), 2013.

156. Malkesman, O., et al., *The female urine sniffing test: a novel approach for assessing reward-seeking behavior in rodents.* Biol Psychiatry, 2010. **67**(9): p. 864-71.

157. Tadmor, H., et al., *Behavioral characterization of blocking the ErbB signaling during adolescent and adulthood in reward-liking (preference) and reward-related learning.* Behav Brain Res, 2017. **326**: p. 139-146.

158. Hildebrand, B.E., et al., *Reduced dopamine output in the nucleus accumbens but not in the medial prefrontal cortex in rats displaying a mecamylamine-precipitated nicotine withdrawal syndrome.* Brain Res, 1998. **779**(1-2): p. 214-25.

159. Carboni, E., et al., *Dissociation of physical abstinence signs from changes in extracellular dopamine in the nucleus accumbens and in the prefrontal cortex of nicotine dependent rats.* Drug Alcohol Depend, 2000. **58**(1-2): p. 93-102.

160. Rada, P., K. Jensen, and B.G. Hoebel, *Effects of nicotine and mecamylamine-induced withdrawal on extracellular dopamine and acetylcholine in the rat nucleus accumbens.* Psychopharmacology (Berl), 2001. **157**(1): p. 105-10.

161. Collins, A.C., et al., *Oral Nicotine Self-Administration in Rodents.* J Addict Res Ther, 2012. **S2**.

162. Benowitz, N.L., J. Hukkanen, and P. Jacob, 3rd, *Nicotine chemistry, metabolism, kinetics and biomarkers.* Handb Exp Pharmacol, 2009(192): p. 29-60.

163. Rose, J.E., et al., *Kinetics of brain nicotine accumulation in dependent and nondependent smokers assessed with PET and cigarettes containing 11C-nicotine.* Proc Natl Acad Sci U S A, 2010. **107**(11): p. 5190-5.

164. O'Dell, L.E. and T.V. Khroyan, *Rodent models of nicotine reward: what do they tell us about tobacco abuse in humans?* Pharmacol Biochem Behav, 2009. **91**(4): p. 481-8.

165. Kasten, C.R., A.M. Frazee, and S.L. Boehm, 2nd, *Developing a model of limited-access nicotine consumption in C57Bl/6J mice.* Pharmacol Biochem Behav, 2016. **148**: p. 28-37.

166. DeBaker, M.C., et al., *Differential patterns of alcohol and nicotine intake: Combined alcohol and nicotine binge consumption behaviors in mice.* Alcohol, 2020. **85**: p. 57-64.

167. Manouze, H., et al., *Effects of Single Cage Housing on Stress, Cognitive, and Seizure Parameters in the Rat and Mouse Pilocarpine Models of Epilepsy.* eNeuro, 2019. **6**(4).

168. Frie, J.A., et al., *OpenVape: An Open-Source E-Cigarette Vapor Exposure Device for Rodents.* eNeuro, 2020. **7**(5).

169. Lippiello, P.M., et al., *TC-5214 (S-(+)-mecamylamine): a neuronal nicotinic receptor modulator with antidepressant activity.* CNS Neurosci Ther, 2008. **14**(4): p. 266-77.

170. Cisewski, D.H., et al., *Approach to buprenorphine use for opioid withdrawal treatment in the emergency setting.* Am J Emerg Med, 2019. **37**(1): p. 143-150.

171. Eissenberg, T., R.R. Griffiths, and M.L. Stitzer, *Mecamylamine does not precipitate withdrawal in cigarette smokers.* Psychopharmacology (Berl), 1996. **127**(4): p. 328-36.

172. Kohlmeier, K.A., *Off the beaten path: drug addiction and the pontine laterodorsal tegmentum.* ISRN Neurosci, 2013. **2013**: p. 604847.

173. Van Dort, C.J., et al., *Optogenetic activation of cholinergic neurons in the PPT or LDT induces REM sleep.* Proc Natl Acad Sci U S A, 2015. **112**(2): p. 584-9.

174. Coimbra, B., et al., *Laterodorsal tegmentum-ventral tegmental area projections encode positive reinforcement signals.* J Neurosci Res, 2021. **99**(11): p. 3084-3100.

175. Nelson, C., et al., *The laterodorsal tegmentum contributes to behavioral sensitization to amphetamine.* Neuroscience, 2007. **146**(1): p. 41-49.

176. Forster, G., et al., *Effects of laterodorsal tegmentum excitotoxic lesions on behavioral and dopamine responses evoked by morphine and d-amphetamine.* Neuroscience, 2002. **114**(4): p. 817-823.

177. Lança, A.J., T.R. Sanelli, and W.A. Corrigall, *Nicotine-induced fos expression in the pedunculopontine mesencephalic tegmentum in the rat.* Neuropharmacology, 2000. **39**(13): p. 2808-2817.

178. Ishibashi, M., C.S. Leonard, and K.A. Kohlmeier, *Nicotinic activation of laterodorsal tegmental neurons: implications for addiction to nicotine.* Neuropsychopharmacology, 2009. **34**(12): p. 2529-2547.

179. Wang, Y., et al., *A selected review of recent advances in the study of neuronal circuits using fiber photometry.* Pharmacol Biochem Behav, 2021. **201**: p. 173113.

180. García-Guillén, I.M., et al., *Netrin-1/DCC Signaling Differentially Regulates the Migration of Pax7, Nkx6.1, Irx2, Otp, and Otx2 Cell Populations in the Developing Interpeduncular Nucleus.* Front Cell Dev Biol, 2020. **8**: p. 588851.

181. Ables, J.L., K. Park, and I. Ibañez-Tallon, *Understanding the habenula: A major node in circuits regulating emotion and motivation.* Pharmacol Res, 2023. **190**: p. 106734.

182. Saleeba, C., et al., *A Student's Guide to Neural Circuit Tracing.* Front Neurosci, 2019. **13**: p. 897.

183. Tran-Van-Minh, A., Z. Ye, and E. Rancz, *Quantitative analysis of rabies virus-based synaptic connectivity tracing.* PLoS One, 2023. **18**(3): p. e0278053.

184. Matos-Ocasio, F., et al., *Female rats display greater nicotine withdrawal-induced cellular activation of a central portion of the interpeduncular nucleus versus males: A study of Fos immunoreactivity within provisionally assigned interpeduncular subnuclei.* Drug Alcohol Depend, 2021. **221**: p. 108640.

185. Lee, H.W., et al., *The Role of the Medial Habenula Cholinergic System in Addiction and Emotion-Associated Behaviors.* Front Psychiatry, 2019. **10**: p. 100.

186. Caputi, A., et al., *The long and short of GABAergic neurons.* Curr Opin Neurobiol, 2013. **23**(2): p. 179-86.

187. Lavin, T.K., et al., *Monosynaptic Tracing Success Depends Critically on Helper Virus Concentrations.* Front Synaptic Neurosci, 2020. **12**: p. 6.

188. Fischer, K.B., H.K. Collins, and E.M. Callaway, *Sources of off-target expression from recombinase-dependent AAV vectors and mitigation with cross-over insensitive ATG-out vectors.* Proc Natl Acad Sci U S A, 2019. **116**(52): p. 27001-27010.

189. Kajita, Y. and H. Mushiake, *Heterogeneous GAD65 Expression in Subtypes of GABAergic Neurons Across Layers of the Cerebral Cortex and Hippocampus.* Front Behav Neurosci, 2021. **15**: p. 750869.

190. Kanaani, J., et al., *Two distinct mechanisms target GAD67 to vesicular pathways and presynaptic clusters.* J Cell Biol, 2010. **190**(5): p. 911-25.

191. Huerta-Ocampo, I., et al., *Whole-brain mapping of monosynaptic inputs to midbrain cholinergic neurons.* Sci Rep, 2021. **11**(1): p. 9055.

192. Souza, R., et al., *Top-down projections of the prefrontal cortex to the ventral tegmental area, laterodorsal tegmental nucleus, and median raphe nucleus.* Brain Struct Funct, 2022. **227**(7): p. 2465-2487.

193. Roman, E., et al., *Untangling the dorsal diencephalic conduction system: a review of structure and function of the stria medullaris, habenula and fasciculus retroflexus.* Brain Struct Funct, 2020. **225**(5): p. 1437-1458.

194. Stevenson, J.G., et al., *Smoking environment cues reduce ability to resist smoking as measured by a delay to smoking task.* Addict Behav, 2017. **67**: p. 49-52.

195. McLaughlin, I., J.A. Dani, and M. De Biasi, *Nicotine withdrawal.* Curr Top Behav Neurosci, 2015. **24**: p. 99-123.

196. Ashare, R.L., M. Falcone, and C. Lerman, *Cognitive function during nicotine withdrawal: Implications for nicotine dependence treatment.* Neuropharmacology, 2014. **76 Pt B**(0 0): p. 581-91.

197. Sherafat, Y., et al., *The Interpeduncular-Ventral Hippocampus Pathway Mediates Active Stress Coping and Natural Reward.* eNeuro, 2020. **7**(6).

198. Malin, D.H., et al., *Bupropion attenuates nicotine abstinence syndrome in the rat.* Psychopharmacology (Berl), 2006. **184**(3-4): p. 494-503.

199. Jackson, K.J., et al., *The role of various nicotinic receptor subunits and factors influencing nicotine conditioned place aversion.* Neuropharmacology, 2009. **56**(6-7): p. 970-4.

200. Stoker, A.K., S. Semenova, and A. Markou, *Affective and somatic aspects of spontaneous and precipitated nicotine withdrawal in C57BL/6J and BALB/cByJ mice.* Neuropharmacology, 2008. **54**(8): p. 1223-32.

201. Klenowski, P.M., et al., *Dynamic activity of interpeduncular nucleus GABAergic neurons controls expression of nicotine withdrawal in male mice.* Neuropsychopharmacology, 2022. **47**(3): p. 641-651.

202. Heyser, C.J. and A. Chemero, *Novel object exploration in mice: not all objects are created equal.* Behav Processes, 2012. **89**(3): p. 232-8.

203. Gorwood, P., *Neurobiological mechanisms of anhedonia.* Dialogues Clin Neurosci, 2008. **10**(3): p. 291-9.

204. Johnson, P.M., J.A. Hollander, and P.J. Kenny, *Decreased brain reward function during nicotine withdrawal in C57BL6 mice: evidence from intracranial self-stimulation (ICSS) studies.* Pharmacol Biochem Behav, 2008. **90**(3): p. 409-15.

205. Alkhlaif, Y., et al., *Assessment of nicotine withdrawal-induced changes in sucrose preference in mice.* Pharmacol Biochem Behav, 2017. **161**: p. 47-52.

206. Molas, S., et al., *A circuit-based mechanism underlying familiarity signaling and the preference for novelty.* Nat Neurosci, 2017. **20**(9): p. 1260-1268.

207. Wingo, T., et al., *Novelty Seeking and Drug Addiction in Humans and Animals: From Behavior to Molecules.* J Neuroimmune Pharmacol, 2016. **11**(3): p. 456-70.

208. Sun, F., et al., *A Genetically Encoded Fluorescent Sensor Enables Rapid and Specific Detection of Dopamine in Flies, Fish, and Mice.* Cell, 2018. **174**(2): p. 481-496.e19.

209. Holmstrand, E.C. and S.R. Sesack, *Projections from the rat pedunculopontine and laterodorsal tegmental nuclei to the anterior thalamus and ventral tegmental area arise from largely separate populations of neurons.* Brain Struct Funct, 2011. **216**(4): p. 331-45.

210. De Biasi, M. and J.A. Dani, *Reward, addiction, withdrawal to nicotine.* Annu Rev Neurosci, 2011. **34**: p. 105-30.

211. Muelken, P., et al., *A Two-Day Continuous Nicotine Infusion Is Sufficient to Demonstrate Nicotine Withdrawal in Rats as Measured Using Intracranial Self-Stimulation.* PLoS One, 2015. **10**(12): p. e0144553.

212. Di Chiara, G., *Nucleus accumbens shell and core dopamine: differential role in behavior and addiction.* Behav Brain Res, 2002. **137**(1-2): p. 75-114.

213. Lecca, D., et al., *Preferential increase of extracellular dopamine in the rat nucleus accumbens shell as compared to that in the core during acquisition and maintenance of intravenous nicotine self-administration.* Psychopharmacology (Berl), 2006. **184**(3-4): p. 435-46.